AFWAL-TR-87-3069
VOLUME IV

EXPERIMENTAL MODAL ANALYSIS AND DYNAMIC COMPONENT SYNTHESIS

VOL IV - System Modeling Techniques

Dr. Randall J. Allemang, Dr. David L. Brown
Structural Dynamics Research Laboratory
Department of Mechanical and Industrial Engineering
University of Cincinnati
Cincinnati, Ohio 45221-0072

Dr. Mohan L. Soni
University of Dayton Research Institute
Dayton, Ohio 45469

December 1987

Final Technical Report for Period November 1983 - January 1987

Approved for public release; distribution is unlimited

FLIGHT DYNAMICS LABORATORY
AIR FORCE WRIGHT AERONAUTICAL LABORATORIES
AIR FORCE SYSTEMS COMMAND
WRIGHT-PATTERSON AIR FORCE BASE, OHIO 45433-6553

NOTICE

This technical report has been reviewed and is approved for publication.

OTTO F. MAURER, Principal Engineer
Structural Dynamics Branch
Structures Division

JEROME PEARSON, Chief
Structural Dynamics Branch
Structures Division

FOR THE COMMANDER

ROBERT M. BADER, Ass't Chief
Structures Division
Flight Dynamics Laboratory

UNCLASSIFIED

SECURITY CLASSIFICATION OF THIS PAGE

REPORT DOCUMENTATION PAGE

1a. REPORT SECURITY CLASSIFICATION: UNCLASSIFIED	1b. RESTRICTIVE MARKINGS
2a. SECURITY CLASSIFICATION AUTHORITY	3. DISTRIBUTION/AVAILABILITY OF REPORT: APPROVED FOR PUBLIC RELEASE; DISTRIBUTION IS UNLIMITED
2b. DECLASSIFICATION/DOWNGRADING SCHEDULE	
4. PERFORMING ORGANIZATION REPORT NUMBER(S)	5. MONITORING ORGANIZATION REPORT NUMBER(S): AFWAL-TR-87-3069 VOL.IV
6a. NAME OF PERFORMING ORGANIZATION: UNIVERSITY OF CINCINNATI; 6b. OFFICE SYMBOL (If applicable)	7a. NAME OF MONITORING ORGANIZATION: AIR FORCE WRIGHT AERONAUTICAL LABORATORIES, FLIGHT DYNAMICS LABORATORY
6c. ADDRESS (City, State and ZIP Code): CINCINNATI OH 45221-0072	7b. ADDRESS (City, State and ZIP Code): AFWAL/FIBG Wright-Patterson AFB OH 45433-6553
8a. NAME OF FUNDING/SPONSORING ORGANIZATION: Armament Test Laboratory; 8b. OFFICE SYMBOL (If applicable): AFATL	9. PROCUREMENT INSTRUMENT IDENTIFICATION NUMBER: F33615-83-C-3218
8c. ADDRESS (City, State and ZIP Code): Eglin AFB FL 32542	10. SOURCE OF FUNDING NOS.: PROGRAM ELEMENT NO. 62201F; PROJECT NO. 2401; TASK NO. 04; WORK UNIT NO. 16

11. TITLE (Include Security Classification) EXPERIMENTAL MODAL ANALYSIS AND DYNAMIC COMPONENT SYNTHESIS (UNCLASSIFIED) Vol. IV - System Modeling Techniques

12. PERSONAL AUTHOR(S) DR. RANDALL J. ALLEMANG DR. DAVID L. BROWN

13a. TYPE OF REPORT	13b. TIME COVERED	14. DATE OF REPORT (Yr., Mo., Day)	15. PAGE COUNT
FINAL	FROM NOV 1983 TO JAN 1987	DECEMBER 1987	153

16. SUPPLEMENTARY NOTATION
The computer software contained herein are theoretical and/or references that in no way reflect Air Force-owned or developed computer software.

17. COSATI CODES			18. SUBJECT TERMS (Continue on reverse if necessary and identify by block number)
FIELD	GROUP	SUB. GR.	MODAL TESTING VIBRATION TESTING DYNAMICS
22	01		

19. ABSTRACT (Continue on reverse if necessary and identify by block number)

System Modeling techniques have become more and more practical in the application of industrial design and troubleshooting of vibration problems in the last few years. Sophisticated commercial codes, such as SDRC's SMURF and SYSTAN, SMS's SDM, are very popularly used by the industrial engineers as one of the integral parts in the state of the art of Computer Aided Engineering. This report presents the reviews of the theoretical basis for the current methods of the System Modeling techniques along with a newly developed Component Mode Synthesis method. The effects of errors existing in the experimental modal model, validation methods of experimental model, and normalization of measured complex modes are also presented as part of the efforts to link the experimental model to the current system modeling techniques. Case studies of a H frame are presented and conclusions are made with respect to the effectiveness of different system modeling techniques.

20. DISTRIBUTION/AVAILABILITY OF ABSTRACT: UNCLASSIFIED/UNLIMITED ☒ SAME AS RPT. ☐ DTIC USERS ☐	21. ABSTRACT SECURITY CLASSIFICATION: UNCLASSIFIED
22a. NAME OF RESPONSIBLE INDIVIDUAL: OTTO F. MAURER	22b. TELEPHONE NUMBER (Include Area Code): (513)255-5236; 22c. OFFICE SYMBOL: AFWAL/FIBG

DD FORM 1473, 83 APR EDITION OF 1 JAN 73 IS OBSOLETE.

SECURITY CLASSIFICATION OF THIS PAGE

SUMMARY

This report reviews the theoretical basis for the current methods used to predict the system dynamics of a modified structure or of combined structures based upon a previously determined, modal or impedance, model of the structure(s). The methods reviewed were:

- Modal modeling Technique
  - Local eigenvalue modification
  - Coupling of Structures Using Eigenvalue Modification
  - Complex Mode Eigenvalue Modification
- Sensitivity Analysis
- Impedance Modeling Technique
  - Building Block Approach
  - Dynamic Stiffness Method
  - Frequency Response Method

The effects of measurement errors, modal parameter estimation error, and truncated modes in the application of modal modeling technique are evaluated. Some of the experimental modal model validation method are also presented.

Several methods to normalize the measured complex modes were reviewed including both the time domain and frequency domain techniques.

A new component mode synthesis method (Superelement Component Dynamic Synthesis) developed by the University of Dayton Research Institute is presented in Section 5 and Appendices.

A complete literature search in the area of System Modeling was performed and is listed in the Bibliography.

PREFACE

This report is one of six Technical Reports that represent the final report on the work involved with United States Air Force Contract F33615-83-C-3218, Experimental Modal Analysis and Dynamic Component Synthesis. The reports that are part of the documented work include the following:

AFWAL-TR-87-3069

Vol. I	Summary of Technical Work
Vol. II	Measurement Techniques for Experimental Modal Analysis
Vol. III	Modal Parameter Estimation
Vol. IV	System Modeling Techniques
Vol. V	Universal File Formats
Vol. VI	Software User's Guide

For a complete understanding of the research conducted under this contract, all of the Technical Reports should be referenced.

Work performed by the University of Dayton Research Institute (UDRI) under a subcontract is included in the above Technical Reports and is in reference to UDRI Report Number UDR-TR-86-117.

ACKNOWLEDGEMENTS

The University of Cincinnati Structural Dynamics Research Laboratory (UC-SDRL) would like to acknowledge the following groups and persons who have contributed to the writing of this report:

- Dr. Mohan L. Soni of the University of Dayton Research Institute has contributed and written Sections 5, 6.3, and Appendices of this report.

- SDRC, particularly John Crowley for assistance with SMURF and Dr. Joe Klaus, for assistance with SYSTAN.

- University of Leuven, for assistance with modal modeling and sensitivity analysis.

- Ottor Maurer, Contract Monitor, for guidance, advice, and assistance during the course of this contract.

The members of the staff of the University of Cincinnati Structural Dynamics Research Laboratory have contributed to the writing of this report as follows:

- Dennis W. Sulisz, for his master thesis work at UC-SDRL (1984 - 1985).

- Phil E. Weber and Vivian Walls, for their preparation and review of Sections 2.8, 4 and 6.1 of this report.

- Alex W. Wang, for his preparation and review of the section on sensitivity analysis and his general support of putting together Sections 2.1 through 2.6, Sections 5 and 8.

- Max L. Wei, for the writing of the normalization methods of the measured complex modes and his assistance and coordination in preparing the final form of this report.

TABLE OF CONTENTS

TABLE OF CONTENTS (concluded)

LIST OF ILLUSTRATIONS

LIST OF TABLES

1. INTRODUCTION

The objective of this report is to document the review of the current methods used to predict the system dynamics of an altered structure or of combined structures based upon a previously defined, modal or impedance, model of the structure(s). Of particular interest is the performance of such modeling methods with respect to experimentally based models.

This report investigates several system modeling techniques to determine their capabilities and limitations from a theoretical and practical viewpoint. Several experimental techniques, practical aspects of the analytical and approximate techniques, test results, modeling results, and analysis of the results are presented to compare and evaluate the various modeling methods. This study presents all of the techniques in a consistent manner from the same origin, using consistent nomenclature, to clearly highlight the similarities and differences inherent in their development which form the basis of the strengths and weaknesses of each technique. To gain practical insights, all of the techniques presented in Sections 2 through 4 are compared with experimental results.

1.1 System Modeling

System modeling is a computer based technique that is used to represent the dynamic characteristics of a structure. This representation takes the form of either experimental data, modal data, or analytical data. Once the dynamic characteristics of a structure are used to form a model or system model, several uses of the model are possible. First, the effects of design changes or hardware changes to the original structure could be studied. Second, the structure could be coupled with another structure to determine the overall resultant dynamic behavior. Finally, the model can be used analytically to apply forces and determine the forced response characteristics of the structure.

The main objective of system modeling is to use a mathematical representation of the dynamic characteristics of a structure in a computer environment to effectively develop a design or trouble shoot a particular problem of a design. Several techniques of various origin have evolved with the advancement of computer technology. Depending on the situation, each is very effective if properly utilized. Design development is generally considered an extensive long range process that results in an optimally designed structure given the constraints of the project. Trouble shooting involves the evaluation of failures or design flaws which must be corrected quickly.

The most obvious way to classify system models is into analytical and experimental methods. The primary approach to analytical modeling is commonly known as finite element Analysis. Finite element analysis is analytical in nature because only knowledge of the physical properties of the structure is used to build a dynamic representation. This is done by subdividing the structure into discrete elements and assembling the linear second order differential equations by estimating the mass, stiffness, and damping matrices from the physical coordinates, material properties, and geometric properties.

Finite Element Analysis is extremely useful because no physical test object is necessary to compute resonant frequencies and mode shapes, forced response simulation, or hardware modifications. Therefore, this method is extremely useful in the development cycle where it can be used to correct major flaws in the dynamic characteristics of a structure before a prototype is built. Since finite element analysis is an approximate analytical technique, experimental modal analysis data is obtained as soon as possible so the analytical model can be validated. Detailed finite element analysis method is not covered in this report.

Experimental modeling techniques are further subdivided into two groups. They are modal models and impedance models. Modal modeling is an experimentally based technique that uses the results of an experimental modal analysis to create a dynamic model based on the estimated poles of the system. The result is a computationally efficient model that is uncoupled due to transformation of the physical coordinates into the modal coordinates which renders the system into a number of lumped mass, single degree of freedom components. This concept is fundamental to modal analysis. This model is then used to investigate hardware changes, couple structures, or compute the forced response. This method is developed fully in Section 2.

Impedance modeling uses measured impedance functions or frequency response functions to represent the dynamic characteristics of a structure in the frequency domain. This method uses the experimentally measured functions to compute the effects of hardware changes or to couple together several components. To use this modeling technique, measurements at the constraint or connection points, driving point, and cross measurements between the two are needed to compute a modified frequency response function. Impedance modeling is fully developed for the compliance method and stiffness method in Section 4.

Both of the experimental modeling methods are quick and easy to use in their basic implementations. Therefore, they are extremely useful in trouble shooting situations but have limited application in the design cycle.

The final classification of system models is experimental/analytical models or mixture methods. Two techniques are considered mixture methods. The first is sensitivity analysis. Sensitivity analysis is an approximate technique that uses the first term or first two terms of a power series expansion to determine the rate of change of eigenvalues or eigenvectors with respect to physical changes (mass, stiffness, and damping). Therefore, this method is used for trend analysis, selection of hardware modification location, and design optimization. This technique is considered a mixture method because it computes sensitivity values for modal parameters which result from either experimental modal analysis or finite element analysis.

The other experimental/analytical method is component mode synthesis. Component mode synthesis and the building block approach are techniques that use experimental or analytical modal representations of the components of a large or complex structure to predict the resultant dynamic characteristics of the entire structure. Furthermore, this technique has evolved to the point where components are combined in either physical or modal coordinates. Therefore, this technique is truly a mixture method where experimental and analytical data are used to optimize a design. This method is very useful in the design cycle of industries that produce large structures, such as the automotive and aerospace industries. A new component mode synthesis method (not a classical mode synthesis method such as SYSTAN) is discussed in detail in Section 5 and the building block approach is discussed in Section 4 along with the development of the impedance modeling technique.

1.2 Practical Application

To determine the practical limitations and capabilities of the various techniques, each is compared with experimental results for four hardware changes to an H frame of hollow tubing, welded construction, and rigid end plates. The four design changes considered are a simple stiffener addition, addition of two masses, beam addition, and plate addition. The modeling techniques were used to predict new dynamic characteristics only when the changes were applicable within the constraints of their intended implementation.

An experimental modal analysis was conducted on the H frame in its original state. The frequency response functions and resulting modal parameters are inputs to the various programs to predict the effects of the design changes.

In summary, system modeling is a diverse field that involves many aspects of structural dynamics. One of the primary goals of this report is to present this material in a concise and consistent manner to reduce unnecessary confusion and better relate the various factions involved. Furthermore, each technique is applied to a structure to gain further insight into the practical aspects of system modeling.

1.3 Boundary Conditions

In the application of the system modeling techniques mentioned above, there are three test configurations used to obtain the frequency response functions or the derived modal data base. These three test configurations involve the boundary condition and can be summarized as free-free, constrained, and actual operating boundary conditions. In terms of analytical modeling technique, such as finite element analysis, various boundary conditions can be easily simulated in the mathematical model to predict the dynamic characteristics of a system. Therefore, this gives the analysts the luxury to evaluate the model using desired boundary condition. In terms of experimental modeling technique, in a laboratory environment, usually it is very difficult and too costly to implement the test fixture to simulate the actual operating condition of a complete system, or the constrained boundary condition of a component. Therefore, most of the modal tests are performed under an environment simulating free-free boundary conditions.

Besides the boundary conditions mentioned above, modal tests can be performed on the mass-loaded structures to predict the shifted dynamic characteristics of the original structure. The advantages of adding lumped masses at the connecting or attachment points of a component under testing are: (1) modal coefficients associated with those connecting degrees of freedom can be more accurately excited and described under the mass loading effect, (2) rotational degrees of freedoms at the connecting degrees of freedom can be computed using rigid body computer programs if sufficient number of accelerometers are mounted on the additive masses, (3) analytically, added masses can be removed from the mass-loaded testing configuration, and the enhanced modal parameters of the original structure can be obtained, (4) if the dynamic characteristics of the original structures are available through analytical or experimental method, then more accurate generalized masses can be obtained through these two sets of data. Examples of applying the mass additive technique can be found in References [1] and [2].

2. MODAL MODELING

2.1 Modal Modeling Overview

This section develops the system modeling technique known as modal modeling. Modal modeling is also known as the Snyder Technique, Local Eigenvalue Modification, Structural Modifications, Dual Modal Space Structural Modification Method, and Structural Dynamic Modification [3-16]. The common thread of the research mentioned is that all utilize a model in generalized or modal coordinates from experimental data upon which to investigate structural changes. Structural changes are transformed into modal coordinates and added to the structure and the result is resolved to yield the modified modal parameters.

The modal modeling technique was initially published by Kron [3] in 1962 and extended by Weissenberger [4], Simpson and Taborrok [5] , and Hallquist, Pomazal and Snyder [6]. Early researchers in this area restricted themselves to a local modification eigensolution technique. Several software packages have been developed employing this technique since the implementation and widespread use of digital Fourier analysis. Notably, Structural Measurement Systems, Inc. first released Structural Dynamics Modification [7] using the local modification procedure. The local modification procedure allows only simple mass, stiffness and damping changes between two general points.

Recent research has progressed in several areas. First, Hallquist and Snyder [8], Luk and Mitchell [9] and SMS [7] have used the local modification technique for coupling two or more structures together. Hallquist [10], O'Callahan [11] and De Landseer [12] have expanded the method to include complex modes. O'Callahan [13] and SMS [14] have found methods to approximate more realistic modifications using local modification for trusses and beams. Mitchell and Elliot [15] and O'Callahan and Chou [16] have developed different methods that use full six degree of freedom representations that depend on the approximation or measurement of the rotational degrees of freedom to make beam or plate modifications.

2.2 Modal Model Development

The equations of motion of a mechanical structure are second order linear differential equations,

$$[M]\{\ddot{x}\} + [C]\{\dot{x}\} + [K]\{x\} = \{f(t)\} \tag{1}$$

where M, C and K are the structure's mass, damping, and stiffness matrices of order N by N. The displacement vector {x} is in physical coordinates, {f} is the applied forcing vector, and N is the number of physical degrees of freedom.

Two techniques are commonly used to find the solution vector {x}. Either a solution is assumed of the form $\{x\} = \{X\}e^{st}$ or Laplace transforms are used to arrive at a set of linear equations.

$$\left[[M]s^2 + [C]s + [K]\right]\{X(s)\} = \{F(s)\} \tag{2}$$

where the initial conditions are equal to zero

Now the substitution

$$[B(s)] = \left[[M]s^2 + [C]s + [K]\right] \tag{3}$$

is made to Equation (2) yielding

$$[B(s)]\{X(s)\} = \{F(s)\} \tag{4}$$

[B(s)] is the system matrix. The eigenvalues of the structure are found by taking the determinant of the system matrix for the nontrivial case when {X(s)} exists. The vector {X} that is associated with each eigenvalue is the eigenvector found from the solution of:

$$[B(s_k)]\{X(s_k)\} = \{0\} \tag{5}$$

The inverse of the system matrix B(s) is called the transfer function matrix of the structure,

$$[H(s)] = [B(s)]^{-1} = \frac{Adj[B]}{Det[B]} \tag{6a}$$

where Adj [B] is the adjoint matrix. The adjoint matrix and determinant of [B] matrix are polynomials in the variables because the elements are functions of s. Therefore, the transfer function matrix is conveniently written in partial fraction form.

$$[H(s)] = \sum_{r=1}^{N}\left\{ \frac{A_r}{(s-\lambda_r)} + \frac{A_r^*}{(s-\lambda_r^*)} \right\} \tag{6b}$$

where the λ_r is the poles or zeroes of the determinant matrix and N is the number of degrees of freedom included in the model. Continuous systems have infinite degrees of freedom; therefore, N modes form a truncated modal model in practice.

The elements of the system matrix are quadratic in s; therefore, the number of poles p is 2N. Furthermore, since M, K, and C are real matrices the poles are in conjugate pairs and are purely imaginary. Also, the residue matrix $[A]_r$ is an N by N matrix of complex values. This concept is critical to experimental modal analysis because the rows and columns of $[A]_r$ are made of a linear combination of the homogeneous solution vector,

$$[A]_r = Q_r\{\phi\}_r\{\phi\}_r^T \tag{7}$$

where Q_r is a scaling constant and $\{\phi\}_r = \{X\}$ is the mode shape vector of mode r.

The physical significance of this is that experimentally, frequency response function is measured in the complex plane at $s = j\omega$. When frequency response functions are measured, either rows or columns of the residue matrix are defined. Thus, the result of an experimental modal analysis parameter estimation is the eigenvalues (frequency and damping) and eigenvectors (mode shapes) from the frequency response functions. Due to the unique orthogonality relationships, modal vectors are linearly independent quantities, which is stated mathematically as:

$$\{\phi\}_i^T[M]\{\phi\}_k = 0 \tag{8}$$

$$\{\phi\}_i^T[K]\{\phi\}_k = 0 \tag{9}$$

for $i \neq k$.

Thus, the projection of one vector on another is zero and is orthogonal with respect to the [M] and [K] matrices. The orthogonality relationships allow a set of simultaneous equations to be transformed into uncoupled equations; this is perhaps the single biggest advantage of the modal domain. An N degree of freedom system is orthogonal in N space. It is desired to transform our system in physical coordinates into modal or generalized coordinates. If $i = k = r$ in Equation (8) and (9).

$$\{\phi\}_r^T[M]\{\phi\}_r = M_r \tag{10}$$

$$\{\phi\}_r^T[K]\{\phi\}_r = K_r \tag{11}$$

M_r and K_r are scalar quantities related to the modal mass and modal stiffness of mode r. Magnitudes of m_r and K_r are dependent on the modal scaling factor Q_r.

The coordinate transformation was required to diagonalize the physical mass and stiffness matrices. As already noted in Equation (8) and (9), when the mass or stiffness matrix is pre-multiplied by the transpose and post-multiplied by different eigenvectors the result is zero. If this same operation is performed with the same vectors, a constant results. Therefore, if all the modal vectors are formed into a matrix it is readily seen that the desired transformation matrix exists in the modal matrix [Φ].

2.3 Local Eigenvalue Modification

The local eigenvalue procedure is a simple technique that transforms modifications into modal space. This is done for simple structural changes hence, a very efficient solution is obtained. Going back to the original equation of motion and assuming proportional damping:

$$[M]\{\ddot{x}\} + [C]\{\dot{x}\} + [K]\{x\} = \{f\} \tag{12}$$

Now, this set of equations is transformed into modal space by substituting the coordinate transformation $\{x\} = [\Phi]\{q\}$ and pre- multiplying by the transpose of the modal matrix [Φ]:

$$[\Phi]^T[M][\Phi] = \lceil M \rfloor \tag{13}$$

$$[\Phi]^T[C][\Phi] = \lceil C \rfloor \tag{14}$$

$$[\Phi]^T[K][\Phi] = \lceil K \rfloor \tag{15}$$

This is a statement of orthogonality with respect to the properties of the modal vectors.

The set of equations in modal coordinates is written as:

$$\lceil M \rfloor \{\ddot{q}\} + \lceil C \rfloor \{\dot{q}\} + \lceil K \rfloor \{q\} = [\Phi]^T\{f\} \tag{16}$$

Note that the mass, stiffness, and damping matrices are assumed to be diagonal. For this case, the system is classically or proportionally damped, and the set of equations yields a real normal mode model. Therefore, this development does not treat the nonproportionally damped case.

To make modifications that have physical significance, the mode shapes must be scaled by some technique so that the equations can be consistently transformed into modal space to yield accurate results. Unity modal mass scaling is used by choosing $Q_r = \frac{1}{2j\omega_r}$ in Equation (7) to put the equations in a convenient form.

$$[I]\{\ddot{q}\} + \lceil 2\varsigma_r\Omega_r \rfloor \{\dot{q}\} + \lceil \Omega_r^2 \rfloor \{q\} = [\Phi]\{f\} \tag{17}$$

where:

$\lceil 2\varsigma_r\Omega_r \rfloor$ - modal damping matrix

$\lceil \Omega_r^2 \rfloor$ - modal stiffness matrix

σ_r - damping coefficient ($= \varsigma_r\Omega_r$)

ς_r - damping ratio for mode r

Ω_r - undamped natural frequency of mode r

Now the orthogonality equations are written as:

$$[\Phi]^T[M][\Phi] = [I] \tag{18}$$

$$[\Phi]^T[C][\Phi] = \lceil 2\sigma_r \rfloor = \lceil 2\varsigma_r\Omega_r \rfloor \tag{19}$$

$$[\Phi]^T[K][\Phi] = \lceil \sigma_r^2 + \omega_r^2 \rfloor \tag{20}$$

The results of a modal test are the eigenvalues (frequency and damping):

$$\lambda_r = \sigma_r + j\omega_r = -\varsigma_r\Omega_r + j\sqrt{1-\varsigma_r^2}\,\Omega_r \tag{21}$$

which are solutions of the characteristic equation:

$$\det\Big[[M]s^2 + [C]s + [K]\Big] = 0 \tag{22}$$

and the eigenvectors are:

$$[\Phi] = [\{\phi\}_1, \{\phi\}_2, \ldots, \{\phi\}_N] \tag{23}$$

which are solved from the homogeneous equation:

$$\Big[[M]\lambda_r^2 + [C]\lambda_r + [K]\Big]\{\phi\}_r = 0 \qquad r = 1, \ldots, N \tag{24}$$

Using the simple relationships (Equation (12) through (24)), modifications can be made to a structure.

$$\Big[[M]+[\Delta M]\Big]\{\ddot{x}\} + \Big[[C]+[\Delta C]\Big]\{\dot{x}\} + \Big[[K]+[\Delta K]\Big]\{x\} = \{f\} \tag{25}$$

where:

$[\Delta M]$ - mass modification

$[\Delta C]$ - damping modification

$[\Delta K]$ - stiffness modification

This equation is transformed into modal coordinates using the standard transformation $[\Phi]$:

$$[\overline{M}]\{\ddot{q}\} + [\overline{C}]\{\dot{q}\} + [\overline{K}]\{q\} = [\Phi]^T\{f\} \tag{26}$$

where:

$[\overline{M}] = [I] + [\Phi]^T[\Delta M][\Phi]$

$[\overline{C}] = \lceil 2\varsigma_r\Omega_r \rfloor + [\Phi]^T[\Delta C][\Phi]$

$[\overline{K}] = \lceil \Omega_r^2 \rfloor + [\Phi]^T[\Delta K][\Phi]$

Note that the bar over a variable denotes that the matrix is modified.

The eigenvalues and eigenvectors of the modified system are found as follows. The eigenvalues are calculated from the determinant equation :

$$\det\left[[\overline{M}]s^2 + [\overline{C}]s + [\overline{K}]\right] = 0 \tag{27}$$

The eigenvectors are calculated as a solution of the homogeneous equation:

$$\left[[\overline{M}]\lambda_r^2 + [\overline{C}]\lambda_r + [\overline{K}]\right]\{\phi\}_r = 0 \qquad r = 1,\ldots,N$$

This results in:

$$[\overline{\Phi}] = [\Phi][\{\phi\}_1,\{\phi\}_2,\ldots,\{\phi\}_N] \tag{28}$$

Therefore, given a set of calibrated frequency response functions from which system parameters are extracted and scaled to unity modal mass, numerous modifications can be investigated. Mass, stiffness, and damping modifications may be made between any two measured degrees of freedom or between ground and a measured degree of freedom.

Frequently, many authors have presented the local modification procedure similar to this development. To better understand the local modification procedure, the form of the modification will be considered more carefully. Only a stiffness modification is handled to simplify the equations.

Consider two modal spaces 1 and 2; 1 is the original modal coordinates and 2 is the modified modal coordinates. A stiffness modification in modal coordinates [77] is written as:

$$[\Delta K_{12}] = [\overline{\Phi}]^T[\Delta K][\overline{\Phi}] \tag{29}$$

where 12 denotes the stiffness change and may be represented in physical form as:

$$[\Delta K_{12}] = [T]\,\lceil D \rfloor\,[T]^T \tag{30}$$

where:

$[T]$ - The matrix containing the eigenvectors of $[\Delta K]$ which represent the *tying* vectors of the physical degree-of-freedoms

$\lceil D \rfloor$ - The eigenvalue spectral matrix of $[\Delta K]$

Equation (30) can be written as a summation over the number of modifications in the system.

$$[\Delta K_{12}] = \sum_{k=1}^{M} \{t\}_k d_k \{t\}_k^T$$

where:

$\{t\}_k$ - The k^{th} tie vector of [T]

d_k- The k^{th} diagonal element of $\lceil D \rfloor$

k - The modification tying index

M - The number of modification(s)

For a single modification, substituting this result into Equation (29) yields:

$$[\Delta K_{12}] = [\Phi]^T \{t\}_k d_k \{t\}_k^T [\Phi] \tag{31}$$

Now, a modal projection vector which indicates the modes affected by the modification is defined.

$$\{v\}_k = [\Phi]^T \{t\}_k \tag{32}$$

This identity is used in Equation (31) to further simplify the expression.

$$[\Delta K_{12}] = \{v\}_k d_k \{v\}_k^T \tag{33}$$

Equation (33) is added to the undamped and homogeneous form of Equation (17) to yield:

$$[I]\{\ddot{q}_{12}\} + \left[\lceil \Omega_r^2 \rfloor + [\Delta K_{12}]\right] \{q_{12}\} = 0 \tag{34}$$

The vector q_{12} describes the change from modal space 1 to 2.

The characteristic Equation of (34) is:

$$[\lceil \Omega_r^2 \rfloor - \omega_2^2]\{q_{12}\} = -\{v\}_k d_k \{v\}_k^T \{q_{12}\} \tag{35}$$

$$\{q_{12}\} = -[\ ^{\lceil}\Omega_r{}^2{}_{\rfloor} - \omega_2{}^2]^{-1}\{\nu\}_k d_k \{\nu\}_k^T \{q_{12}\} \tag{35a}$$

where:

Ω_r - Natural frequency of the r^{th} mode of the original structure in the modal space 1

ω_2 - Modified natural frequency

multiply both sides of Equation (35a) by $\{\nu\}_k^T$:

$$\{\nu\}_k^T\{q_{12}\} = -\{\nu\}_k^T[\ ^{\lceil}\Omega_r{}^2{}_{\rfloor} - \omega_2{}^2]^{-1}\{\nu\}_k d_k \{\nu\}_k^T \{q_{12}\} \tag{36}$$

since $\{\nu\}_k^T\{q_{12}\} \neq 0$, therefore :

$$1 = -d_k\{\nu\}_k^T[\ ^{\lceil}\Omega_r{}^2{}_{\rfloor} - \omega_2{}^2]^{-1}\{\nu\}_k \tag{37}$$

which is manipulated into the summation form:

$$\frac{1}{d_k} = \sum_{r=1}^{N}\left\{\frac{\nu_r{}^2}{(\Omega_r{}^2 - \omega_2{}^2)}\right\} \tag{37a}$$

Equation (37) is the modified characteristic polynomial equation in modal space 2 relative to modal space 1. Although the use of tie vectors confuses the development, it lends much insight to the understanding of the relationships between the two modal spaces. Once the eigenvalues are determined, the eigenvectors of the modified system are found using standard eigenvalue/eigenvector decomposition algorithms to yield the eigenvectors in modal coordinates. They are scaled to unity modal mass in relative space:

$$[\Phi_{12}]^T[\overline{M}][\Phi_{12}] = [I]$$

and transformed back into modal space by multiplying by $[\Phi_{12}]$.

$$[\Phi_2] = [\Phi_1][\Phi_{12}] \tag{38}$$

The local eigenvalue modification procedure allows the projection of the physical space into modal space 1 using the tie vector approach originated by Kron [3]. Therefore, a complete eigenvalue solution is not necessary. The largest advantage of this method is that it is very quick because a full rank eigenvalue/eigenvector extraction is not needed.

2.4 Coupling of Structures Using Eigenvalue Modification

Modal synthesis is used primarily to find the resultant dynamic characteristics of a large structure by adding smaller components together. It is assumed that the components have been measured and data exists at the connection points. The modal synthesis technique has been implemented using the local eigenvalue modification technique. This implementation is extremely simple because it eliminates the need for attachment modes, residuals, and constraints that are discussed in Sections 4 and 5. Only the mass, stiffness, and damping at the coupling points are necessary, along with the modal data of the two structures.

Recalling the original differential Equations (12), it can be readily seen that for n components, the equation becomes:

$$[\hat{M}]\{\hat{\ddot{x}}\} + [\hat{C}]\{\hat{\dot{x}}\} + [\hat{K}]\{\hat{x}\} = \{\hat{f}\} \tag{39}$$

where:

$$[\hat{M}] = \begin{bmatrix} [M_1] & [0] & [0] & \dots & [0] \\ [0] & [M_2] & [0] & \dots & [0] \\ \vdots & \vdots & & \ddots & \vdots \\ [0] & [0] & [0] & \dots & [M_n] \end{bmatrix}$$

$$[\hat{K}] = \begin{bmatrix} [K_1] & [0] & [0] & \dots & [0] \\ [0] & [K_2] & [0] & \dots & [0] \\ \vdots & \vdots & & \ddots & \vdots \\ [0] & [0] & [0] & \dots & [K_n] \end{bmatrix}$$

$$[\hat{C}] = \begin{bmatrix} [C_1] & [0] & [0] & \dots & [0] \\ [0] & [C_2] & [0] & \dots & [0] \\ \vdots & \vdots & & \ddots & \vdots \\ [0] & [0] & [0] & \dots & [C_n] \end{bmatrix}$$

$$\hat{f} = \begin{Bmatrix} \{f_1\} \\ \{f_2\} \\ \vdots \\ \{f_n\} \end{Bmatrix} \qquad \hat{x} = \begin{Bmatrix} \{x_1\} \\ \{x_2\} \\ \vdots \\ \{x_n\} \end{Bmatrix}$$

The total size of this system of equations is the sum of the size of each of the component equations.

Now, the modifications can be made by adding the ΔM, ΔK, or ΔC terms to the stacked matrices (39). This results in the following equation:

$$[\hat{M}+\Delta M]\{\ddot{\hat{x}}\} + [\hat{C}+\Delta C]\{\dot{\hat{x}}\} + [\hat{K}+\Delta K]\{\hat{x}\} = \{\hat{f}\} \tag{40}$$

This equation is transformed into modal coordinates as before:

$$[\underline{M}]\{\ddot{\hat{q}}\} + [\underline{C}]\{\dot{\hat{q}}\} + [\underline{K}]\{\hat{q}\} = [\hat{\Phi}_1]^T\{\hat{f}\} \tag{41}$$

where:

$$[\underline{M}] = [\hat{M}] + [\hat{\Phi}_1]^T[\Delta M][\hat{\Phi}_1]$$

$$[\underline{C}] = [\hat{C}] + [\hat{\Phi}_1]^T[\Delta C][\hat{\Phi}_1]$$

$$[\underline{K}] = [\hat{K}] + [\hat{\Phi}_1]^T[\Delta K][\hat{\Phi}_1]$$

$$\{\hat{x}\} = [\hat{\Phi}_1]\{\hat{q}\}$$

$$\left[\hat{\Phi}_1\right] = \begin{bmatrix} [\Phi_1] & [0] & [0] & \cdots & [0] \\ [0] & [\Phi_2] & [0] & \cdots & [0] \\ \cdot & \cdot & & \cdots & \cdot \\ \cdot & \cdot & & \cdots & \cdot \\ \cdot & \cdot & & \cdots & \cdot \\ [0] & [0] & [0] & \cdots & [\Phi_n] \end{bmatrix}$$

Assuming that the structure is proportionally damped, the equations of motion of the stacked matrices take the form of Equation (40). Therefore, the resultant dynamics depend only on the modal parameters of each structure plus the stiffness, damping, and mass of the connections.

The modal parameters of the two structures are combined by the coupling system transformed into modal space 12. The eigenvalues $\overline{\lambda}_r = \sigma_r + j\omega_r$ are computed from the determinant equation:

$$\det\left[[\underline{M}]s^2 + [\underline{C}]s + [\underline{K}]\right] = 0 \tag{42}$$

and the eigenvectors:

$$[\Phi_2] = [\Phi_1][\{\phi\}_1, \{\phi\}_2, \ldots, \{\phi\}_n]_{12}]$$

are found from:

$$\left[[\underline{M}]\overline{\lambda}_r^2 + [\underline{C}]\overline{\lambda}_r + [\underline{K}]\right]\{\overline{\phi}_{12}\}_r = 0 \qquad r = 1, \ldots, n \tag{43}$$

Once again, the addition of the connections $[\Delta K]$ is made using a tie vector approach, Once again, the addition of the connections $[\Delta K]$ is made using a tie vector approach,

$$[\Delta K] = [T] \lceil D_{\rfloor} [T]^T \qquad (44)$$

where the tie vector {t} designates the coordinates to be joined. Using the modal transformation $[\Phi]$ the new eigenvalue problem of the total modified system is formulated. The tie vector provides the connection or tie between the original modal space and the modified modal space. Once again, the characteristic equation is Equation (37) and the eigenvectors are the vectors associated with the nontrivial solution of the eigenvalue problem. Once they are obtained in the modified modal space 12 they are transformed into modal space 2 using Equation (38).

2.5 Complex Mode Eigenvalue Modification

Thus far, only real normal modes have been considered. This approximation is very accurate for most physically realizable structures. Some systems have heavier damping or exhibit nonproportional damping. In this limited case complex modes are needed to adequately describe the modal characteristics. Another situation may arise when complex modes are necessary. When investigating a modification that tends to make the damping nonproportional or increase the damping ratio, a real normal mode method will not accurately model the structure. Complex modes provide an exact solution but make the development and understanding of the technique more difficult.

For the nonproportional damped case the undamped normal modes do not uncouple the equations of motion. Frazer, Duncan, and Collar [17] proposed a method to reduce the nonproportional damped second order differential equation of motion:

$$[M]\{\ddot{x}\} + [C]\{\dot{x}\} + [K]\{x\} = \{f\} \qquad (45)$$

to a form that results in a 2N first order differential set of symmetric equations using an auxiliary vector {y(t)}. The resulting standard eigenvalue form is

$$-\begin{bmatrix} [M] & [0] \\ [0] & -[K] \end{bmatrix} \begin{Bmatrix} \{\dot{x}\} \\ \{x\} \end{Bmatrix} + \begin{bmatrix} [0] & [M] \\ [M] & [C] \end{bmatrix} \begin{Bmatrix} \{\ddot{x}\} \\ \{\dot{x}\} \end{Bmatrix} = \begin{Bmatrix} 0 \\ \{f\} \end{Bmatrix} \qquad (46)$$

or as:

$$-[U]\{y\} + [V]\{\dot{y}\} = \{f\} \qquad (47)$$

where:

$$[U]_{2m\times 2m} = \begin{bmatrix} [M] & [0] \\ [0] & -[K] \end{bmatrix} \qquad [V]_{2m\times 2m} = \begin{bmatrix} [0] & [M] \\ [M] & [C] \end{bmatrix}$$

$$\{y\}_{2m\times 1} = \begin{Bmatrix} \{\dot{x}\} \\ \{x\} \end{Bmatrix} \qquad \{\dot{y}\} = \begin{Bmatrix} \{\ddot{x}\} \\ \{\dot{x}\} \end{Bmatrix}$$

Now the transformation from physical coordinates y to modal coordinates q of rank 2m by 2N is:

$$\{y\}_{2m\times 1} = [\overline{\Psi}]_{2m\times 2N}\{q\} \tag{48}$$

The state vector velocity transformation is found by taking the derivative with respect to time:

$$\{\dot{y}\}_{2m\times 1} = [\overline{\Psi}]\lceil\Lambda\rfloor\{q\} \tag{49}$$

where:

$\lceil\Lambda\rfloor$ - The diagonal spectral matrix of rank 2N by 2N *of* the original complex eigenvalues λ_r

N - The number of degree of freedom in modal coordinates

m - The number of degree of freedom in physical coordinates

Applying the standard coordinate transformation to the homogeneous form of Equation (46)

$$[\overline{\Psi}]^T[U][\overline{\Psi}]\{q\} = [\overline{\Psi}]^T[V][\overline{\Psi}]\lceil\Lambda\rfloor\{q\} \tag{50}$$

Since original equations are symmetric and real, the right and left hand eigenvectors are equal.

Using the orthogonality conditions the equations become diagonal which is the advantage of the U and V formulation. U unity scaling method is used by letting Q_r = 1.0 to make Equation (50) valid :

$$[\overline{\Psi}]^T[U][\overline{\Psi}] = \lceil\Lambda\rfloor \tag{51}$$

$$[\overline{\Psi}]^T[V][\overline{\Psi}] = [I] \tag{52}$$

The modal matrix $[\Psi]$ may be partitioned with respect to the state vector defined in Equation (48) as:

$$[\overline{\Psi}] = \begin{bmatrix}[\Psi]\lceil\Lambda\rfloor \\ [\Psi]\end{bmatrix} \tag{53}$$

where $[\overline{\Psi}]$ is the modal matrix of rank (m by 2N) used to transform physical coordinates into modal coordinates for the complex case.

$$\{x\} = [\overline{\Psi}]\{q\} \tag{54}$$

Once again, since the necessary coordinate transformations exist, a structural modification or coupling of systems can be made using a local eigenvalue technique. Changes are represented as ΔM, ΔC and ΔK. The original modal space is modal space 1 and the modified modal space is modal space 2. Since the equations are reformulated into U and V matrices the appropriate ΔU and ΔV must be found.

Modifications in the original system of Equation (45) appear as:

$$\Big[[M]+[\Delta M]\Big]\{\ddot{x}\}+\Big[[C]+[\Delta C]\Big]\{\dot{x}\}+\Big[[K]+[\Delta K]\Big]\{x\}=\{f\} \tag{55}$$

Taking advantage of the transformation for the homogeneous solution:

$$[\overline{\Psi}_1]^T\Big[[U_1]+[\Delta U_{12}]\Big][\overline{\Psi}_1]\{q_1\} = [\overline{\Psi}_1]^T\Big[[V_1]+[\Delta V_{12}]\Big][\overline{\Psi}_1]\lceil\Lambda_1\rfloor\{q_1\} \tag{56}$$

where:

$$[\Delta U_{12}] = \begin{bmatrix}[\Delta M] & [0]\\ [0] & -[\Delta K]\end{bmatrix} \qquad [\Delta V_{12}] = \begin{bmatrix}[0] & [\Delta M]\\ [\Delta M] & -[\Delta C]\end{bmatrix}$$

The $[\Delta U_{12}]$ and $[\Delta V_{12}]$ matrices are the modifications that transform the system from modal space 1 to modal space 2. Utilizing Equations (50) through (54) on Equation (55) produces:

$$\Big[\lceil\Lambda_1\rfloor + [\overline{\Psi}_1]^T[\Delta U_{12}][\overline{\Psi}_1]\Big]\{q_1\} = \Big[[I] + [\overline{\Psi}_1]^T[\Delta V_{12}][\overline{\Psi}_1]\Big]\lceil\Lambda_1\rfloor\{q_1\} \tag{57}$$

This equation can be solved to produce the modified eigenvalues and eigenvectors in space 12 which maps space 1 into space 2. Therefore, a transformation exists:

$$\{q_1\} = [\Psi_{12}]\{q_2\}$$

where: $[\Psi_{12}]$ is the modal matrix of rank 2N by 2N found from Equation (56)

The eigenvectors are normalized to unity $[B_{12}]$ matrix and transformed into modified space 2 by:

$$[\overline{\Psi}_2] = [\overline{\Psi}_1][\Psi_{12}]$$

Thus, $[\overline{\Psi}_2]$ is the new modal matrix of the modified structure. It was obtained by projecting information into the new modal space which eliminates the need for a new eigenvalue solution.

2.6 Realistic Modal Modifications

Several researchers have developed techniques to make more realistic modifications. Rarely is a physical structural change realistically modeled as a local modification between two points. This has led to the development of truss and beam type modifications in local modification schemes. Another major problem in the prediction of realistic structural modifications is the lack of rotational degrees of freedom in a modal model. Yasuda and Brown [18], Martinez [19], O'Callahan and Lieu [20], and Smiley and Brinkman [21] have proposed various methods to measure or predict the rotational frequency response at a point.

The details of these techniques are beyond the scope of this investigation so they are not fully developed. Structural Measurement Systems [14] has proposed making a series of local eigenvalue modifications to approximate a realistic modification. For a rib element a three point technique is used to make three modifications locally to approximate a rib. This technique does not require rotational degrees of freedom.

O'Callahan and Chou [13] have proposed two techniques to make beam modifications. The first is a local eigenvalue modification technique that requires data for the rotational degrees of freedom through measurement or calculation at the modification points. A three dimensional symmetric beam stiffness element is approximated by making six individual modifications. This is accomplished by adding the axial, shear, and bending stiffness to each of the two connection points.

The second technique [16] is a general technique that introduces the concept of group eigenvalue modifications. Rather than using only a single tie vector to make the modification, a group of tie vectors is developed for the stiffness matrix to transform: normalized coordinates into the principal axes, principal bending axes into a centroidal set of coordinates, centroidal axes to a local reference through the centroid, local coordinates from the centroid to a geometric reference point, local bending axes at the reference point to a parallel set through the attachment, and local coordinates of the beam element into global coordinates.

Also, a global mass tie matrix is derived by using only the last three tie matrices mentioned above. Six spectral coefficients are needed to formulate the final matrix. Three are the translational mass, one the torsional inertia, and the last two are rotary inertia. The only remaining information needed to develop the stiffness tie matrix is the six spectral coefficients which define axial stiffness, torsional stiffness, shear about the two principal axes, and moments about the two principal axes. This formulation requires rotational information at the modification points. This formulation results in the general mass and stiffness matrices for an offset beam.

Elliot and Mitchell [22] have proposed an alternate technique to transfer the mass and stiffness matrix of a beam into a dynamic stiffness matrix. Therefore, the modal model is also formed using the dynamic stiffness.

$$\left[[K] - \omega^2 [M] \right] = \textit{Dynamic Stiffness Matrix} \tag{58}$$

The beam transfer matrix is more flexible than the previous method because a number of structural elements already exist in this form. This technique also transforms the elements in a group sense which makes it very efficient.

The need for more realistic modifications has led to research in the area of beam modifications using modal modeling techniques. The main drawback to these techniques is that rotational degrees of freedom are required to properly formulate the beam dynamic matrix. Currently, several techniques are being researched to provide the necessary rotational information experimentally. Until a technique becomes commercially available, beam modifications will not be a useful tool in modal modeling.

2.7 Normalization of Measured Complex Modes

2.7.1 Introduction and Background

Experimental modal analysis is carried out to extract a set of modal parameters from the measured time or frequency domain data of the structure under test. The identified eigenvectors are in general complex modes due to several possible reasons:

1. The damping is nonproportional, i.e., [C] matrix is not proportional to [K] and [M] matrices.
2. Measurement errors due to mass loading effects, noise, nonlinearities etc.
3. Digital processing errors due to finite frequency resolution, leakages, high modal density, and frequency response functions estimation procedure (H_1, H_2, H_v).
4. Modal parameter estimation errors due to invalid estimation of number of degrees of freedom.

The identified complex modes can be used directly in the applications of modal modeling, structural dynamic modifications ,sensitivity analysis, and validation and optimization of an analytical model. On the other hand, real normal modes are sometimes more desirable in those applications due to the facts that (i) normal modes are numerically easier to handle than complex modes and (ii) analysts usually compute normal modes rather complex modes in the finite element analysis. Therefore, if the normal modes are desired, a real-normalization procedure is needed to be implemented. Some of the proposed normalization methods are summarized in the following.

2.7.2 Normalization Using Direct Parameter Estimation Technique

The Direct Parameter Estimation technique [23] is a multi-degree-of-freedom frequency domain parameter estimation algorithm. This technique manipulates multiple response functions from a single reference location to obtain global least-square estimates of the modal properties.

Consider the equation of motion in the frequency domain,

$$-\omega_i^2[M]\{X_i\} + j\omega_i[C]\{X_i\} + [K]\{X_i\} = \{F_i\} \tag{59}$$

where:

ω_i = frequency i
$[M]$ = $N_p \times N_p$ mass matrix
$[C]$ = $N_p \times N_p$ viscous damping matrix
$[K]$ = $N_p \times N_p$ stiffness matrix
$\{X_i\}$ = vector of N_p responses at frequency i
$\{F_i\}$ = vector of N_p forces at frequency i
N_p = number of physical degrees of freedom

For the single reference case, the force vector would be made up of all zeroes except at the reference location. Premultiplying Equation (59) by the inverse of the mass matrix,

$$-\omega_i^2\{X_i\} + j\omega_i[\alpha]\{X_i\} + [\beta]\{X_i\} = \{-\nu\} \tag{60}$$

where:

$$[\alpha] = [M]^{-1}[C]$$
$$[\beta] = [M]^{-1}[K]$$
$$\{\nu\} = -[M]^{-1}\{F\}$$

Reordering Equation (60):

$$j\omega_i[\alpha]\{X_i\} + [\beta]\{X_i\} + \{\nu\} = \omega_i^2\{X_i\} \tag{61}$$

Dropping vector and matrix notation for simplicity:

$$\begin{bmatrix}\alpha & \beta & \nu\end{bmatrix} \begin{Bmatrix} j\omega_i X_i \\ X_i \\ 1 \end{Bmatrix} = \omega_i^2 X_i \tag{62}$$

Let

$$D_i = \begin{Bmatrix} j\omega_i X_i \\ X_i \\ 1 \end{Bmatrix} \qquad and \qquad E_i = \omega_i^2 X_i \tag{63}$$

Consider k spectral lines at $\omega = \omega_1, \omega_2, \ldots, \omega_k$,

$$[\,\alpha\ \beta\ \nu\,]\ [D_1\,|\,D_2\,|\,\ldots\,|\,D_k] = [E_1\,|\,E_2\,|\,\ldots\,|\,E_k] \tag{64}$$

Equation (64) can be solved using a least square technique. The system matrices α and β can be used to solve for the eigenvalues and eigenvectors of the system using a companion matrix approach.

The companion matrix for the general case of nonproportional damping:

$$\begin{bmatrix} -\alpha & -\beta \\ I & 0 \end{bmatrix}$$

where [I] is the identify matrix.

Since the α matrix contains all the damping information, and the β matrix contains the mass and stiffness information, the companion matrix can also be defined to solve for the undamped natural frequencies and a set of normal modal vectors of the system. For this case, the α matrix is neglected and the resulting companion matrix is shown below:

$$\begin{bmatrix} 0 & -\beta \\ I & 0 \end{bmatrix}$$

An estimate of the proportional damping can be obtained using the left and right eigenvectors, resulting from this solution, to diagonalize the damping matrix. Using the diagonal elements and the natural frequency of the system, the estimates of proportional damping can be obtained.

Principal Response Analysis [24] is applied to improve the numerical efficiency of the algorithm by allowing a large number of response functions to be used in the analysis.

2.7.3 Ibrahim's Time Domain Technique

S.R. Ibrahim indicated [25,26] that large errors may result from simplified normal mode approximations to complex modes.

$$\psi_i = R_i + jI_i \tag{65}$$

where:

ψ_i = i^{th} element of a complex modal vector
R_i = real part of ψ_i
I_i = imaginary part of ψ_i

The approximated normal mode element ϕ_i corresponding to ψ_i is:

$$\phi_i = \pm\sqrt{R_i^2 + I_i^2} \tag{66}$$

where:

ϕ_i = ith element of the normal modal vector

The ± sign in Equation (66) is determined by the phase angle of the the complex modal coefficient ψ_i. For example, if a normal modal vector has zero phase angle, then ϕ_i has "+" sign if the phase angle of the complex ψ_i is between $\pm 90^0$.

A time domain technique has been proposed to compute a set of normal modes from the identified complex modes. The required data are a set of modal parameters such as may be identified from a modal survey test. These modal parameters are namely a set of complex modes $\{\psi\}_r$, r=1,....,N and a set of corresponding roots λ_r, r=1,....,N(and their complex conjugates). The modal vectors have N_p elements where $N_p >> N$. To compute the normal modes, two approaches were suggested in the following way:

2.7.3.1 Approach 1: Using an Oversized Mathematical Model

From the given modal parameters, displacement, velocity, and acceleration responses are formed according to the equations,

$$\{x(t)\} = \sum_{r=1}^{2N}\{\psi\}_r e^{\lambda_r t} + \{n_1(t)\} \tag{67}$$

$$\{\dot{x}(t)\} = \sum_{r=1}^{2N} \lambda_r \{\psi\}_r e^{\lambda_r t} + \{n_2(t)\} \tag{68}$$

$$\{\ddot{x}(t)\} = \sum_{r=1}^{2N} \lambda_r^2 \{\psi\}_r e^{\lambda_r t} + \{n_3(t)\} \tag{69}$$

where $n_1(t), n_2(t), n_3(t)$ are added random noise of uniform distribution. These responses are then used in the state vector equation,

$$\begin{Bmatrix} \dot{x}(t) \\ \ddot{x}(t) \end{Bmatrix} = \begin{bmatrix} [0] & [I] \\ -[[M]^{-1}[K]] & -[[M]^{-1}[C]] \end{bmatrix} \begin{Bmatrix} x(t) \\ \dot{x}(t) \end{Bmatrix} \tag{70}$$

or

$$\{y\} = [E]\{\dot{y}\} \tag{71}$$

where $\{y\}$ is now system's state vector containing the displacements and velocity responses. By repeating Equation (71) $2N_p$ time instants, the following equation is satisfied:

$$[\dot{y}] = [E][y] \tag{72}$$

where $[y]$ and $[\dot{y}]$ contain responses measured at the $2N_p$ time instants. From Equation (72) the [E] matrix can be identified as,

$$[E] = [\dot{y}][y]^{-1} \tag{73}$$

By computing matrix [E], the $[M]^{-1}[K]$ matrix gives normal modes according to the eigenvalue equation,

$$\left[[M]^{-1}[K]\right] \{\phi\} = \omega^2 \{\phi\} \tag{74}$$

Naturally, without any noise, the matrix $[y]$ is singular since the number of degrees of freedom is larger than the number of modes present in the responses. A small amount of noise makes the inversion of [y] possible for the purpose of extracting modal information. The mechanism on which the success of this approach is based is explained in Reference [26].

2.7.3.2 Approach 2: Using Assumed Modes

The given set of complex modal parameters satisfy the equation

$$\left[[M]^{-1}[K]\ \ [M]^{-1}[C]\right]\begin{Bmatrix}\psi_r\\ \lambda_r\psi_r\end{Bmatrix}=\{-\lambda_r^2\psi_r\}\qquad (r=1,\ldots,N) \tag{75}$$

Since there are only N modes and the system has N_p degrees of freedom, Equation (75) cannot be solved for $\left[[M]^{-1}[K]\ \ [M]^{-1}[C]\right]$. Let us assume that there exists a set of vectors Y_k and a set of characteristic roots s_k, k= N+1, N+2,...., N_p. This set of assumed parameters are selected such that

$$\lambda_r \neq s_k$$

$$Y_k \neq [\psi_1\ \psi_2\ \ldots.\ \psi_N]\{a\}$$

where $\{a\}$ is any vector of coefficients. This implies that Y_k and $\{\psi\}_r$ for all r and k from a linearly independent set of vectors. In such case, it can be written that

$$\left[[M]^{-1}[K]\ \ [M]^{-1}[C]\right]\begin{Bmatrix}Y_k\\ s_kY_k\end{Bmatrix}=\{-s_k^2Y_k\}\qquad (k=N+1,N+2,\ldots,N_p) \tag{76}$$

and Equations (75) and (76) can be solved for $\left[[M]^{-1}[K]\ \ [M]^{-1}[C]\right]$ from which normal modes are computed according to Equation (74).

2.7.4 Frequency Domain Normalization Technique using orthogonality constraints

Zhang and Lallement [27] proposed a numerical method to determine the real eigenvalues and eigenvectors of the associated undamped structure from the identified complex eigensolutions.

2.7.4.1 Recall of General Relations

Under autonomous conditions, the dynamic behavior of a mechanical system is assumed to be represented by a second order linear differential equation,

$$[M]\{\ddot{x}(t)\}+[C]\{\dot{x}(t)\}+[K]\{x(t)\}=0 \tag{77}$$

where [M],[C],[K] are $N_p \times N_p$ positive definite real matrices.

The solution of Equation (77) is of the form: $\{x(t)\}=\{X\}e^{\lambda t}$. This leads to the eigenvalue problem,

$$\left[\lambda^2[M]+\lambda[C]+[K]\right]\{\psi\}=0 \tag{78}$$

Assuming the case of nonproportional damping, the $2N_p$ eigensolutions (λ_r, $\{\psi\}_r$) are then found by conjugate pairs. Introducing the spectral matrix $\lceil\Lambda\rfloor$ and the modal matrix $[\Psi]$ defined by

$$\lceil \Lambda \rfloor_{2N_p \times 2N_p} = \begin{bmatrix} \lceil \Lambda \rfloor_{N_p \times N_p} & \\ & \lceil \Lambda^* \rfloor_{N_p \times N_p} \end{bmatrix} \tag{79}$$

and

$$[\Psi]_{N_p \times 2N_p} = \left[[\Psi]_{N_p \times N_p} \,|\, [\Psi^*]_{N_p \times N_p} \right] \tag{80}$$

the first N_p relations of Equation (78) are collected in the form:

$$[M][\Psi]_{N_p \times N_p} \lceil \lambda^2 \rfloor + [C][\Psi]_{N_p \times N_p} \lceil \lambda \rfloor + [K][\Psi]_{N_p \times N_p} = 0 \tag{81}$$

The transformation of Equation (77) into the space of state variable y(t) gives:

$$[U]\{\dot{y}(t)\} = [V]\{y(t)\} \tag{82}$$

where:

$$[U] = \begin{bmatrix} [C] & [M] \\ [M] & [0] \end{bmatrix} \quad [V] = \begin{bmatrix} -[K] & [0] \\ [0] & [M] \end{bmatrix} \quad \{y(t)\} = \begin{Bmatrix} x(t) \\ \dot{x}(t) \end{Bmatrix} \tag{83}$$

The solutions of Equation (82) are also of the form: $\{y(t)\} = \{y\} e^{\lambda t}$. This leads to the eigenvalue problem:

$$\left[[V] - \lambda [U] \right] \{y\} = 0. \tag{84}$$

Introducing the modal matrix $[Y]_{N_p \times N_p}$, where [Y] == [....,$\{y\}_r$,....], and it can be shown directly that [Y] is of the form:

$$[Y] = \begin{bmatrix} [\Psi] & [\Psi^*] \\ [\lambda \Psi] & [\lambda^* \Psi^*] \end{bmatrix} \quad \text{and} \quad \{y\}_r = \begin{Bmatrix} \psi_r \\ \lambda_r \psi_r \end{Bmatrix} \tag{85}$$

and that the matrices [U], [V], $\lceil \Lambda \rfloor$ and [Y] satisfy the orthogonality relations:

$$[Y]^T[U][Y] = \lceil R \rfloor; \quad [Y]^T[V][Y] = \lceil R \rfloor \lceil \Lambda \rfloor \tag{86}$$

where $\lceil R \rfloor_{2N_p \times 2N_p} = diagonal\{r_r\} = \begin{bmatrix} \lceil R \rfloor_{N_p \times N_p} & \\ & \lceil R^* \rfloor_{N_p \times N_p} \end{bmatrix}$, and r_r characterizes the norm chosen for the eigenvector $\{y\}_r$.

Considering the partition into submatrices of [V],[Y], $\lceil R \rfloor$, and $\lceil \Lambda \rfloor$, the two following equations are directly deduced from Equation (86):

$$\lceil \Lambda \rfloor [\Psi]^T [M][\Psi] \lceil \Lambda \rfloor - [\Psi]^T[K][\Psi] = \lceil R \rfloor \lceil \Lambda \rfloor \quad (N_p \times N_p) \tag{87}$$

$$\lceil \Lambda^* \rfloor [\Psi^*]^T [M][\Psi] \lceil \Lambda \rfloor - [\Psi]^T[K][\Psi] = 0 \quad (N_p \times N_p) \tag{88}$$

The conservative system associated with Equation (77) is finally characterized by:

$$[M]\{\ddot{x}(t)\} + [K]\{x(t)\} = 0 \tag{89}$$

It is known that its solutions of the following form: $\{x(t)\} = \{X\}e^{\pm j\omega t}$, yield the eigenvalue problem:

$$\Big[[K] - \Omega^2[M]\Big] \{\phi\} = 0 \tag{90}$$

Collecting these m eigenvalues $(\Omega_r, \{\psi\}_r)$ in the spectral matrix $\lceil \Omega_r \rfloor = diagonal\{\Omega_r\}$, and in the modal matrix $[\Phi] = \Big[\dots, \{\phi\}_r, \dots \Big]$, these matrices satisfy the orthonormality relations:

$$[\Phi]^T[M][\Phi] = [I] \;;\; [\Phi]^T[K][\Phi] = \lceil \Omega_r \rfloor \tag{91}$$

2.7.4.2 Data and Hypothesis

The problem considered here has the following assumptions:

1. The matrices [M],[C],[K] are unknown.

2. From dynamic tests carried out on the structure, N ($N << N_p$) eigensolutions are identified by means of N_m ($N \leq N_m \leq N_p$) measurement points located on the structure. These N eigensolutions are characterized by the spectral submatrix: $\lceil \Lambda \rfloor_{N \times N} = diagonal\{\lambda_r\}$, and the modal matrix: $[\Psi]_{N_m \times N}$.

3. $\lceil \Omega_r \rfloor_{N \times N}, [\Phi]_{N_m \times N}$, corresponding submatrices of the associated conservative system, are to be determined from $\lceil \Lambda \rfloor, [\Psi]$.

The hypotheses to solve the unknowns are described as follows:

Hypothesis 1: It is assumed that the identified eigenvectors can be represented by a linear combination of the corresponding normal eigenvectors of the associated conservative systems:

$$[\Psi] = [\Phi][\Gamma], \quad \textit{where:} \quad [\Gamma] \textit{ is a complex } N{\times}N \textit{ matrix} \tag{92}$$

Let:

$$[\Psi] = [\Psi]_{re} + j[\Psi]_{im} \quad (N_m{\times}N) \quad \textit{where: } re = \textit{real part}, \; im = \textit{imaginary part}$$

$$[\Gamma] = [\Gamma]_{re} + j[\Gamma]_{im} \quad (N{\times}N) \tag{93}$$

$$\lceil \Lambda \rfloor = \lceil \Lambda \rfloor_{re} + j\lceil \Lambda \rfloor_{im} \quad (N{\times}N)$$

Hypothesis 2: The matrices $[\Psi]$ and $[\Phi]$ are assumed to have rank N. Therefore, matrix $[\Gamma]$ is nonsingular. The matrix $[\Gamma]_{re}$ is also assumed to be nonsingular.

Hypothesis 1 leads to the following relationship:

$$[\Psi] = [\Psi]_{re}\,[\Gamma]_{re}^{-1} \tag{94a}$$

$$[\Gamma]_{im} = [\Gamma]_{re}\,[W] \qquad \textit{where: } [W] \textit{ is a real } N{\times}N \textit{ matrix.} \tag{94b}$$

The combination of Equations (92) and (94b) yields:

$$[\Psi]_{im} = [\Psi]_{re}\,[W] \tag{95}$$

The best estimation of [W], by means of the least squares method, is then

$$[W] = \left[[\Psi]_{re}^T [\Psi]_{re} \right]^{-1} [\Psi]_{re}^T [\Psi]_{im} \tag{96}$$

According to Hypotheses 1 and Equation (94b), it can be then written:

$$[\Psi] = [\Phi] [\Gamma]_{re} \left[[I]_{N_p \times N_p} + j[W] \right] \tag{97}$$

$$[\Phi] = [\Psi]_{re} [\Gamma]_{re}^{-1} \tag{98a}$$

The matrix $[\Psi]_{re}$ being known, the problem is now to determine the matrix $[\Gamma]_{re}^{-1}$ first, then the matrix $^{\lceil}\Omega_{r\rfloor}$.

The solution procedure, therefore, is briefly described as follows:

– By substituting Equation (92) and (97) into Equation (87) and (88), and then separating the real and imaginary parts, expressions of the symmetrical matrices $[\Gamma]_{re}^T [\Gamma]_{re}$ and $[\Gamma]_{re}^T \, ^{\lceil}\Omega_{r\rfloor} [\Gamma]_{re}$ can be derived. These matrices can be expressed as functions of matrices $[\Psi]$, $^{\lceil}\Lambda_{\rfloor}$ and [W].

– Calculate matrices $[\Gamma]_{re}^T [\Gamma]_{re}$ and $[\Gamma]_{re}^T \, ^{\lceil}\Omega_{r\rfloor} [\Gamma]_{re}$.

– Matrices $[\Gamma]_{re}$ and $^{\lceil}\Omega_{r\rfloor}$ are determined by solving the following eigenvalue problems:

$$[[B_1] - \lambda_r [B_2]]\{\nu_r\} = 0, \qquad \{\nu_r\}^T[B_2]\{\nu_r\} = 1, \qquad r = 1, \cdots, N \tag{98b}$$

where $[B_1] = [\Gamma]_{re}^T \, ^{\lceil}\Omega_{r\rfloor} [\Gamma]_{re}$ and $[B_2] = [\Gamma]_{re}^T [\Gamma]_{re}$.

and

$$^{\lceil}\Omega_{r\rfloor} = diagonal\{\lambda_r\}, \qquad \text{and} \qquad [V] = [\cdots\{\nu_r\}\cdots] = [\Gamma]_{re}^{-1} \tag{98c}$$

2.7.5 Normalization Using Improved Computational Model

Natke and Rotert [28] proposed to obtain a set of normal modes by improving an existing computational model using measured eigenquantities (incomplete and erroneous) in a subsystem formulation. This improved computational model is then used to compute the eigenquantities of the associated undamped system. Since this method assumes the use of a analytical or finite element model, detailed discussion of this technique will not be presented here.

2.7.6 Time Domain Technique using Principal Response Analysis

A time-domain technique is presented to compute a set of normal modes from the measured complex modes. The number of degrees of freedom which is equal to the number of measurements, in general, is much larger than the number of measured modes. By using the proposed method , a large number of physical coordinates are reduced to a smaller number of principal coordinates using principal response analysis technique. From the given modal parameters, free decay responses are calculated using properly scaled complex modal vectors. The companion matrix for the general case of nonproportional damping is also derived in the principal coordinates. Normal modes are obtained through eigenvalue solutions of the $[M]^{-1}[K]$ and transformed back to the physical coordinates to get a set of normalized real modes. A numerical example is presented to support the outlined theory.

2.7.6.1 Theory and Formulation: computation of normal modes

Assume there exists a set of measured modal parameters from a modal test. These modal parameters consists of N complex modes(and their complex conjugates), λ_r, r=1,....,N and $\{\psi\}_r$, r=1,....,N. Each modal vector has dimensions N_m and in general $N_m >> N$. To compute a set of normal modes from the given complex modes, a time-domain approach is formulated as follows:

Free decay displacement, velocity and acceleration responses can be expressed as:

$$\{x(t)\} = \sum_{r=1}^{2N} \{\psi\}_r e^{\lambda_r t} \tag{99}$$

$$\{\dot{x}(t)\} = \sum_{r=1}^{2N} \lambda_r \{\psi\}_r e^{\lambda_r t} \tag{100}$$

$$\{\ddot{x}(t)\} = \sum_{r=1}^{2N} \lambda_r^2 \{\psi\}_r e^{\lambda_r t} \tag{101}$$

The equations of motion for the general case of nonproportional damping is:

$$\begin{bmatrix} [C] & [M] \\ [M] & [0] \end{bmatrix} \begin{Bmatrix} \dot{x}(t) \\ \ddot{x}(t) \end{Bmatrix} + \begin{bmatrix} [K] & [0] \\ [0] & -[M] \end{bmatrix} \begin{Bmatrix} x(t) \\ \dot{x}(t) \end{Bmatrix} = \begin{Bmatrix} \{f\} \\ \{0\} \end{Bmatrix} \tag{102}$$

Another form of the homogeneous Equation (102) can be written as:

$$\begin{Bmatrix} \dot{x}(t) \\ \ddot{x}(t) \end{Bmatrix} = \begin{bmatrix} [0] & [I] \\ -[M]^{-1}[K] & -[M]^{-1}[C] \end{bmatrix} \begin{Bmatrix} x(t) \\ \dot{x}(t) \end{Bmatrix} \tag{103}$$

or

$$\{\dot{y}(t)\} = [E]\{y(t)\} \tag{104}$$

where {y(t)} is now the system's state vector containing the displacement and velocity responses. In the physical coordinates, dropping vector notation, Equation (104) can also be written as:

$$[\dot{y}(t_1), \ldots, \dot{y}(t_{2N_m})] = [E]\,[y(t_1), \ldots, y(t_{2N_m})] \tag{105}$$

Therefore, [E] matrix can be computed as:

$$[E] = [\dot{y}]\,[y]^{-1} \tag{106}$$

where [E], [y] and $[\dot{y}]$ are all $2N_m \times 2N_m$ matrices.

By computing the matrix [E], $[M]^{-1}[K]$ matrix gives the normal modes according to the eigenvalue solution:

$$\left[[M]^{-1}[K]\right][\Phi] = \omega^2\,[\Phi] \tag{107}$$

The matrix [y] is always singular due to the number of degrees of freedom N_m is larger than the number of measured modes N. Therefore, it is numerically difficult and unstable to solve [E] matrix in the physical coordinates. Therefore, it is proposed to compute the companion matrix [E] in the principal coordinates in the following way:

Define $[\hat{\Phi}]$ = modulus matrix of complex modal vector matrix $[\Psi]$, i.e., $[\hat{\Phi}]$ is real modal vector approximation according to Equations (65) and (66), and

$$[\Psi] = [\hat{\Phi}]\,[W] \tag{108}$$

where [W] is a $N \times N$ complex matrix and can be obtained through pseudo inverse technique.

Using singular value decomposition technique and assume $[\hat{\Phi}]$ has full rank N (which is true if an independent set of modal vectors is used), $[\hat{\Phi}]$ can be decomposed as:

$$[\hat{\Phi}] = [P]\,\lceil\Sigma\rfloor\,[S]^T \tag{109}$$

where:

$[P]$ = orthonormal matrix $(N_m \times N)$
$\lceil\Sigma\rfloor$ = diagonal matrix consists of eigenvalues of $[\hat{\Phi}]^T[\hat{\Phi}]$ $(N \times N)$
$[S]$ = unitary matrix consists of eigenvectors of $[\hat{\Phi}]^T[\hat{\Phi}]$ $(N \times N)$

By using matrix [P] as the transformation matrix, physical coordinates can be transformed to principal coordinates as follows:

$$\{p(t)\} = [P]^T \{x(t)\} \tag{110}$$

substitute Equations (99) and (108) into (110), we get

$$\begin{aligned}\{p(t)\} &= [P]^T [\Psi] \lceil e^{\lambda t} \rfloor \\ &= [P]^T [\hat{\Phi}] [W] \lceil e^{\lambda t} \rfloor \\ &= [P]^T [P] \lceil \Sigma \rfloor [S]^T [W] \lceil e^{\lambda t} \rfloor \\ &= \lceil \Sigma \rfloor [S]^T [W] \lceil e^{\lambda t} \rfloor\end{aligned} \tag{111}$$

Similarly,

$$\{\dot{p}(t)\} = [P]^T [\Psi] \lceil \lambda e^{\lambda t} \rfloor \tag{112}$$

$$\{\ddot{p}(t)\} = [P]^T [\Psi] \lceil \lambda^2 e^{\lambda t} \rfloor \tag{113}$$

Therefore, free decay displacement, velocity and acceleration responses can be evaluated using Equations (111) through (113) in the principal coordinates. Once $\{q(t)\}$ and $\{\dot{q}(t)\}$ are computed at 2N time points , companion matrix [E] (2N by 2N) can be computed in the principal coordinates accordingly as:

$$[E] = [\dot{q}][q]^{-1} \tag{114}$$

where: $\{q(t)\} = \begin{Bmatrix} p(t) \\ \dot{p}(t) \end{Bmatrix}, \quad \{\dot{q}(t)\} = \begin{Bmatrix} \dot{p}(t) \\ \ddot{p}(t) \end{Bmatrix}$

Since [q] is a full rank matrix, it is always invertible and the computation is numerically stable and accurate.

Based on the result of matrix [E], the N by N $[M]^{-1}[K]$ matrix gives the normal mode solutions $[\underline{\Phi}]$ in the principal coordinates according to Equation (106).

A set of normal modes,[Φ] in the physical coordinates can be obtained through the coordinate transformation:

$$[\Phi] = [P][\underline{\Phi}] \tag{115}$$

2.7.6.2 Discussion and Conclusion

From the numerical example of a nonproportionally damped discrete system described later in Section 6.2, it indicates that a set of real-normalized modal vectors can be obtained using this proposed method. Nevertheless, unless a complete set of complex modal vectors are included in the analysis, analysis results are subject to modal truncation errors to certain extent.

Finite element modes can be added to the measured modal data set outside the measurement band to improve the analysis results. The analysis modes can be real normal modes with proportional damping or complex modes with nonproportional damping.

For a very lightly damped system the magnitude of the $M^{-1}C$ matrix is in general, much smaller than the magnitude of the $M^{-1}K$ matrix. Based on past experiences, the real-normalized modal vectors will be similar to those normal modes by taking the magnitudes of the complex modes.

The true free decay responses of a system are dependent on the initial conditions of the structure, but the modal properties of a system are independent of the initial conditions. With the proposed method, it is recommended that all modal vectors included in the analysis band be scaled to the same order of magnitude before computing the free decay responses according to Equations (99) to (101). And by doing so, the diagonal matrix $\lceil \Sigma \rfloor$ in Equation (109) will always have rank N and make the coordinate transformation feasible in the application of principal response analysis.

2.8 Errors in the Experimental Model

Since the structural dynamic modification method uses the modal parameters of the unmodified structure to predict the effects of the modification , it is apparent that the accuracy of the results is dependent on the validity of the data base supplied. For this reason, it is important that all errors associated with the data acquisition and processing of the unmodified structure are minimized.

Among the sources of error that must be addressed are nonlinearity, standard FFT errors (aliasing and leakage), scaling errors, as well as truncation errors of the modal model itself. Only the most serious of these errors will be addressed at this time.

One of the assumptions in the experimental modal analysis is linearity of the system. Therefore, all methods discussed here are based on this assumption. In reality, inaccurate results will arise when linear system coupling algorithm is used to predict the dynamic characteristics of structure(s) coupled together by nonlinear joints.

Leakage is a measurement error that arises from the processing of signals that are not periodic in the time window of the signal analyzer. Because of this truncation in the time domain, the Fourier coefficients of the sampled signal do not lie on the Δf of the analyzer. This causes energy at a specific frequency to spread out into adjacent frequency bands, and results in an amplitude distortion at the actual frequency. It is this amplitude error that causes scaling errors in the modal mass and stiffness estimates associated with each mode. This in turn affects the modification process by scaling the predicted modes of the modified structure by an amount that is proportional to the amplitude error of the original data.

This leakage problem can be reduced by: (1) using periodic excitation, or transient excitation signals such as burst random, or, (2) using the H_v frequency response function procedure, or, (3) using cyclic averaging technique in the measurement stage, or, (4) taking data with smaller Δf, or, (5) using windows on the time domain measurement, such as, impact with exponential window applied to the response signals. If exponential window is used, it must be accounted for in the parameter estimati on because it adds artificial damping to the structure. Care must be taken not to overcompensate for this damping allowing the poles of the system to become negatively damped.

Modification errors often arise from using a modal data base that is not properly scaled relative to the system of units used by the modeling software. This type of error will occur if the modal parameters are estimated using frequency response functions which were measured using improper transducer calibrations. This improper scaling once again results in improper estimates of modal mass and stiffness used by the modeling software.

Up to this point, it has been shown that the accuracy of the results is dependent on the amount of error in the data base. Another concern that needs to be addressed is the validity of the modal model. Because the effects of a structural modification are calculated in modal space, if an insufficient number of modes are included in the original data base, there will be a limit to the number of modal vectors that can be predicted. This phenomena is known as modal truncation and should be considered in choosing a frequency range for the analysis. It may be desirable in some cases to extend the frequency range of data acquisition above the actual frequency range of interest for the data base to include a few extra modes. This extended frequency range will improve the calculation of out of band residuals, and may help for the case where these out of band modes are shifted into the frequency range of interest by the modification. Care must be taken in extending the frequency range, to prevent an excessive loss of frequency resolution.

Another concern in the development of the modal model is the number of degrees of freedom to include in the analysis. By definition, the number of degrees of freedom must be equal to or greater than the number of modes in the frequency range of interest. Realistically, the number of DOF should be much larger than the number of modes of interest to accurately define the individual modal vectors. Since modal coefficients exist only at points where data has been taken, it is possible to miss nodal lines of the structure if too few points are included in the analysis. This generally becomes a more significant problem for higher order mode shapes.

Once the original data base has been established, the modal parameters can be estimated using any of several existing parameter estimation algorithms. All of these algorithms attempt to yield a best estimate of the actual parameters. Because there will always be some degree of experimental error in the data, the resulting estimates of modal parameters will be subject to error. In order to minimize this error, it is advantageous to use some sort of least squares implementation to yield a best estimate of modal parameters.

The use of SDOF versus MDOF parameter estimation algorithms is determined by the modal density of the structure being analyzed. If a SDOF method is used for a structure with closely coupled modes, poor estimates of modal mass and stiffness are obtained, and the modification routine will yield poor results.

The various errors mentioned in the previous paragraphs are commonly committed, and easily overlooked when performing a modal test. This is not intended to be an exhaustive list of errors affecting modal modeling, but an indication of the types of things that must be kept in mind when establishing a valid modal data base. Without good estimates of the original structures modal parameters, there can be no serious attempt at accurately predicting the characteristics of the modified structure.

2.9 Validation of Experimental Modal Model

As mentioned in the previous section, the accuracy of the modal modeling or structural modification results is dependent on the validity of the modal model supplied. There will always be some degrees of experimental and modal parameter estimation errors in the data base. Therefore, it is important for the users to qualitatively, and if possible, quantitatively, examine the validity and errors of the modal model before it is used to predict the system modeling or modification results. Although perfect results should not be desired in the application of modal modeling technique, it is important to realize that any modal model obtained experimentally is far from being perfect. Therefore, it is suggested that the experimental modal model be validated, or optimized , before the model is input to any modal modeling algorithm. In this section, some of the validation methods are briefly summarized as follows:

2.9.1 Frequency Response Function Synthesis

Synthesizing a frequency response function (not used in the estimation of modal parameters) using extracted modal parameters and compared with a measured frequency response function at the synthesized measurement degree of freedom is, in general, a common practice during the modal parameter estimation process. If a good match exists between these two sets of frequency response functions, then it is a good indication that the extracted modal parameters are agreeable with the measurement data. But this doe s not guarantee that there is no error exist in the modal data base.

2.9.2 MAC

Modal Assurance Criteria (MAC) [29] is commonly used to check the consistency of the extracted modal parameters, when more than one estimate of each mode is available.

2.9.3 Detection of Mode Overcomplexity

This method qualifies each mode by a number called the Mode Overcomplexity Value (M.O.V.) and the global Modal Model by the Mode Overcomplexity Ratio (M.O.R.) [30]. The basic idea of the Mode Overcomplexity test is that, for good modal models with complex modes, the frequency sensitivity for an added mass change should be negative. If it happens that the sensitivity is positive, it is caused by either an incorrect scale factor (modal mass) or by the fact that the phase angle of the complex modes compared to the normal mode phase angle exceeds a certain limit; in other words, it is due to an overcomplexity of the mode shape.

The MOV is defined as the ratio of the number of positive frequency sensitivities over the number of all the frequency sensitivities for a particular mode. To give more weight to points with a high modal displacement compared to points with a small modal displacement, a weighted sum is introduced to give a more general evaluation of the modal model. The value of MOV is between 1 and 0, the bigger the value is, the modal model is more overcomplex.

The MOR is defined as the ratio of $\sum_{i=1}^{m} MOV_i$ over ($1 - \sum_{i=1}^{m} MOV_i$) which gives a one figure assessment of the modal model with respect to its overcomplexity. The MOR ranges from zero to infinity. A low MOR value indicates good modal data, while a large MOR indicates a scale factor problem or a overcomplexity problem.

2.9.4 Mass Additive/Removal technique

This technique employs a mass additive or removal procedure to verify or validate experimental modal model in the application of modal modeling technique. Modal model can be obtained from either the original structure, or, mass-loaded structure [2]. If modal model is obtained from the original structural configuration, then, comparisons can be made between the analytically predicted dynamic characteristics of the mass-loaded structure from the modal modeling algorithm, and the test results (such as modified resonant frequencies) obtained from the physically modified mass-loaded structure. If there is no good agreement between these two sets of results for the mass-loaded structure, then this is an indication that global or local scaling errors, or overcomplexity of some measured complex modes, existing in the experimental modal model. If high quality data are desired in predicting the system dynamics of the altered structure or combined structure(s), then the previously determined experimental modal model needs to be validated, if possible, or, a new set of data needs to be recollected before any modeling application is attempted.

For the second case, i.e., if modal model is obtained from the physically mass-loaded structure, then comparisons can be made between the analytically predicted and experimentally measured dynamic characteristics of the mass-removed structure. Similarly, if there is no good agreement between these two sets of data, this indicates some errors existing in the original modal model. In Reference [2], using approximated real modes from the measured complex modes, a modal scaling procedure can be used to correct the global scaling errors in the experimental modal model.

The number of masses and the size/weight of each additive mass, can be added to the structure is dependent on the total mass and size of the structure(s). In general, the following rules can be used as guidelines in considering the number and size(s) of the additive mass(es):

- The added mass(es) can be considered rigid in the frequency range of interest.
- With small amount of mass(es) added or removed to or from the structure, the mode shapes can be considered unchanged before and after the modification.
- Sensitivity of the change of system dynamics is dependent on the location(s) of the added mass(es). In other words, if there is only one mass added to a large structure, then some of the modes may not be sensitive enough to alter their frequencies due to the fact that the added single mass is near the nodal points of such modes.
- Rotational degrees freedom, if permitted, can be extracted from the rigid body motion of the lumped mass(es). This information is very useful if the mass mounting point(s) is(are) the connection or coupling point(s) of the structure(s).

2.9.5 Improvement of Norms of Modal Vectors

Zhang and Lallement [31] proposed a method to improve the norms of the measured modal vectors and then calculate the generalized modal masses of the original structure. This method will correct modal scaling errors in the modal data base. This method requires a set of modal data from the initial structure and a set of data from the mass loaded (perturbated) structure.

2.9.6 Conclusion

There are many other techniques currently being studied in order to evaluate and improve the accuracy of the experimental modal model. Some involve the use of a finite element model. The validation methods described in this section serve under the assumption that the experimental modal model needs to be verified, and furthermore, validated through an acceptable engineering procedure. This procedure, which is needed to guarantee the accuracy of the modal modeling results within an acceptable limit, has been proven to be a missing link between the modal data base and the analytical model modeling technique.

2.10 Summary

In summary, modal modeling has been discussed from its inception by Kron through present day research on beam modifications in the modal domain. Modal modeling is a technique that is very quick because the generalized coordinates have a reduced number of degrees of freedom. Therefore, many modifications can be investigated in a short time. Earlier, One this technique was presented mainly as a trouble shooting technique. In fact, researchers [16] have found this method to be three to six times faster than analytical techniques. This ratio increases with the size of the problem. The speed of this technique and its interactive implementation make it well-suited for on-site problem solving and initial design cycle work.

Many limitations are apparent from the development. First, if experimental data is used, the frequency response functions must be carefully calibrated. This technique is extremely sensitive to experimental errors in general. Data must be carefully acquired to avoid bias errors such as leakage and aliasing. Errors made in the estimation of the frequency response functions translate into errors in the modal model and modal matrix $[\Psi]$. Modal parameter estimation is extremely critical in modal modeling. Parameter estimation is a two-stage process that estimates eigenvalues which are used to compute the modal model (see Equation (17)) and the modal vectors which make up the transformation matrix.

Recall that a convenient form of the model is for unity modal mass or unity [V] (see Equation (52)) scaling. This results in equations of the form of those in Equations (18) through (20). Examination of the modal stiffness and damping matrix reveals that the estimate of the damping ratio ς is involved in both matrices. Unfortunately, damping is a difficult parameter to estimate. This is one of the major limitations of the accuracy of an experimental modal model. Fortunately, if great care is taken in the measurements, the magnitudes of this error are not great enough to cause more variation than found in normal experimental error.

Another source of error is truncation. Truncation errors occur in two forms: geometry and modal. Geometry truncation is a problem that occurs when not enough physical coordinates are defined to adequately describe the dynamics of the structure. Higher order mode shape patterns are not properly defined unless enough points are defined along the shape to describe it. A good rule of thumb is to apply Shannon's sampling theorem to the highest order mode expected. Geometry truncation also occurs when all pertinent translational and rotational degrees of freedom are not measured. If a structure exhibits motion in all translational degrees of freedom and only one is measured, the associated error is defined as geometry truncation. In general, the number of data points should be much greater than the number of modes of interest to avoid geometry truncation.

Modal truncation refers to the number of modes included in the data set. From Equation (38), the modified mode shapes are a linear combination of the original mode shapes. Therefore, the rank of the original modal matrix limits the possible dynamic changes that can be calculated. The lower limit of the number of modes required for even simple structures is six [32], to have sufficient rank to accurately predict the results for the first few modes. A good rule of thumb is to include several modes beyond the frequency range of interest to insure the validity of the results within the frequency range of interest. Another serious modal truncation error occurs when the rigid body modes of a free-free structure are not included when that structure is tied to ground.

Based on the preceding discussion it is apparent that the use of modal modeling programs with experimental data requires carefully acquired data and good parameter estimation results. These problems can be overcome by carefully designing the modal test and using the proper parameter estimation algorithms for the given data [33]. This technique works equally well with analytical data and has been implemented in this manner by Structural Measurement Systems [34].

The issue of complex versus real modes has been debated greatly in recent years. To be completely accurate the complex form of the modal modeling technique should be used when nonproportional or heavy damping exists in a structure. Using a real normal mode in this case will cause erroneous results [11]. One compromise is to use a normalized set of real modes derived from the measured complex modes described in Section 2.7.

The use of beam modifications greatly increases the capability of modal modeling. Simple scalar modifications and lumped masses are limiting and unrealistic. Beam modifications require rotational information at the modification points. This information is not readily available but can be obtained with some effort experimentally or analytically. Once rotational information is readily available from experimental sources, modal modification will become a more powerful trouble shooting tool.

3. SENSITIVITY ANALYSIS

3.1 Sensitivity Analysis Overview

Sensitivity Analysis is an approximate technique that determines the rate of change of eigenvalues and eigenvectors using a Taylor expansion of the derivatives. This technique was developed by Fox and Kappor [35] and Garg [36] initially in the late Sixties and early Seventies. Van Belle and VanHonacker [20,37] further developed its use with mechanical structures and implemented it for use directly on modal parameters. This technique is approximate because only one term (differential) or two terms (difference) of the series expansion are used to approximate the derivative.

Sensitivity Analysis is useful in two ways. First, if a certain type of modification of a structure is required, Sensitivity Analysis determines the best location to make effective structural changes. Sensitivity Analysis also is used to predict the amount of change by linearly interpolating the amount of change from the sensitivity to achieve the desired dynamic behavior. This last method is very time consuming, especially when using difference sensitivities to maintain accuracy.

3.2 Formulation of Sensitivity Analysis

Van Belle initially developed the expression for differential and difference sensitivities using the theory of adjoint structures. A design problem is reduced to a classical optimization problem and Tellogen's Theorem is applied. Wang and De Landsheer [12] independently derived the sensitivity of the dynamic transfer function by direct algebraic manipulation and partial differentiation. This results in a general expression for the derivative of the transfer function matrix. Starting with the basic second order differential equation of a mechanical structure:

$$[M]\{\ddot{x}\}+[C]\{\dot{x}\}+[K]\{x\} = \{f(t)\} \tag{116}$$

where M, C and K are the structure's mass, damping and stiffness matrices of order n by n. Laplace transforms are used to arrive at a set of linear equations.

$$[B(s)]\{x\} = \{F(s)\} \tag{117}$$

where,

$$[B(s)] = \Big[[M]s^2+[C]s+[K]\Big]$$

or,

$$[H]\{F\} = \{x\} \tag{118}$$

where,

$$[H] = \Big[[M]s^2+[C]s+[K]\Big]^{-1}$$

From Equations (117) and (118), an identity equation can be formulated as:

$$[B][H] = [H][B] = [I] \tag{119}$$

For a modified system with an added mass, damper or stiffener, a similar identity equation can be derived :

$$[B]_m [H]_m = [H]_m [B]_m = [I] \tag{120}$$

$$[H]_m = [H] + [\Delta H]$$

$$[B]_m = [B] + [\Delta B]$$

where $[\Delta H]$ and $[\Delta B]$ are formed by applying Equation (117) and (118) with added mass(es), damper(s) or stiffener(s). Substitution is made to Equation (120) yielding :

$$[H]_m [B]_m = [H][B] + [H][\Delta B] + [\Delta H][B] + [\Delta H][\Delta B] = [I] \tag{121}$$

By the identity Equation (119), Equation (121) can be simplified as:

$$[\Delta H]\Big[[B] + [\Delta B]\Big] = -[H][\Delta B]$$

By postmultipling the equation above by [H] and then taking the inverse of $([I] + [\Delta B][H])$, an expression for $[\Delta H]$ can be obtained as:

$$[\Delta H] = -[H][\Delta B][H]\Big[[I] + [\Delta B][H]\Big]^{-1} \tag{122}$$

Recall the Macalaurin series and Taylor series as :

$$(1 + x)^{-1} = 1 + x - \frac{x^2}{2} - \ldots \tag{123}$$

$$\Delta f = f - f(x_0) = f'(x_0)\Delta x + \frac{f''(x_0)}{2}(\Delta x)^2 \tag{124}$$

Applying Equation (123), Equation (122) can be expanded as a matrix polynomial form:

$$[\Delta H] = -[H][\Delta B][H] + [H][\Delta B][H][\Delta B][H] + \ldots \tag{125}$$

The first and second order derivative of the transfer function matrix [H] can then be obtained according to Equation (124):

$$[H]' = \frac{\partial [H]}{\partial p} = -[H]\frac{[\Delta B]}{\Delta p}[H] \tag{126}$$

$$[H]'' = \frac{\partial^2 [H]}{\partial p^2} = 2[H]\frac{[\Delta B]}{\Delta p}[H]\frac{[\Delta B]}{\Delta p}[H] \tag{127}$$

The transfer function matrix [H(s)] can be conveniently expressed as a summation of modal vectors in partial fraction form by expanding Equation (119) as :

$$[H(s)] = \sum_{r=1}^{2N} \frac{\{\psi\}_r \{\psi\}_r^T}{(s - \lambda_r)} \tag{128}$$

where,

$$\lambda_{r+N} = \lambda_r^*, \quad \{\psi\}_{r+N} = \{\psi\}_r^*, \quad r = 1, 2, 3, \ldots, N$$

Differentiating Equation (128) with a general variable p (could be mass, damping or stiffness), the derivative of the transfer function matrix can be found as :

$$\frac{\partial[H(s)]}{\partial p} = [H]' = \sum_{r=1}^{2N}\left[\{\psi\}_r\{\psi\}_r^T \frac{\partial\lambda_r}{\partial p}\frac{1}{(s-\lambda_r)^2} + \frac{\partial(\{\psi\}_r\{\psi\}_r^T)}{\partial p}\frac{1}{(s-\lambda_r)}\right] \qquad (129)$$

With the substitution of Equation (128) into Equation (126), the derivative of the transfer function matrix can be clearly shown as a summation of power series of $\frac{1}{(s-\lambda_r)}$ through the use of partial fraction expansion :

$$[H]\frac{[\Delta B]}{\Delta p}[H] = \left(\sum_{r=1}^{2N}\frac{\{\psi\}_r\{\psi\}_r^T}{(s-\lambda_r)}\right)\frac{[\Delta B]}{\Delta p}\left(\sum_{r=1}^{2N}\frac{\{\psi\}_r\{\psi\}_r^T}{(s-\lambda_r)}\right)$$

$$= \sum_{r=1}^{2N}\left[\frac{\{\psi\}_r\{\psi\}_r^T}{(s-\lambda_r)}\frac{[\Delta B]}{\Delta p}\frac{\{\psi\}_r\{\psi\}_r^T}{(s-\lambda_r)}\right]$$

$$+ \sum_{r=1}^{2N}\sum_{m=1_{m\neq r}}^{2N}\left[\frac{\{\psi\}_r\{\psi\}_r^T}{(s-\lambda_r)}\frac{[\Delta B]}{\Delta p}\frac{\{\psi\}_m\{\psi\}_m^T}{(s-\lambda_m)}\right]$$

$$= \sum_{r=1}^{2N}\left[\{\psi\}_r\{\psi\}_r^T\left(\frac{[\Delta B]}{\Delta p}\right)_{s=\lambda_r}\{\psi\}_r\{\psi\}_r^T\frac{1}{(s-\lambda_r)^2}\right]$$

$$+ \sum_{r=1}^{2N}\left[\{\psi\}_r\{\psi\}_r^T\left(\frac{\partial}{\partial s}\frac{[\Delta B]}{\Delta p}\right)_{s=\lambda_r}\{\psi\}_r\{\psi\}_r^T\frac{1}{(s-\lambda_r)}\right]$$

$$+ \sum_{r=1}^{2N}\sum_{m=1_{m\neq r}}^{2N}\left[\{\psi\}_r\{\psi\}_r^T\left(\frac{[\Delta B]}{\Delta p}\right)_{s=\lambda_m}\{\psi\}_m\{\psi\}_m^T\frac{1}{(\lambda_r-\lambda_m)}\frac{1}{(s-\lambda_r)}\right]$$

$$+ \sum_{r=1}^{2N}\sum_{m=1_{m\neq r}}^{2N}\left[\{\psi\}_r\{\psi\}_r^T\left(\frac{[\Delta B]}{\Delta p}\right)_{s=\lambda_m}\{\psi\}_m\{\psi\}_m^T\frac{1}{(\lambda_m-\lambda_r)}\frac{1}{(s-\lambda_r)}\right]$$

$$+ \sum_{r=1}^{2N}\left[\{\psi\}_r\{\psi\}_r^T\frac{1}{2}\left(\frac{\partial^2}{\partial s^2}\frac{[\Delta B]}{\Delta p}\right)_{s=\lambda_r}\{\psi\}_r\{\psi\}_r^T\right]$$

$$+ \sum_{r=1}^{2N}\sum_{m=1_{m\neq r}}^{2N}\left[\{\psi\}_r\{\psi\}_r^T\frac{1}{2}\left(\frac{\partial^2}{\partial s^2}\frac{[\Delta B]}{\Delta p}\right)_{s=\lambda_m}\{\psi\}_m\{\psi\}_m^T\right]$$

By factoring out the same terms, the derivative of the transfer function matrix can be simplified as :

$$[H]\frac{[\Delta B]}{\Delta p}[H] = \sum_{r=1}^{2N}\left[\frac{1}{(s-\lambda_r)^2}A + \frac{1}{(s-\lambda_r)}B + C\right] \qquad (130)$$

where,

$$A = \{\psi\}_r\{\psi\}_r^T\left(\frac{[\Delta B]}{\Delta p}\right)_{s=\lambda_r}\{\psi\}_r\{\psi\}_r^T$$

$$B = \{\psi\}_r \{\psi\}_r^T \left(\frac{\partial}{\partial s} \frac{[\Delta B]}{\Delta p} \right)_{s=\lambda_r} \{\psi\}_r \{\psi\}_r^T$$

$$+ \sum_{m=1_{m \neq r}}^{2N} \frac{1}{(\lambda_r - \lambda_m)} \left[\{\psi\}_r \{\psi\}_r^T \left(\frac{[\Delta B]}{\Delta p} \right)_{s=\lambda_m} \{\psi\}_m \{\psi\}_m^T + \{\psi\}_m \{\psi\}_m^T \left(\frac{[\Delta B]}{\Delta p} \right)_{s=\lambda_m} \{\psi\}_r \{\psi\}_r^T \right]$$

$$C = \{\psi\}_r \{\psi\}_r^T \frac{1}{2} \left(\frac{\partial^2}{\partial s^2} \frac{[\Delta B]}{\Delta p} \right)_{s=\lambda_r} \{\psi\}_r \{\psi\}_r^T$$

$$+ \sum_{m=1_{m \neq r}}^{2N} \{\psi\}_r \{\psi\}_r^T \frac{1}{2} \left(\frac{\partial^2}{\partial s^2} \frac{[\Delta B]}{\Delta p} \right)_{s=\lambda_m} \{\psi\}_m \{\psi\}_m^T$$

A comparison between Equations (129) and (130) related to Equation (126) yields :

$$A = -\{\psi\}_r \{\psi\}_r^T \frac{\partial \lambda_r}{\partial p} \tag{131}$$

$$B = -\frac{\partial(\{\psi\}_r \{\psi\}_r^T)}{\partial p} \tag{132}$$

$$C = 0 \tag{133}$$

Expanding Equation (131), the eigenvalue sensitivity can be obtained through the following procedure,

$$\{\psi\}_r \{\psi\}_r^T \frac{\partial \lambda_r}{\partial p} = -\{\psi\}_r \, a_{rr} \{\psi\}_r^T$$

where a_{rr} is a scalar and,

$$a_{rr} = \{\psi\}_r^T \left(\frac{\partial [B]}{\partial p} \right)_{s=\lambda_r} \{\psi\}_r$$

Hence, the eigenvalue sensitivity is :

$$\frac{\partial \lambda_r}{\partial p} = -a_{rr} = -\{\psi\}_r^T \left(\frac{\partial [B]}{\partial p} \right)_{s=\lambda_r} \{\psi\}_r \tag{134}$$

Also, expanding Equation (132), the eigenvector sensitivity can be acquired.

$$\frac{\partial(\{\psi\}_r \{\psi\}_r^T)}{\partial p} = -b_r \{\psi\}_r \{\psi\}_r^T - \sum_{m=1_{m \neq r}}^{2N} \frac{a_{rm}}{(\lambda_r - \lambda_m)} (\{\psi\}_r \{\psi\}_m^T + \{\psi\}_m \{\psi\}_r^T)$$

where,

$$b_r = \{\psi\}_r^T \left(\frac{\partial}{\partial s}\frac{\partial [B]}{\partial p}\right)_{s=\lambda_r} \{\psi\}_r$$

$$a_{rm} = \{\psi\}_r^T \left(\frac{\partial [B]}{\partial p}\right)_{s=\lambda_m} \{\psi\}_m$$

Investigating the equation above, a further detailed expression of eigenvector sensitivity about each modal coordinate can be found as :

$$\frac{\partial(\psi_{ir}\psi_{jr})}{\partial p} = -b_r\,\psi_{ir}\psi_{jr} - \sum_{m=1_{m\neq r}}^{2N} \frac{a_{rm}}{(\lambda_r - \lambda_m)}(\psi_{im}\psi_{jr} + \psi_{ir}\psi_{jm})$$

A comparison between the next two equations yields the eigenvector sensitivity expression,

- $$\frac{\partial(\psi_{ir}\psi_{ir})}{\partial p} = -b_r\,(\psi_{ir})^2 - \sum_{m=1_{m\neq r}}^{2N} \frac{2a_{km}}{(\lambda_r - \lambda_m)}\psi_{ir}\,\psi_{im}$$
- $$\frac{\partial(\psi_{ir}\psi_{ir})}{\partial p} = \frac{\partial(\psi_{ir})^2}{\partial p} = 2\psi_{ir}\frac{\partial\psi_{ir}}{\partial p}$$

$$\frac{\partial\psi_{ir}}{\partial p} = \frac{1}{2\psi_{ir}}\left[-b_r\,(\psi_{ir})^2 - \sum_{m=1_{m\neq r}}^{2N} \frac{2a_{km}}{(\lambda_r - \lambda_m)}\psi_{ir}\,\psi_{im}\right] \tag{135}$$

$$= -\frac{b_r}{2}\psi_{ir} - \sum_{m=1_{m\neq r}}^{2N} \frac{a_{km}}{(\lambda_r - \lambda_m)}\psi_{im}$$

Following the same derivation process, starting from Equation (127), the second order eigenvalue sensitivity equation is :

$$\frac{\partial^2\lambda_r}{\partial p^2} = 2\left(a_{rr}\,b_r + \sum_{m=1_{m\neq r}}^{2N} \frac{a_{rr}^{\,2}}{(\lambda_r - \lambda_m)}\right) \tag{136}$$

where,

$$b_r = \{\psi\}_r^T \left(\frac{\partial}{\partial s}\frac{\partial [B]}{\partial p}\right)_{s=\lambda_r} \{\psi\}_r$$

$$a_{km} = \{\psi\}_r^T \left(\frac{\partial [B]}{\partial p}\right)_{s=\lambda_m} \{\psi\}_m$$

3.3 Analysis

The differential sensitivity analysis technique utilizes the term on right hand side of Equation (126). Different expressions are developed for the mass, stiffness and damping cases. For the calculation of the sensitivity of an eigenvalue, λ_k, only the corresponding eigenvector is necessary. Calculation of eigenvalue derivations do not require complete information on the dynamics of the structure [38].

Finite difference or difference sensitivities use the terms on the right hand side of Equations (126) and (127) trying to improve the approximation of the differential sensitivity. Nevertheless, a better approximation is obtained only when the change of the structure parameter is small. If the magnitude of change is increased beyond a certain value, the result will be even worse. Equation (136) shows that a term $\frac{1}{(\lambda_k - \lambda_m)}$ is involved in the second order derivative of an eigenvalue. If there are two close modes, the term will become large so the second order derivative contribution dominates the approximation. Further more, if two adjacent modes are very close to each other, the term will diverge so the result will be unacceptable. Hence, care must be taken when a set of modal data shows repeated eigenvalues.

From this discussion, it is seen that the expressions used to compute differential or difference sensitivity from modal parameters are in the form of the transfer function matrix. Because only one or two terms are used from the Taylor expansion, the technique is an approximate one. Since only modal parameters are necessary, this technique is equally applicable to experimental or analytical data. Currently it is implemented with experimental data [38].

VanHonacker [38] has shown this method to be accurate for only small incremental changes. The differential method is far less accurate than the difference method. For small changes of mass, stiffness, or damping the differential technique will accurately predict the eigenvalue shift. For more significant parameter changes, the difference technique is recommended. Therefore, sensitivity analysis has only limited application in the prediction of the effects of structural modifications.

Sensitivity is extremely useful as a preprocessor to Modal Modeling or Finite Element Analysis techniques. The sensitivities of a structure can be computed rapidly from the modal parameters to determine the optimal location at which to investigate a modification. Furthermore, the sensitivity value is useful in determining how much of a modification is required. Therefore, Sensitivity Analysis is a valuable tool in the optimization of a design.

This technique has several limitations. First, the results are only as good as the modal parameters used in the calculations. Therefore, all of the experimental errors and parameter estimation limitations which hinder other modeling methods apply to sensitivity techniques as well. Notably, a limited number of modes are available from zero to the maximum frequency measured. Although not currently implemented with analytical data, any inaccuracies in an analytical model would similarly deteriorate the calculations when used with modal data. In the experimental case, geometry truncation errors are significant due to the exclusion of rotational degrees of freedom.

As a preprocessor to other modeling techniques, sensitivity has advantages. The computations are fast and stable, especially when compared with a complete eigensolution. It is intuitive in nature because it provides rates of change that allow the selection of the best type and location of modification as well as a comparison of different modifications. This provides a large amount of information that offers much insight into the dynamic behavior of a structure.

4. IMPEDANCE MODELING

4.1 Impedance Modeling Overview

The general impedance method was first introduced by Klosterman and Lemon [39] in 1969. Due to the state of measurement equipment at that time the method was not pursued further. As the ability of Fourier analyzers to accurately measure frequency response functions improved in the late Seventies, the interest in General Impedance Techniques was renewed. Two techniques are developed in this chapter using experimental data. Both methods use measured frequency response functions or synthesized frequency response functions.

The general impedance technique is formulated in two ways: frequency response and dynamic stiffness. The dynamic stiffness approach was initially developed by Klosterman [40] and implemented by Structural Dynamics Research Corporation as SABBA (Structural Analysis using the Building Block Approach) [41]. This technique is primarily used to couple together structures to predict the total dynamic characteristics using the concept of superposition. Thus, the phrase building block approach was applied to this technique.

The frequency response method was published and implemented by Crowley and Klosterman [42] at the Structural Dynamics Research Corporation in 1984 and referred to as SMURF (Structural Modifications Using Response Functions). It is primarily a trouble shooting technique. It operates on frequency response functions; therefore, no modal model is necessary to investigate structural modifications. Problems may be solved by acquiring several frequency response functions and investigating the effects of modifications. The modified frequency response function is computed as a function of frequency by simple block operation using the original frequency response function and a frequency representation of the structural modification.

Consider once again the multiple degree of freedom linear second order differential equation:

$$[M]\{\ddot{x}\}+[C]\{\dot{x}\}+[K]\{x\}=\{f\} \tag{137}$$

which describes the equations of motion of a structure. Laplace transforms or assumption of the solution $\{x\}=\{X\}e^{st}$ yields:

$$[[M]s^2+[C]s+[K]]=F(s) \tag{138}$$

where the initial conditions are assumed to be zero. The substitution:

$$[B(s)] = [[M]s^2+[C]s+[K]]$$

is made to Equation (138) to yield:

$$[B(s)]\{X(s)\}=\{F(s)\} \tag{139}$$

where [B(s)] is the system matrix. The system transfer function [H(s)] is defined as $[B(s)]^{-1}$ allowing Equation (140) to be written as:

$$[H(s)] = \frac{X(s)}{F(s)} \tag{140}$$

In practice, the transfer function matrix is not measured. Experimentally, the Fast Fourier Transform measures only the frequency response function at $s=j\omega$ in the complex plane yielding:

$$[H(\omega)] = \frac{X(\omega)}{F(\omega)} \tag{141}$$

This expression is expanded using partial fractions and including inertial restraint and residual flexibility for mass and stiffness as:

$$[H(\omega)] = [R_I] + \sum_{r=k}^{n}\left[\frac{[A_k]_r}{(j\omega - \sigma - j\omega_d)} + \frac{[A_k^*]_r}{(j\omega - \sigma + j\omega_d)}\right] + [R_F] \tag{142}$$

where:

$$[R_I] = Re\left[\sum_{i=1}^{n-1}\left[\frac{[A_k]}{(j\omega - \sigma - j\omega_d)} + \frac{[A_k^*]}{(j\omega - \sigma + j\omega_d)}\right]\right]$$

$$[R_F] = Re\left[\sum_{i=n+1}^{\infty}\left[\frac{[A_k]}{(j\omega - \sigma - j\omega_d)} + \frac{[A_k^*]}{(j\omega - \sigma + j\omega_d)}\right]\right]$$

$$A_r = Q_r\{\psi_r\}\{\psi_r\}^T$$

Equation (142) is the expression that forms the basis of impedance methods. Measured frequency response functions are represented analytically by this equation. If the modal parameters exist from either Finite Element Analysis or an experimental modal model, the frequency response function can be synthesized from the model by substituting in the eigenvalue and eigenvector information. The use of residual terms increases the validity of the analytical expression.

4.2 Dynamic Stiffness Method

Historically, the dynamic stiffness method was implemented first by Klosterman and Lemon as a building block approach. This approach is used to predict the response of two components coupled together or the effects of a structural change, when the dynamic characteristics are available in dynamic stiffness form.

$$\{F\} = [H]^{-1}\{X\} \tag{143}$$

or as

$$\{F\} = \left[-\omega^2 [M] + [K] + j\omega[C] \right] \{X\}$$

$[H]^{-1}$ is the inverse of the frequency response function matrix. The dynamic stiffness matrix may consist of experimental, analytical, or general matrix components in their dynamic stiffness form.

A system with two points p and q has inputs at both points. Frequency response functions are linear for linear, time invariant systems. Therefore, the principle of superposition is used to write the steady state response.

$$\{F_p\} = [H_{pp}]^{-1} \{X_p\} + [H_{pq}]^{-1} \{X_q\} \tag{144}$$

$$\{F_q\} = [H_{qp}]^{-1} \{X_p\} + [H_{qq}]^{-1} \{X_q\}$$

Now consider a technique to couple two systems, 1 and 2, at points p and s. The equations for sinusoidal input on the second structure at points s and t are:

$$\{F_s\} = [H_{ss}]^{-1} \{X_t\} + [H_{st}]^{-1} \{X_t\} \tag{145}$$

$$\{F_t\} = [H_{ts}]^{-1} \{X_p\} + [H_{tt}]^{-1} \{X_t\}$$

Now, equilibrium and compatibility conditions are enforced upon the system

$$F_p + F_s = 0 \tag{146}$$

$$X_p = X_s$$

to combine the two sets of equations into a system matrix.

$$\begin{bmatrix} [H_{qq}]^{-1} & [H_{qt}]^{-1} & [0] \\ [H_{tq}]^{-1} & [H_{tt}]^{-1} + [H_{ss}]^{-1} & [H_{sq}]^{-1} \\ [0] & [H_{ts}]^{-1} & [H_{tt}]^{-1} \end{bmatrix} \begin{Bmatrix} \{X_q\} \\ \{X_p\} \\ \{X_t\} \end{Bmatrix} = \begin{Bmatrix} \{F_q\} \\ 0 \\ \{F_t\} \end{Bmatrix} \tag{147}$$

This set of equations represents a set of complex linear simultaneous equations of the form $F=KX$.

This method can be used with several sources of frequency response function data. The first is direct computation of mass and stiffness matrices to satisfy Equation (143). The second is to utilize the impedance properties of many components. For example, mass, stiffness, beam, or bearings are modeled using a library of impedance representations [41] in SDRC's SABBA modeling program. The third is the direct measurement of frequency response functions and inverting them to assemble the dynamic stiffness matrix. Last is the computation of frequency response function data from the Equation (141) from a modal model.

The last two methods require an inversion of the matrix [H]. Care must be taken to prevent this inversion from becoming ill-conditioned. The use of frequency response function data was found to be undesirable by Klosterman initially, due to instability in the numerical calculations caused by poor measurement quality. Hence, the general impedance technique is implemented using synthesized frequency response functions from modal data. The possible errors associated with using a modal model are discussed in Section 2.8 . Considering the possible errors associated with a modal model, this technique is still preferable to direct frequency response function calculations.

The modal method is implemented in two fashions, the unconstrained modal method and the constrained modal method. Both methods are compatible with modal models or Finite Element Analysis. These methods are used when a structure is free or constrained respectively during test or analysis.

Consider the degrees of freedom of the connection point to be designated by q_m in modal coordinates, and $[\Phi]$ is the eigenvector abbreviated to include only the coordinates at the connection points. The modal model of a component is expressed as:

$$\left\{ \lceil K_\rfloor - \omega^2 \lceil M_\rfloor \right\} [q_m] = [\Phi]^T \{F_m\} + [\Phi]^T \{F_n\} \tag{148}$$

where: $\{F_m\}$ - forces due to external connection of another component

$\{F_n\}$ - additional external forces

This set of equations could represent an experimental modal component.

Now consider a finite element component in standard form

$$\left[\begin{bmatrix} K_{ii} & K_{im} \\ K_{mi} & K_{mm} \end{bmatrix} - \omega^2 \begin{bmatrix} M_{ii} & M_{im} \\ M_{mi} & M_{mm} \end{bmatrix} \right] \begin{Bmatrix} X_i \\ X_m \end{Bmatrix} = \begin{Bmatrix} F_i^2 \\ -F_m + F_n^2 \end{Bmatrix} \tag{149}$$

where: $\{F^2\}$ is external forces on the second component

$\{X_i\}$ is remaining coordinates

$\{X_m\}$ is the coordinates of the connection points

The two systems, modal and analytical, are combined by enforcing the compatibility and equilibrium conditions yielding:

$$\begin{bmatrix} \lceil K \rfloor - \omega^2 \lceil M \rfloor & 0 & 0 & -[\Phi]^T \\ 0 & [K_{ii}] - \omega^2 [M_{im}] & [K_{im}] - \omega^2 [M_{im}] & 0 \\ 0 & [K_{mi}] - \omega^2 [M_{mi}] & [K_{mm}] - \omega^2 [M_{mm}] & I \\ [\Phi] & 0 & -I & 0 \end{bmatrix} \begin{Bmatrix} q_m \\ X_i \\ X_m \\ F_m \end{Bmatrix} = \begin{Bmatrix} [\Phi]^T \{F_n\} \\ F_i^? \\ F_m \\ 0 \end{Bmatrix} \tag{150}$$

This matrix can be condensed into the general form of:

$$\Big[[K] - \omega^2 [M] \Big] \{X\} = \{F\} \tag{151}$$

by substitution.

This is the standard form used by finite element programs. Recall that the dynamic matrix is formed from frequency response function information and must be solved frequency by frequency using a determinant search algorithm [41] to determine the new model properties. In its initial implementation the series of equations were used to solve for the modified frequency response due to a structural modification or coupling with another structure. The unconstrained modal method requires a large number of degrees of rreedom depending upon the severity of the constraints placed upon the component. This led to the development of the constrained modal method.

The constrained modal method is used when the test or analysis is conducted with the structure constrained in some manner. This is desirable in several situations. Rigid body modes are eliminated which is desirable in light of the fact that they are difficult to determine in experimental tests. A constrained mode model closely represents the final structure. Klosterman has shown [40] that the damping characteristics are *frequency* dependent; therefore, a minimal shift in the dominant modes will result in a more accurate representation of damping. Fewer modes or degrees of freedom are necessary if the structure is analyzed or tested with constraint similar to the final composite structure.

Klosterman has proposed a method to derive a representation when the connection coordinates $\{X_m\} = 0$. This result is:

$$\begin{bmatrix} \lceil K \rfloor - \omega^2 \lceil M \rfloor & [R]^T \\ [R] & [K'_{mm}] + [R]\{\lceil K \rfloor\}^{-1} [R]^T \end{bmatrix} \begin{Bmatrix} \{q_i\} \\ \{X_m\} \end{Bmatrix} = \begin{Bmatrix} [\Phi]^T \{F_i\} \\ \{F_m\} \end{Bmatrix} \tag{152}$$

where: m = fixed connection coordinates

i = remaining coordinates

$\{q_i\}$ = modal coordinate of the remaining points

$[R] = -[\Phi]^T \lceil K \rfloor$ = forces applied at the connections to restrain each normal mode

$K_{mm'} = [K_{mm}] - [K_{im}]^T [\Phi][K]^{-1} [\Phi]^T [K_{im}]$

When the coordinates $\{q_m\}$ are not redundant, $[K_{mm'}] = 0$ and Equation (152) is the best form to use. All of the information necessary to use with Equation (152) is available from any modal analysis if all of the forces of constraint are available. This point is the largest disadvantage to this technique. A more detailed development is found in Reference 4.

The dynamic stiffness approach has evolved from the level where single frequency response functions were computed for modified structures, to where complex beam and matrix constraints can be placed on a structure and the resulting modal parameters are found using a frequency dependent determinant search method. This technique has been implemented on super mini-computers [41] and is available for on-test-site trouble shooting and design cycle applications. It relies on modal data; therefore, any limitations noted on modal parameter identification in Section 2.8 are relevant to this technique.

4.3 Frequency Response Method

The frequency response method is a pure trouble shooting technique that operates on measured data or synthesized data. It is implemented [42] to be used for on-site structural modifications or verification of a modal model. Only single constraint structural modifications are practical. This technique is an extension of the technique originally proposed by Klosterman. It became feasible because the numerical problems associated with using measured data were reduced as measurement techniques improved in recent years.

Frequency response testing results in equations of the general form:

$$\{X\} = [H]\{F\} \tag{153}$$

In the following section, equations will be developed using simple block manipulations of frequency response functions to couple two structures, add mass to a structure, add a stiffener to a structure, and constrain a point on a structure to ground.

First, the coupling of two structures is treated. The forcing vector is split into external $\{F_e\}$ and internal $\{F_i\}$ forces, yielding:

$$\{X\} = [H]\{F_e\} + [H]\{F_i\} \tag{154}$$

which is manipulated into:

$$\begin{bmatrix}[I] & -[H]\end{bmatrix}\begin{Bmatrix}\{X\}\\ \{F_i\}\end{Bmatrix} = [H]\{F_e\} \tag{155}$$

The uncoupled equations of two structures, 1 and 2, become:

$$\begin{bmatrix}[I] & -[H_1] & 0 & 0\\ 0 & 0 & [I] & -[H_2]\end{bmatrix}\begin{Bmatrix}\{X_1\}\\ \{F_{i1}\}\\ \{X_2\}\\ \{F_{i2}\}\end{Bmatrix} = \begin{Bmatrix}[H_1]\{F_{e1}\}\\ [H_2]\{F_{e2}\}\end{Bmatrix} \tag{156}$$

Now the equilibrium and compatibility equations are applied at the connections to compute the frequency response $\overline{H}_{pq}$ of the modified structure. The bar denotes the combined structures 1 and

2, p refers to the response point on 1, q refers to the input point on 1, and k is the connection point. The equation to compute the new frequency response is:

$$\overline{H}_{pq} = H_{pq1} - \frac{H_{pq1}\, H_{kq1}}{H_{kk1}\, H_{kk12}} \tag{157}$$

Now consider structure 1 with point m tied to ground such that $X_m = 0$ The new frequency response between p and q is found by writing the response of point m due to input at m and q as:

$$X_m = H_{mm}\, F_m + H_{mq}\, F_q \tag{158}$$

since $X_m = 0$

$$F_m = -H_{mm}^{-1}\, H_{mq}\, F_q \tag{159}$$

The response of point p is also written in terms of the reaction force at m and input at q.

$$X_p = H_{pm}\, F_m + H_{pq}\, F_q \tag{160}$$

Equation (158) is substituted into (159) to obtain the constrained response at point p.

$$X_p = (\, H_{pq} - H_{pm}\, H_{mm}^{-1}\, H_{mq}\,)\, F_q \tag{161}$$

By simply dividing by F_q the frequency response function H_{pq} is found.

$$\overline{H}_{pq} = H_{pq} - H_{pm}\, H_{mm}^{-1}\, H_{mq} \tag{162}$$

H_{pq} is computed frequency by frequency from the measured frequency response functions. Note that if a structure is to be constrained at a point m, a driving point measurement at m and cross measurements between m, p, and q are necessary to compute the modified frequency response function.

Fixing a point to ground is a special case of the more general one of constraining a single point of a structure. Crowley has shown [42] that the constraint is modeled by finding a stationary point of the constrained quadratic functional by minimizing the strain energy:

$$\frac{1}{2}\,\{X\}^H\,[H]^{-1}\,\{X\} - \{X\}^H\,\{F\} \tag{163}$$

subject to the constraint $[J]^T\,\{X\} = 0$

where: J is a matrix of constraint coefficients

Employing Lagrange multipliers $\{\beta\}$ is equivalent to solving a linear equation system.

$$\begin{bmatrix} [H]^{-1} & [J] \\ [J]^T & [0] \end{bmatrix} \begin{Bmatrix} \{X\} \\ \{\beta\} \end{Bmatrix} = \begin{Bmatrix} \{F\} \\ \{0\} \end{Bmatrix} \tag{164}$$

Algebraic manipulation results in the general form for constrained response:

$$[H]' = \left[[I] - [H]\,[J] \left([J]^T [H]\,[J] \right)^{-1} [J]^T \right] [H] \tag{165}$$

Equation (165) is used to develop general equations for addition of mass at a point, and a stiffener addition between two points. The cases of constraining one point to ground and coupling two structures are already developed.

To compute the effect of addition of mass at point q to H_{pq} Equation (165) takes the form:

$$\overline{H}_{pk} = H_{pk} - (H_{pq})\,[H_{qq} + H_{mm}]^{-1}\,(H_{qk}) \tag{166}$$

where: H_{mm} is the analytical driving point of the mass addition at point q.

The equation for the addition of a stiffener between q and m for the modified response at H_{pk} in general form is:

$$\overline{H}_{pk} = H_{pk} - \frac{(H_{pq} - H_{pm})\,(H_{qk} - H_{mk})}{(H_{qq} - H_{mq}) - (H_{qm} - H_{mm})} \tag{167}$$

The expression for adding stiffness at points q and m is computed by adding the analytical stiffness to H_{qq} and H_{mm}

The frequency response method is a simple technique to utilize in trouble shooting situations. Measurements are required at and between the driving point and all points of constraint as well as the desired response point. Generally, driving point information is needed at the driving point and points of constraint. Cross measurements are also needed between each of these points. Crowley suggests only one constraint be applied at a time to avoid matrix inversions [42] . Based on the current implementation, it appears that an impact testing technique is best suited to quickly acquire the necessary frequency response functions to investigate modifications using the frequency response method.

4.4 Analysis

The general impedance technique is a method that employs the use of frequency response data to investigate coupling of structures and structural modifications. The dynamic stiffness approach is the more powerful of the two. The advantage of this technique is that a large array of investigations may be conducted. Also, the method is not as cumbersome as the component modal synthesis technique (Section 5) because it has a reduced number of degrees of freedom.

Due to the dynamic stiffness formulation, modal models of experimental or analytical origin may be combined or modified using an array of mass, stiffness, damping, beam, or matrix elements represented in impedance form. This brings more analytical capability directly to an engineer in a mini-computer environment as implemented currently [41] when compared with modal modeling techniques.

Due to numerical problems, Klosterman recommends use of synthesized frequency response functions to build the dynamic stiffness matrix. This introduces errors made in modal parameter estimation, but reduces numerical problems associated with noisy frequency response functions measurements because the parameter estimation process fits a smooth curve through the measured data. Modeling of this type requires carefully acquired, and properly calibrated, data to obtain the best modal model possible.

One of the major problems with the dynamic stiffness approach is the determination of the $[H]^{-1}$ matrices. The inverse of the matrix must exist. This problem forces the use of modal data because the inversion process is numerically unstable [43]. The number of modes must be much greater than the number of constraint points to insure the existence of the inverse.

The most serious limitation of the dynamic stiffness approach is the computational speed and stability. When implemented initially, only individual frequency response functions were computed for the resultant structure. This implementation is efficient, but the computations are somewhat unstable unless synthesized frequency response functions are used. This led to the application of a determinant search algorithm to compute the resultant eigenvalues and eigenvectors. This algorithm is not computationally efficient because the equations are solved frequency by frequency. This fact has led to more widespread use of component modal synthesis techniques that are described in Chapter 5.

The frequency response method is implemented for single constraint situations to avoid the matrix inversion problem. This makes it useful for trouble shooting situations. Since measured frequency response functions are used in the calculations, no modal model is necessary. Therefore, if the necessary frequency response functions exist, modifications may be made directly to obtain the modified frequency response. This makes the frequency response technique the fastest trouble shooting technique, but only modified frequency response functions are computed not modal data. This technique is slower than modal modeling when modal data is desired.

Data is required for driving points and cross measurements at the constraints, response point, and driving point to compute the modified frequency response. Therefore, the impact testing or multiple reference techniques are most convenient for the frequency response method. Synthesized frequency response functions can be used in this technique when the desired frequency responses are not available, but the advantage of avoiding modal parameter estimation is lost. Modal modeling is a better alternative at this point because the entire set of modified modal parameters is computed. Only individual modified frequency response functions result from the frequency response method.

The frequency response technique is sensitive to measurement errors such as leakage, aliasing, and random noise. Wang [44] has found the errors largest at anti-resonance. This is due to the fact that the signal to noise ratio is poor at anti-resonance. Therefore, as the magnitude of modification or constraint increases, the more the accuracy of the calculations will deteriorate because frequencies will shift closer to or past anti-resonances.

5. COMPONENT DYNAMIC SYNTHESIS

5.1 Introduction

Component dynamic synthesis is an analytical procedure for modeling dynamical behavior of complex structures in terms of the properties of its components or substructure. The procedure involves explicitly every component in the structure the advantages of which are many-fold: analysis and design of different components of the structure can proceed independently, component properties can be obtained from tests and/or analysis, and the size of the built-up structure analysis problem can be reduced to manageable proportions.

Component synthesis with static condensation [45,46] has long been used for improving efficiency of static analysis. In this method, known as substructuring technique, unique or functionally distinct components of a structural system are analyzed separately, condensed, and then combined to form a reduced model. This reduced model, having fewer degrees of freedom, is generally more economical to analyze than the original structural model. The static condensation is an exact reduction procedure.

In dynamic analysis, exact reduction of an individual component is dependent upon the natural frequencies of the total structural system which are yet unknown at the component level. Frequency independent or iterative reduction methods must therefore be used, which introduce approximations. The various reduction methods are collectively known as component dynamic synthesis or modal synthesis (CMS).

The objectives of this section are to review the state of the art in component dynamic synthesis and to develop and implement an improved dynamics synthesis procedure.

5.1.1 Dynamic Synthesis Methods

In order to review the existing dynamic synthesis procedures, it is necessary to define certain frequently-used terms. A component or substructure is one which is connected to one or more adjacent components by redundant interfaces. Discrete points on the connection interface are called boundary points and the remainder are called interior points. The following classes of modes are commonly used as basis components in component dynamic model definition. Details of these mode sets is given later in this report.

1. Normal Modes: These are free vibration eigenmodes of an elastic structure that result in a diagonal generalized mass and stiffness matrix. The normal modes are qualified as free or fixed interface modes, depending on whether the connection interfaces are held free or fixed. Loaded interface normal modes simulate intermediate fixity of the interfaces.

2. Constraint Modes: These are static deflection shapes resulting from unit displacements imposed on one connection degree of freedom and zero displacements on all the remaining degrees of freedom.

3. Attachment Modes: The attachment modes are static deflection shapes defined by imposing a unit force on one connection degree of freedom while the remaining connection degrees-of-freedom (DOFs) are force free. If the structure is unrestrained, this mode set will consist of inertia relief modes. Attachment modes are also static modes.

4. Rigid-body Modes: These are displacement shapes corresponding to rigid body degrees of

freedom. They may be considered a subset of normal modes corresponding to null eigenvalues or else defined directly by geometrical consideration.

5. Admissible Shape Functions: These are any general distributed coordinates or space functions, linear combinations of which simultaneously approximate the displacement of all points of an elastic structure. The only requirements are that the admissible functions satisfy geometry boundary conditions of the component over which they are defined, and satisfy certain differentiability conditions. These are analogous to finite element shape functions.

Static condensation or Guyan Reduction [46] is the simplest of all component dynamic synthesis techniques. The approach is a direct extension of static condensation. The transformation matrix of static constraint modes which is used to reduce the order of the stiffness matrix in static analysis is also used to reduce the order of the structure mass matrix. The kinetic energy of the interior nodes is represented by only static mode shapes. Drawbacks of this approach are obvious. The static modes are not the best Ritz modes for component dynamic representation.

The concept of Component Modal Synthesis (CMS) was first proposed by Hurty [47]. Component members were represented by admissible functions (low- order polynomials) to develop a reduced order model. This procedure is essentially the application of the Rayleigh-Ritz procedure at the component level. Hurty extended the method to include discrete finite element models[48]. This method proposed that the connect DOF of a component were fixed or had a zero displacement. Hurty then partitioned the modes of the structure into rigid body modes, constraint modes, and normal modes. The constraint and rigid body modes were found by applying unit static load to each of the connection points individually to obtain static deformation shapes of the structure. These modes were added to the constrained normal modes to form a truncated mode set used in the synthesis of the entire structure. A simplification of Hurty's fixed interface method was presented by Craig and Bampton [49]. Substructure component modes were divided into only two groups: constraint modes and normal modes. This resulted in a procedure which is conceptually simpler, easier to implement in analysis software. Bamford [50] further increased the accuracy of the method by adding attachment modes which improve the convergence of the method. The attachment modes are the displaced configurations of a component when a unit force is applied to one boundary degree of freedom while all other boundary DOF remain free of loads.

Goldman [51] introduced the free interface method, employing only rigid body modes and free-free normal modes in substructure dynamic representation. This technique eliminates the computation of static constraint modes, but their advantage is negated by the poor accuracy of the method. Hou [52] presented a variation of Goldman's free-interface method in which no distinction is made between rigid body modes and free-free normal modes. Hou's approach also includes an error analysis procedure to evaluate convergence.

Gladwell [53] developed "branch mode analysis" by combining free interface and fixed interface analysis to reduce the order of the stiffness and mass matrices for individual substructures. The reduction procedure depends upon the topological arrangement of the substructures in the model. Thus, reduction of any one substructure requires knowledge of the arrangement of all substructures in the model.

Bajan, et al. [54] developed an iterative form of the fixed interface method. He showed that significant improvements in synthesis accuracy can be achieved by repeating the reduction, based on updated estimates of system frequencies and mode shapes.

Benfield and Hruda [55] introduced inertia and stiffness loading of component interfaces to account for adjacent substructures. The use of loaded interface modes is shown to have superior convergence characteristics.

Motivated by the need to use experimental test data, MacNeal [56] introduced the use of hybrid modes and inertia relief modes for component mode synthesis. Hybrid modes are substructure normal modes computed with a combination of fixed and free boundary conditions. Inertia relief attachment modes are attachment modes for components with rigid body freedoms. MacNeal also included residual inertia and flexibility to approximate the static contribution of the truncated higher order modes of a component. Rubin [57] extended the residual flexibility approach for free interface method by introducing higher order corrections to account for the truncated modes. Klosterman [58] more fully developed the combined experimental and analytical method introduced by MacNeal. Hintz discussed the implications of truncating various mode sets and developed guidelines for retaining accuracy with a reduced size model[59].

Many authors have compared the techniques discussed. No method clearly appears to be superior to the other. The constrained interface method of Craig and Bampton and Hurty is expected to be the most accurate when the connect degrees of freedom have little motion. The free interface method with the use of residuals as proposed by Rubin appears to be more accurate than the constrained approach.

Recent research has centered on comparisons of the various methods. Baker [60], for example, compares the constrained and free-free approach using experimental techniques and also investigates using mass additive techniques and measured rotational DOF [45]. This investigation was motivated by a need to find the best method for rigidly connected flexible structures. In this connection, the constrained method produced the best result. Klosterman [58] has shown the free-free method to be accurate for relatively stiff structures connected with flexible elements. This supports Rubin's conclusion [57] that the free-free method is at least as accurate when residual effects are accounted for. These conclusions are intuitive because the type of boundary condition imposed in the analysis that best represents the boundary of the assembled structure provides the best accuracy in the modal synthesis.

Meirovitch and Hale [61] have developed a generalized synthesis procedure by broadening the definition of the admissible functions proposed by Hurty [47]. This technique is applicable to both continuous and discrete structural models. The geometric compatibility conditions at connection interfaces are approximately enforced by the method of weighted residuals.

The method due to Klosterman [58] has been implemented in an interactive computer code SYSTAN [62] and that due to Herting [63] is available in NASTRAN. The latter is the most general of the modal synthesis techniques. It allows retention of an arbitrary set of component normal modes, inertia relief modes, and all geometric coordinates at connection boundaries. Both the fixed-interface method of Craig and Bampton, and the MacNeal's residual flexibility method, are special cases of the general method. Other analyses presented in the literature based on modal synthesis techniques are not incorporated into general structural analysis codes. In general, there is a lack of sophistication in available software.

5.1.2 Damping Synthesis Methods

The methods of dynamic synthesis are particularly useful and sometimes the only alternative available in damping prediction for built-up structures. Most frequently, damping has been synthesized in the manner analogous to stiffness and mass synthesis with the assumption of proportional damping. Hasselman and Kaplan [64] used complex modes of components with nonproportional damping. Obtaining damping matrices in the presence of general energy dissipating mechanisms in a complex structure is one of the complicating factors, however. In such cases an average damping behavior can be obtained from tests in the form of cyclic energy dissipated versus peak stored energy correlation or damping law. Kana et al. [65] synthesized system damping based on substructure stored energy at the system modal frequency. Soni [66] developed a substructure damping synthesis method applicable to cases where substructure damping varies greatly and irregularly from mode to mode. The procedure has been validated in experimental studies [67]. Jezequel [68] employed fixed interface component modes together with mass loaded interface modes replacing the static constraint mode in his damping synthesis method. Mass loading results in an improved representation of interface flexibility and dissipation; however, the use of constrained interface modes make it difficult to implement it in experimental testing.

The subject of component dynamic synthesis has received increasing attention in recent years. Reference [69] presents several detailed reviews, applications, and case histories, with particular emphasis on experimental characterization of component dynamics.

5.1.3 A Comparison of the Synthesis Methods

While differing in their detailed treatment, all the synthesis methods have the following objectives: (1) to efficiently predict the dynamics of a structure within required accuracy for a minimum number of DOFs; (2) to analyze the components totally independent of other components so the design process is uncoupled, and (3) to use component properties derived from tests and/or analyses. The various methods discussed in the preceding paragraphs only partially satisfy the three basic requirements. Common to all modal synthesis methods discussed in the preceding is the complexity of the matrix manipulations involved in setting up the coupling and assembly procedure to obtain the final reduced equation system.

The major limitation on the use of the existing modal synthesis methods is their lack of compatibility with practical experimental procedures. Although various types of component dynamic representations have been proposed, only those requiring normal modal properties are practical. Test derived modal representation is, in general, incomplete; the component normal modes obtained assuming any type of support conditions at the interfaces are, in general, different from those occurring when the components are acting within the compound of the total system. Since only a limited set of modal data is obtainable, the interface flexibility is not adequately modeled. Depending upon the synthesis method used, additional information is therefore usually required to approximate the effect of interface condition or modal truncation.

Fixed interface mode synthesis methods employ static deflection shapes. In an experimental setup, constraining interface degrees of freedom proves impractical, particularly when large dimensions or a large number of connection points are involved. Also, damping data associated with static modes is unavailable. For these reasons the free interface based modal synthesis methods are best suited for achieving test compatibility. These methods also lend themselves to accuracy improvements via the artifice of interface loading or by augmenting the normal modal data with residual flexibility and inertia effects of truncated modes.

5.1.4 Objectives and Scope

The objective of this work is to investigate and develop component dynamic synthesis procedures and associated computer software which (a) combines component dynamic characteristics obtained from modal tests or analyses or both; (b) accounts for the effects of differences in interface boundary constraints of the component structures in the modal test and in the comparison of total structure; and c) reduces inaccuracies due to modal truncation.

In view of the above objectives and the assessment of existing synthesis methods made in the preceding section, the free interface modal synthesis methods are studied further in this work. For completeness, the fixed interface and the discrete element representations are also considered. For certain components the use of constrained interface conditions may be unavoidable. Structural components such as panels, stringers, simple masses, vibration control devices, etc. are conveniently input to the synthesis procedure via discrete elements.

A principal feature of the work developed here is the component dynamic model reduction procedure that leads to an exact and numerically stable synthesis. In order to affect component coupling, neither the specification of external coupling springs nor an user-specified selection of independent coordinate is required. Existing synthesis procedures suffer from these drawbacks. Component dynamic models considered include free-free normal modes with or without interface loading, up to second order stiffness and inertia connections accounting for the effect of modal truncation, fixed interface modes, and also the physical coordinate components. The modal reduction procedure involves interior boundary coordinate transformations which explicitly retain connection interface displacement coordinates in the reduced component dynamic representations. Interior coordinates may include physical, modal, or any admissible coordinates. Components in this reduced form are termed "superelement" because they are a generalization of the conventional finite elements of structural mechanics. The problem of component dynamic synthesis is then reduced to the assembly of the superelement. The direct stiffness approach and all subsequent processing operations of the finite element method are then applicable.

The remainder of this section presents the formulation implementation aspects of the superelement component dynamic synthesis method. Section 5.2 contains a discussion of various types of component dynamic models, a synopsis of coupling methods followed by a detailed derivation of the superelement component dynamic equations. The derivation of component dynamic models from measurements is described in Section 5.3. A verification study of the developed technique is presented in Section 6. The computer software implementation of the superelement synthesis method is described in the Appendix B.

5.2 Superelement Method

In order to develop an improved component dynamics synthesis procedure, there are two key issues to focus on: the modeling of component dynamics and the coupling of component coordinates. As seen in the review, no one method of component dynamic modeling is shown to be superior to any other. The methods of synthesis developed in the literature use one or other type of component representation. Aerospace structures involve a wide variety of components and any single component dynamic modeling method may not be uniformly suitable to all the components. With this in mind, a generalized synthesis method is develop which permits different types of component models and an associated coupling procedure. In Section 5.2.1 various component dynamic models are described. In Section 5.2.2 coupling procedures are described, illustrating the accuracy and computational efficiency of direct matrix assembly procedures to affect component coupling. A basic requirement of the superelement method is discussed. In order to implement the direct matrix assembly procedure for components described in any general coordinates, the necessary transformations are derived in Section 5.2.3. The coupled systems equations are derived in Section 5.2.4.

5.2.1 Component Dynamic Model

The equation of motion of a component undergoing motion within the compound of a total structural system may be expressed as

$$[M]\{\ddot{x}\} + [C]\{\dot{x}\} + \left[[K] + j[\hat{K}]\right]\{x\} = \{f\} \tag{168}$$

where M, C, K and $\hat{K}$ are respectively the mass, viscous damping, stiffness, and hysteretic damping matrices and {x} the column matrix of displacement due to internal forces {F} at the interface degrees of freedom connected with adjacent components. External forces are assumed to be applied only at connect degrees of freedom. In the following derivations we ignore damping. Further, we use the same notation for the time dependent quantities and their amplitudes, that is, $\{x(t)\} = \{x\} e^{j\omega t}$, $\{F\} = \{F\} e^{j\omega t}$, to minimize the number of symbols. For later discussion the system of Equation (168) is partitioned according to boundary $\{x\}_B$ and remainder $\{x\}_O$ degrees of freedom as

$$\begin{bmatrix} [M]_{OO} & [M]_{OB} \\ [M]_{BO} & [M]_{BB} \end{bmatrix} \begin{Bmatrix} \ddot{x}_O \\ \ddot{x}_B \end{Bmatrix} + \begin{bmatrix} [K]_{OO} & [K]_{OB} \\ [K]_{BO} & [K]_{BB} \end{bmatrix} \begin{Bmatrix} x_O \\ x_B \end{Bmatrix} = \begin{Bmatrix} 0 \\ F_B \end{Bmatrix} \tag{169}$$

The above represents a total of n $(= n_B + n_O)$ number of equations where n_B and n_O are, respectively, the number of boundary and other degrees of freedom. The boundary degrees of freedom include the connection interface DOFs as well as any other DOF that need to be carried to system synthesis in physical coordinates. Thus the grid point DOFs associated with supports, external excitations, response monitoring stations, concentrated weights and attachment to other components for higher level synthesis are also termed boundary DOFs.

In order to reduce the size of the above system equation and also to obtain the model from experimental tests the displacements $\{x\}$ of the component are represented by a linear combination of a finite number of displacement functions as

$$\{x\} = [\Phi]\{q\} \tag{170}$$

where $\{q\}$ is the vector of generalized coordinates and $[\Phi]$ is the matrix of generalized displacement functions. Using the above transformation in Equation (168) leads to the equation of motion in generalized coordinates as

$$[M]_q\{\ddot{q}\} + [K]_q\{q\} = [\Phi]^T\{F\} \tag{171}$$

where :

$[M]_q = [\Phi]^T[M][\Phi]$: Generalized mass matrix

$[K]_q = [\Phi]^T[K][\Phi]$: Generalized stiffness matrix

Equation (171) defines the component dynamic model in generalized coordinates. This definition is very general in the sense that no restriction is placed on the coordinate {q} other than the requirements that the columns of this transformation matrix $[\Phi]$ be linearly independent admissible shape functions [61] whose linear combination adequately represents the deformed configuration of the elastic component. In the following, however, in view of the objectives of this work, attention is focused on the use of component normal modal coordinates. Some auxiliary displacement functions are also used in order to improve the accuracy of component dynamic representation. The normal mode and auxiliary displacement functions for different interface fixity conditions are described next.

5.2.1.1 Free Interface Modal Models

The generalized displacement functions in Equation (170) are obtained from the solution of the eigenproblem

$$\left[[K]-\lambda_r^2[M]\right]\{\phi\}_r=0 \tag{172}$$

where the boundary forces $\{F\}_B$ in Equation (169) are set to zero. The displacement functions include rigid body modes if any, and the flexural modes of the component. The generalized mass and stiffness matrices are diagonal with coefficients given as

$$\begin{aligned} M_r &= \{\phi\}_r^T[M]\{\phi\}_r \\ K_r &= \{\phi\}_r^T[K]\{\phi\}_r \\ \lambda_r^2 &= \frac{K_r}{M_r} \end{aligned} \tag{173}$$

The equation of motion of the modal component is

$$\lceil M \rfloor\{\ddot{q}\}+\lceil K \rfloor\{q\}=\{f\} \tag{174}$$

In practice, only a partial set of normal modes is available which fails to adequately represent the component dynamic behavior. The two models, loaded interface modal model and the residual flexibility modal model discussed in the following, approximate the effects of high frequency truncated modes and improve the accuracy of the component dynamic representation.

The loaded interface modal model is obtained from a modified eigenproblem of the component. The modifications account for the stiffness and inertia loading of the component interfaces. Let $[\Delta K]_{BB}$ and $[\Delta M]_{BB}$ be the connection point stiffness and mass loading matrices respectively. The modified component eigenproblem becomes

$$\left(\begin{bmatrix}[K]_{OO} & [K]_{OB} \\ [K]_{BO} & \left[[K]_{BB}+[\Delta K]_{BB}\right]\end{bmatrix}-\lambda_r^2\begin{bmatrix}[M]_{OO} & [M]_{OB} \\ [M]_{BO} & \left[[M]_{BB}+[\Delta M]_{BB}\right]\end{bmatrix}\right)\begin{Bmatrix}\phi_O \\ \phi_B\end{Bmatrix}=\begin{Bmatrix}0 \\ 0\end{Bmatrix} \tag{175}$$

The computed eigenvectors $\{\phi\}_r$ diagonalize the modified stiffness and mass matrices and satisfy the orthogonality relations of the types given by Equations (173).

The residual flexibility model accounting for the effects of modal truncation is derived using the residual flexibility attachment modes used in a number of previous works [56,57,58,63,69,70]. In the following a derivation of the model including inertia as well as flexibility effects is given.

Partitioning the complete modal matrix $[\Phi]$ into orthogonal subsets $[\Phi]_K$ and $[\Phi]_D$, where $[\Phi]_K$ is a n by m_K matrix of kept normal modes and $[\Phi]_D$ is a n by m_D matrix of omitted high frequency modes, n and m_K being the total number of component degrees of freedom and the number of retained modes, respectively, m_D is the number of omitted modes ($m_D = n - m_K$). The physical displacement, Equation (170), can be written as

$$\{x\} = [\Phi]_K\{q\}_K + [\Phi]_D\{q\}_D \tag{176}$$

where,

$$[\Phi] = \Big[[\Phi]_K \;\;|\;\; [\Phi]_D\Big]$$

Substituting Equation (176) into Equation (171) gives the equations of motion for generalized coordinates $\{q\}$ as

$$\{\ddot{q}\}_K + \lceil\Lambda\rfloor_K\{q\}_K = [\Phi]_K^T\{f\} \tag{177}$$

$$\{\ddot{q}\}_D + \lceil\Lambda\rfloor_D\{q\}_D = [\Phi]_D^T\{f\} \tag{178}$$

where modes are orthonormalized with respect to the mass matrix, and $\lceil\Lambda\rfloor_K$ and $\lceil\Lambda\rfloor_D$ are defined as per Equations (173) corresponding to the kept and detailed modes respectively. For harmonic motion of the component at frequency ω, solving Equation (178) for the generalized coordinate $\{q\}$ and substituting the result into Equation (176) leads to

$$\{x\} = [\Phi]_K\{q\}_K + \sum_{r=m_K+1}^{N} \frac{\{\phi\}_r\{\phi\}_r^T}{(\lambda_r^2 - \omega^2)}\{f\} \tag{179}$$

The second series in the above expression represents the dynamic flexibility or simply the residual flexibility of the modes $[\Phi]_D$. Approximation for the residual effects of the truncated modes is arrived at indirectly since the modes and frequencies in the second series are not known. Following Rubin [57], the static contribution of the truncated modes is obtained by neglecting inertia in Equation (178) and solving for $\{q\}_D$:

$$\{q\}_D = \lceil\Lambda\rfloor_D^{-1}[\Phi]_D^T\{f\} \tag{180}$$

Substitution of the above into Equation (176) gives component displacements as

$$\{x\} = [\Phi]_K\{q\}_K + [\Phi]_D\lceil\Lambda\rfloor_D^{-1}[\Phi]_D^T\{f\} \tag{181}$$

Using the definition of the generalized stiffness

$$\lceil\Lambda\rfloor = [\Phi]^T[K][\Phi]$$

the total static flexibility is given as

$$[G] = [K]^{-1} = [\Phi]\lceil\Lambda\rfloor^{-1}[\Phi]^T$$

for constrained components, and $[G] = [A]^T [\hat{G}] [A]$ for free components where $[A]$ is a matrix operator [71] which filters out rigid body modes:

$$[A] = [I] - [M][\Phi]_R [M]_R [\Phi]_R^T$$

$[\Phi]_R$ and $[M]_R$ being respectively the matrix of rigid body modes and corresponding mass matrix. $[\hat{G}]$ is the flexibility of the component subjected to arbitrary statically determinate constraints. Using the partitioned form of the modal matrix $[\Phi]$ the above equation becomes:

$$[G] = [\Phi]_K \lceil \Lambda \rfloor_K^{-1} [\Phi]_K^T + [\Phi]_D \lceil \Lambda \rfloor_D^{-1} [\Phi]_D^T \tag{182}$$

Therefore the component displacements can be written in terms of the known modes $[\Phi]_K$ and the static flexibility as

$$\{x\} = [\Phi]_K \{q\}_K + \left[[G] - [\Phi]_K \lceil \Lambda \rfloor_K^{-1} [\Phi]_K^T \right] \{f\} \tag{183}$$

or

$$\{x\} = [\Phi]_K \{q\}_K + [G]_R \{f\}$$

where,

$$[G]_R = \left[[G] - [\Phi]_K \lceil \Lambda \rfloor_K^{-1} [\Phi]_K^T \right] \tag{184}$$

represents the residual flexibility of the truncated modes.

Correction for the inertial effects of the truncated modes is obtained using Equation (180) to approximate the inertia term in Equation (178). Thus,

$$\{q\}_D = \lceil \Lambda \rfloor_D^{-1} \left[[I] + \omega^2 [G]_R \right] \{f\} \tag{185}$$

Correspondingly,

$$\{x\} = [\Phi]_K \{q\}_K + [G]_R \left[[I] + \omega^2 [G]_R \right] \{f\} \tag{186}$$

The approximation for the flexibility and inertia of the truncated modes is clearly seen in the displacement transformation relations given by Equations (183) and (186). These transformations, however, are not suitable for component coordination reduction because of the force term $\{F\}$. A Rayleigh- Ritz representation for Equation (183) is readily obtained by considering the residual displacement term in Equation (181)

$$\{x\}_R = [G]_R \{f\}$$

This equation defines residual displacement of the component due to interface force $\{F\}$. Comparing it with the definition of an attachment mode, this equation leads to the definition of a residual flexibility attachment mode for a unit force imposed at the interface coordinate. The residual displacement vector is the column of residual flexibility matrix corresponding to the interface coordinate degree of freedom. Component displacement $\{x\}_R$ can therefore be expressed as a superposition of residual flexibility attachment modes $[G]_B$:

$$\{x\}_R = [G]_B \{q\}_B \tag{187}$$

where $\{q\}_B$ is the associated generalized coordinate and $[G]_B$ is the $(n \times n_B)$ partition of the $(n \times n)$ residual flexibility vector $[G]_B$. That is,

$$[G]_R = \begin{bmatrix} [G]_{OO_{n_O \times n_O}} & [G]_{OB_{n_O \times n_B}} \\ [G]_{BO_{n_B \times n_O}} & [G]_{BB_{n_B \times n_B}} \end{bmatrix} \tag{188}$$

Rayleigh-Ritz transformation for the component displacement then becomes

$$\{x\} = [T]_1 \{q\}$$

where,

$$[T]_1 = \begin{bmatrix} [\Phi]_K & | & [G]_B \end{bmatrix} \quad , \ \{q\} = \begin{Bmatrix} q_K \\ q_B \end{Bmatrix} \tag{189}$$

Equation (182) governs component dynamic equilibrium in the generalized coordinates $\{q\}$ given by Equation (189) with the modal parameters defined as

$$[M]_q = [T]_1^T [M] [T]_1 = \begin{bmatrix} \lceil M \rfloor_K & [0] \\ [0] & [H]_{BB} \end{bmatrix} \tag{190}$$

$$[K]_q = [T]_1^T [K] [T]_1 = \begin{bmatrix} \lceil \Lambda \rfloor_K & 0 \\ 0 & [G] \end{bmatrix} \tag{191}$$

where $\lceil M \rfloor_K$ and $\lceil \Lambda \rfloor_K$ are respectively the generalized mass and stiffness matrices of the kept normal modes, and $[H]_{BB}$ and $[G]_{BB}$ are the boundary partitions of the residual mass and flexibility matrices.

$$
\begin{aligned}
\lceil M \rfloor_{K} &= [\Phi]_K^T [M][\Phi]_K \\
[H]_{BB} &= [G]_B^T [M][G]_B \\
\lceil \Lambda \rfloor_{K} &= [\Phi]_K^T [K][\Phi]_K \\
[G]_{BB} &= [G]_B^T [K][G]_B
\end{aligned}
\tag{192}
$$

The following orthogonality properties of the modes are used in the above derivation:

$$
\begin{aligned}
&[\Phi]_K^T [M][G]_B = [G]_B^T [M][\Phi]_K = 0 \\
&[\Phi]_K^T [K][G]_B = [G]_B^T [K][\Phi]_K = 0 \\
&[G]_R^T [K][G]_R = [\Phi]_D \lceil \Lambda \rfloor_D^{-1} [\Phi]_D^T = [G]_R
\end{aligned}
\tag{193}
$$

It should be noted that in contrast to Equation (183), through the use of residual flexibility attachment modes, the Raleigh-Ritz transformation of Equation (189) requires the measurement of residual flexibilities at connection DOFs only. Furthermore, the transformation of Equation (189) is amenable to superelement assembly procedure as is shown later in this section. An estimate of the improvement in accuracy of component displacement representation with the introduction of the residual flexibility effects is obtained as follows. Comparing Equations (179) and (184), the error in displacement given by the two equations is less than or equal to

$$
\left(\frac{\lambda}{\omega_K}\right)^2 \left|\left| \sum_{i=m_K+1}^{N} \{\phi\}_r^T \{\phi\}_r \frac{\{f\}}{(\omega_i^2 - \kappa^2)} \right|\right|
$$

where ω_K is the frequency of the highest retained mode of the component.

5.2.1.2 Constrained Interface Modal Model

A constrained interface modal model is derived using the displacement transformation given as

$$
\{X\} = \begin{bmatrix} [\Phi]_K & [\Phi]_C \\ [0] & [I] \end{bmatrix} \{q\}
\tag{194}
$$

where the columns of the $[\Phi]_K$ and $[\Phi]_C$ matrices are respectively the constrained interface normal modes and the static constraint deflection shapes of the component obtained as follows. For forced harmonic motion of the component at system frequency λ, the component equilibrium Equation (169) can be written as

$$
\left(\begin{bmatrix} [K]_{OO} & [K]_{OB} \\ [K]_{BO} & [K]_{BB} \end{bmatrix} - \lambda^2 \begin{bmatrix} [M]_{OO} & [M]_{OB} \\ [M]_{BO} & [M]_{BB} \end{bmatrix} \right) \begin{Bmatrix} x_O \\ x_B \end{Bmatrix} = \begin{Bmatrix} 0 \\ f_B \end{Bmatrix}
\tag{195}
$$

Since the interior DOFs are force free, their motion can be written in terms of the boundary DOFs as

$$
\{x\}_O = -\left[[K]_{OO} - \lambda^2 [M]_{OO}\right]^{-1} \left[[K]_{OB} - \lambda^2 [M]_{OB}\right]\{x\}_B
\tag{196}
$$

The static constraint modes are derived by ignoring inertia forces on the interior coordinates. Thus,

$$\{x\}_O = [\Phi]_C \{x\}_B \tag{197}$$

where

$$[\Phi]_C = -[K]_{OO}\,[K]^{-1}_{OB}$$

$[\Phi]_C$ is the constraint mode transformation.

Physically a static constraint mode is the displacement configuration of the component resulting from a unit displacement applied to one boundary DOF while all other boundary DOFS are held fixed.

Inertia of the interior DOFs is accounted for by considering the motion of the component with all interface DOFs held fixed and solving the eigenproblem

$$\left[[K]_{OO} - \lambda^2 [M]_{OO}\right]\{x\}_O = \{0\} \tag{198}$$

The solution of this eigenproblem yields the matrix of fixed interface normal modes $[\Phi]_O$ having the same order as $[K]_{OO}$ and $[M]_{OO}$. The computed eigenfrequencies λ_i^2 are those of the component with its boundaries fixed.

The complete set of component normal modes $[\Phi]_O$ plus the static constraint modes $[\Phi]_C$ provide the means to transform the displacement vector $\{x\}$ from geometric coordinates to an equivalent set of generalized coordinates $\{q\}$ as given in Equation (194), where $[\Phi]_K$ is a subset of $[\Phi]_O$ chosen so as to yield a reduced order model. The reduced order stiffness and mass matrices in generalized coordinates are obtained as

$$[k] = [T]_1^T [K][T]_1 = \begin{bmatrix} [\Lambda]_K & [0] \\ [0] & [K]_{CC} \end{bmatrix}$$

$$[m] = [T]_1^T [M][T]_1 = \begin{bmatrix} [m]_{KK} & [m]_{KC} \\ [m]_{CK} & [m]_{CC} \end{bmatrix} \tag{199}$$

where

$$
\begin{aligned}
&[T]_1 = \begin{bmatrix} [\Phi]_K & [\Phi]_C \\ [0] & [I] \end{bmatrix} \\
&\lceil \Lambda \rfloor_K = [\Phi]_K^T [K] [\Phi]_K = \lceil \lambda_i^2 \rfloor \\
&[m]_{KK} = [\Phi]_K^T [M] [\Phi]_K = \lceil m_{i_j} \rfloor \\
&[k]_{CC} = [\Phi]_C^T [K] [\Phi]_C = [K]_{BB} + [K]_{BO} [\Phi]_C \\
&[m]_{CC} = [\Phi]_C^T [M] [\Phi]_C = [M]_{BB} + [\Phi]_C^T [M]_{OO} [\Phi]_C + [\Phi]_C^T [M]_{OB} + [M]_{BO} [\Phi]_C \\
&[m]_{KC} = [M]_{BO} [\Phi]_K + [\Phi]_C^T [M]_{OO} [\Phi]_K \\
&[m]_{CK} = [m]_{KC}^T
\end{aligned}
\qquad (200)
$$

Two characteristics should be noted concerning the generalized coordinates of the constrained interface model: (1) the generalized coordinates associated with the constraint modes are simply the boundary displacement coordinates; and (2) the generalized coordinates associated with their normal modes of the component are unique to the component and do not require compatibility with other components. It is in this regard that the fixed interface model mimics the general characteristics of a displacement based finite element. Assimilation of this and the other models, namely the interface modal models, finite element models in the system synthesis is discussed in the next section.

Procedures for constructing the component dynamic models discussed in the preceding from experimental test data are summarized later in this Section 5. Detailed discussions may be found elsewhere [57,58,60,69,72].

5.2.2 Component Coordinate Coupling

The assembly of the component dynamics models and the enforcement of the compatibility constraints at their connection interfaces to form coupled system equations is the key step in a synthesis procedure. The accuracy and efficiency of synthesis depends on the manner in which these interface constraints are enforced, which in turn depends upon the type of basis coordinates used in the component dynamics representation. In the following, several coupling procedures are discussed. Observe that the direct matrix approach is the only exact and most efficient coupling procedure. Finally, observations are made regarding the form of the component dynamics model needed to affect synthesis using direct matrix assembly approach.

In the following, the coupling of two components described in physical coordinates (Equation (168)), generalized coordinates (Equation (171)), and mixed coordinates are considered. In discussing the generalized coordinate model full generality of the basis coordinates is permitted, that is, the columns of the modal matrix $[\Phi]$ in Equation (170) are not required to be orthogonal vibration modal vectors, the generalized stiffness and mass matrices are in general fully populated.

The problem of component coordinate coupling can be approached in basically two ways depending on how the compatibility condition at connection interfaces is enforced. In the direct or implicit method, the component matrices are partitioned into interior and boundary DOFs and then assembled in the manner of direct matrix assembly approach used in conventional finite element method. Thus the coupling system governing equations are

$$\begin{bmatrix} [M]^1_{OO} & [0] & [M]^1_{OB} \\ [0] & [M]^2_{OO} & [M]^2_{OB} \\ [M]^1_{BO} & [M]^2_{BO} & [M]^1_{BB}+[M]^2_{BB} \end{bmatrix} \begin{Bmatrix} \ddot{x}^1_O \\ \ddot{x}^2_O \\ \ddot{x}_B \end{Bmatrix} + \begin{bmatrix} [K]^1_{OO} & [0] & [K]^1_{OB} \\ [0] & [K]^2_{OO} & [K]^2_{OB} \\ [K]^1_{BO} & [K]^2_{BO} & [K]^1_{BB}+[K]^2_{BB} \end{bmatrix} \begin{Bmatrix} x^1_O \\ x^2_O \\ x_B \end{Bmatrix} = \{0\} \tag{201}$$

where the vectors and matrices are partitioned as

$$[M]^\alpha = \begin{bmatrix} [M]^\alpha_{OO} & [M]^\alpha_{OB} \\ [M]^\alpha_{BO} & [M]^\alpha_{BB} \end{bmatrix}, \; [K]^\alpha = \begin{bmatrix} [K]^\alpha_{OO} & [K]^\alpha_{OB} \\ [K]^\alpha_{BO} & [K]^\alpha_{BB} \end{bmatrix}, \; \{x\}^\alpha = \begin{Bmatrix} x^\alpha_O \\ x^\alpha_B \end{Bmatrix} \tag{202}$$

The superscripts identify the component, and the subscripts B and O represent respectively the boundary, and the other than boundary degrees of freedom. The interface displacement and force compatibility conditions

$$\begin{aligned} \{x\}^1_B &= \{x\}^2_B \\ \{f\}^1_B &= -\{f\}^2_B \end{aligned} \tag{203}$$

are implicitly satisfied in obtaining the coupled system equations (Equation (201)). Note that the presence of boundary DOFs $\{X\}^\alpha_B$ in the component representation permitted the use of direct matrix assembly. In the event the components are described in terms of generalized coordinates the constraints in Equation (203) need to be enforced explicitly as shown below.

Consider the coupling of the components described by Equation (171). The governing equations are

$$\begin{bmatrix} [M]^1_q & [0] \\ [0] & [M]^2_q \end{bmatrix} \begin{Bmatrix} \ddot{q}^1 \\ \ddot{q}^2 \end{Bmatrix} + \begin{bmatrix} [K]^1_q & [0] \\ [0] & [K]^2_q \end{bmatrix} \begin{Bmatrix} q^1 \\ q^2 \end{Bmatrix} = \begin{Bmatrix} f^1_{q_B} \\ f^2_{q_B} \end{Bmatrix} \tag{204}$$

or

$$[M]_q\{\ddot{q}\} + [K]_q\{q\} = \{f\}_{q_B}$$

together with the interface compatibility constraints

$$[A]\{q\} = \{0\} \tag{205}$$

which are generalized coordinate analog of Equation (203), [A] is the matrix of connection point modal coefficients, and {q} is the uncoupled system coordinate vector. The constraint Equation (205) implies a reduction of the number of system DOFs by the number of constraints. This reduction is denoted by

$$\{q\} = [T]\{\hat{q}\} \tag{206}$$

where [T] is coordinate coupling or synthesis transformation and $\{\hat{q}\}$ is the coupled system coordinate vector. The manner in which the constraints Equation (206) are inserted into the system Equation (205) significantly affects the accuracy and efficiency of the synthesis procedure. Possible alternates are as follows.

5.2.2.1 Lagrange Multiplier Method

The constraints are introduced by extending the system of Equation (204) through the use of nodeless variable of Lagrange multiplier γ_i, $i=1,2,\ldots,N_B$, N_B being the total number of connection DOF. The overall system equations become

$$\begin{bmatrix} [M]_q & [0] \\ [0] & [0] \end{bmatrix} \begin{Bmatrix} q \\ 0 \end{Bmatrix} + \begin{bmatrix} [K]_q & [A]^T \\ [A] & [0] \end{bmatrix} \begin{Bmatrix} q \\ \gamma \end{Bmatrix} = \begin{Bmatrix} f_q \\ 0 \end{Bmatrix} \tag{207}$$

Contrary to the reduction in the number of coordinates, the system size is extended by the number of compatibility constraints. Also, it leads to some extraneous system frequencies and mode shapes.

The system size reduction can be achieved by applying Guyan condensation to the system Equation (207). This involves assumptions concerning the inertia and mass of the condensed out DOFs and also the reduction is nonunique. An inappropriate selection of master DOFs may lead to meaningless results.

5.2.2.2 Elimination of Coordinates

The rectangular matrix [A] of Equation (205) is partitioned into an invertible, nonsingular, square matrix $[A]_D$ and the remainder $[A]_I$, the coordinate vector {q} is also partitioned likewise. Then, since

$$\begin{bmatrix} [A]_D [A]_I \end{bmatrix} \begin{Bmatrix} q_D \\ q_I \end{Bmatrix} = \{0\}$$

$$\{q\}_D = -[A]_D^{-1}[A]_I\{q\}_I$$

and therefore

$$\{q\} = \begin{bmatrix} \begin{bmatrix} -[A]_D^{-1}[A]_I \end{bmatrix} \\ [I] \end{bmatrix} \{q\}_I \tag{208}$$

or,

$$\{q\} = [T]\{\hat{q}\}$$

which leads to system equations in $\{\hat{q}\}$ coordinates alone at the expense of computations implied in Equation (208). Note that the coefficients of matrix [A] are the connection point modal coefficients, finding an invertible partition of which may present computational difficulties.

5.2.2.3 Orthogonal Complement Method

The coordinate reduction transformation [T] is generated by means of an orthogonal complement of [A]. The orthogonal complement $[\beta]$ of [A] consists of the eigenvectors corresponding to the zero eigenvalues of the following problem:

$$[A]^T[A]\{q\} = \lambda\{q\} \tag{209}$$

The uncoupled system coordinates may then be represented in terms of the coupled coordinates $\{\hat{q}\}$ through the relation $\{\hat{q}\} = [\beta]\{q\}$. The size of the above eigenproblem is equal to the total number of generalized coordinates in the system. Further, due to roundoff errors the zero eigenvalues may not be discernible from small eigenvalues.

5.2.2.4 Elastic Coupling Element

Between each DOF to be coupled an artificial coupling spring is introduced which leads to coupled system equation as

$$[M]_q\{\ddot{q}\} + \left[[K]_q + [\Delta K]\right]\{q\} = \{f\}_q \tag{210}$$

where $[\Delta K]$ is additional stiffness due to coupling spring given as

$$[\Delta K] = [\Phi]_C^T[K]_C[\Phi]_C \tag{211}$$

where

$$[\Phi]_C = \begin{bmatrix} [\Phi]_{\uparrow C}^A & [0] \\ [0] & [\Phi]_{\uparrow C}^B \end{bmatrix}$$

is the matrix of modal coefficients corresponding to coupling DOFs. $[\Phi]_{\uparrow C}^A$ and $[\Phi]_{\uparrow C}^B$ are the row partition corresponding to the connection DOFs of the modal matrices for the components A and B respectively and $[K]_C$ is the stiffness of the coupling spring. The nature of the coupled system so obtained may be altered drastically by an inappropriate choice of the coupling spring stiffness.

In view of the above, it is obvious that the direct matrix assembly procedure of coupling component coordinates is the most efficient and exact. All other methods introduce added computations and/or approximations. In order to be able to use the direct matrix assembly procedure, it is necessary to have the connection DOFs explicitly represented in the component dynamics model. On the other hand, the dynamic representation given in Equation (170) is more practical and obtainable from experimental tests. The superelement dynamic reduction procedure developed in the following section makes use of the dynamic model given by Equation (170) and reduces it to a form amenable to direct matrix assembly procedure. All the component dynamic models described in Section 5.2.1 are reducible to this form, thus leading to a unified treatment for any general component representation.

5.2.3 Superelement Model Reduction

In this section the mathematical transformations are derived for reducing the component dynamic models to a form involving physical DOFs of the connection interface nodes plus some additional DOFs related to the interior nodes. The component dynamic models in this reduced form possess a structure similar to that of the displacement finite element method and are therefore termed superelements. The superelement components can be assembled to other similarly reduced components by the direct stiffness method, leading to an efficient and exact component dynamics synthesis. Four different types of component dynamic models are considered in the following: (1) finite element model; (2) fixed interface modal model with static constraint modes; (3) free interface modal model with residual flexibility attachment modes; and (4) free interface model with normal modes alone. The superelement reduction procedure can also be applied to the component dynamic models involving other than normal modes of the component as long as certain requirements for matrix partitioning and invertibility are satisfied, the model type 4 above includes this model as well. A system may involve any combination of the above types of component dynamics model since the models are reduced to a common form before assembly. Furthermore, the component dynamic models chosen above are such that the component independence is preserved. Thus the superelement method leads to a very general synthesis procedure.

The finite element model described in Equation (168) or in partitioned form by Equation (169) naturally contains the connection interface DOFS and is already in the required superelement form.

The constrained interface modal model described by Equations (194) through (201) is also in the required superelement form since the generalized coordinates associated with the constraint modes are the physical DOFs of the connection interface nodes as seen in Equation (197). It should be noted that as the number of modes in $[\Phi]_K$ is reduced, the transformation relation, Equation (195), shrinks to just the static constraint modes and the fixed interface model degenerates to a Guyan reduced component. Likewise, as the number of kept normal modes in $[\Phi]_K$ is increased, the Equation (195) approaches an exact transformation. Selection of these normal modes accounts for the accuracy of the constrained interface superelement.

Next, consider the free interface modal model with residual flexibility attachment modes. The displacement transformation of Equation (189) can be written in partitioned form as

$$\begin{Bmatrix} X_O \\ X_B \end{Bmatrix} = \begin{bmatrix} [\Phi]_{KO} & [G]_{OB} \\ [\Phi]_{KB} & [G]_{BB} \end{bmatrix} \begin{Bmatrix} q_K \\ q_B \end{Bmatrix} \tag{212}$$

To obtain the superelement reduction transformation, solve the lower partition of the equation for $\{q\}_B$. Thus,

$$\{q\}_B = -[G]_{BB}^{-1}[\Phi]_{KB}\{q\}_K + [G]_{BB}\{x\}_B \tag{213}$$

and therefore,

$$\begin{Bmatrix} q_K \\ q_B \end{Bmatrix} = [T]_2 \begin{Bmatrix} q_K \\ q_B \end{Bmatrix} \tag{214}$$

where

$$[T]_2 = \begin{bmatrix} [I] & [0] \\ \left[-[G]^{-1}_{BB}[\Phi]_{KB}\right] & \left[[G]^{-1}_{BB}\right] \end{bmatrix} \tag{215}$$

The above transformation reduces the residual flexibility attachment model to the superelement form. The net transformation can be obtained by combining Equations (212) and (214), leading to

$$\begin{Bmatrix} x_O \\ x_B \end{Bmatrix} = [T] \begin{Bmatrix} q_K \\ x_B \end{Bmatrix} \tag{216}$$

where

$$[T] = \begin{bmatrix} \left[[\Phi]_{KO} - [G]_{OB}[G]^{-1}_{BB}[\Phi]_{KB}\right] & \left[[G]_{OB}[G]^{-1}_{BB}\right] \\ [0] & [I] \end{bmatrix} \tag{217}$$

The generalized coordinates $\{q\}_K$ are now the participation factors of the modified modes $([\Phi]_{KO} - [G]_{OB}[G]^{-1}_{BB}[\Phi]_{KB})$ The internal partitions of the modified normal modes are in effect free interface normal mode partitions minus a set of constraint modes internal partitions and therefore represent modes constrained at boundary degrees of freedom. Note the similarity of the transformation of Equation (216) with that of Equation (194). It can be shown that the $\begin{bmatrix} [G]_{OB}[G]_{BB}^{-1} \\ [I] \end{bmatrix}$ partition of the transformation is in fact the matrix of residual constraint modes [73], which represents the static deflection of the component due to the residual portion of the stiffness matrix resulting from a unit displacement at each of the boundary degrees of freedom. The superelement equations of motion are obtained by transforming the Equation (168) leading to

$$\begin{bmatrix} \left[[M]_{KK} + [\Phi]^T_{KB}[J]_{BB}[\Phi]_{KB}\right] & \left[-[\Phi]^T_{KB}[J]_{BB}\right] \\ sym. & [J]_{BB} \end{bmatrix} \begin{Bmatrix} \ddot{q}_K \\ \ddot{x}_B \end{Bmatrix} \tag{218}$$

$$+ \begin{bmatrix} \left[\lceil \Lambda \rfloor_{KK} + [\Phi]^T_{KB}[G]^{-1}_{BB}[\Phi]_{KB}\right] & \left[-[\Phi]^T_{KB}[G]^{-1}_{BB}\right] \\ sym. & [G]^{-1}_{BB} \end{bmatrix} \begin{Bmatrix} q_K \\ x_B \end{Bmatrix} = \begin{Bmatrix} 0 \\ f_B \end{Bmatrix}$$

where

$$[J]_{BB} = [G]^{-1}_{BB}[H]_{BB}[G]_{BB}.$$

The modification of the component generalized mass and stiffness matrices by the contributions from the residual flexibility of the deleted modes is clearly seen in the above equation. To recapitulate, $[M]_{KK}$ and $\lceil \Lambda \rfloor_{KK}$ are generalized mass and stiffness matrices respectively. $\lceil \Lambda \rfloor_{KK}$ and $[H]_{BB}$ are the generalized stiffness and mass associated with the residual flexibility attachment modes obtained from transformations given in Equation (192).

In the event only a truncated set of free interface normal modes is used to represent component displacements, the superelement reduction transformation is obtained from a partial inversion of the modal matrix as described in the following. Consider the free interface normal mode transformation

$$\begin{Bmatrix} x_O \\ x_B \end{Bmatrix} = \begin{bmatrix} [\Phi]_{KO} \\ [\Phi]_{KB} \end{bmatrix} \{q\}_K \tag{219}$$

where $[\Phi]_{KO}$ and $[\Phi]_{KB}$ are $(n_O \times m_K)$ and $(n_B \times m_K)$ size partitions of the component modal matrix corresponding to the interior and boundary degrees of freedom $\{x\}_O$ and $\{x\}_B$, respectively. Consider the lower portion of Equation (219),

$$\{x\}_B = [\Phi]_{KB}\{q\}_K \tag{220}$$

and partition $[\Phi]_{KB}$ into a nonsingular invertible square matrix $[\Phi]_{KB1}$ and remainder $[\Phi]_{KB2}$. Thus,

$$\{x\}_B = \begin{bmatrix} [\Phi]_{KB1} & [\Phi]_{KB2} \end{bmatrix} \begin{Bmatrix} q_{K1} \\ q_{K2} \end{Bmatrix} \tag{221}$$

which requires that the number of kept modes be greater than the number of boundary degrees of freedom. Solving the above equation for $\{q\}_{K1}$ gives

$$\{q\}_{K1} = -[\Phi]_{KB1}^{-1}[\Phi]_{KB2}\{q\}_{K2} + [\Phi]_{KB1}^{-1}\{x\}_B \tag{222}$$

and

$$\{q\}_K = \begin{Bmatrix} q_{K1} \\ q_{K2} \end{Bmatrix} = \begin{bmatrix} \left[-[\Phi]_{KB1}^{-1}[\Phi]_{KB2}\right] & \left[[\Phi]_{KB1}^{-1}\right] \\ [I] & [0] \end{bmatrix} \begin{Bmatrix} q_{K2} \\ X_B \end{Bmatrix} \tag{223}$$

or

$$\{q\} = [T]_2 \begin{Bmatrix} q_{K2} \\ X_B \end{Bmatrix} \tag{224}$$

The generalized coordinates $\{q\}_{K2}$ are called reduced modal coordinates since they are associated with modified modes as seen in the above equation. Combining Equations (219) and (224), a net transformation from physical coordinates $\{X\}$ to free interface normal mode superelement coordinates can be written as

$$[T] = [\Phi]_K[T]_2 = \begin{bmatrix} \left[-[\Phi]_{KO1}[\Phi]_{KB1}^{-1}[\Phi]_{KB2} + [\Phi]_{KO2}\right] & \left[[\Phi]_{KO1}[\Phi]_{KB1}^{-1}\right] \\ [0] & [I] \end{bmatrix} \tag{225}$$

where $[\Phi]_{KO1}$ and $[\Phi]_{KO2}$ are partitions of $[\Phi]_{KO}$ created using the partitioning information generated in Equation (221). Analogous to Ritz transformation for constrained interface modal model Equation (194) and the transformation for residual flexibility modal model Equation (217), the left and right partitions of the transformation of Equation (225) may be interpreted as expressing modal matrices of modified normal modes and boundary constraint modes, respectively. The component equations of motion in superelement coordinates ($\{q\}_2$, $\{x\}_B$) are obtained from pre- and post-multiplication of Equation (169) with the transformation [T] of Equation (225).

$$[T]^T \begin{bmatrix} [M]_{OO} & [M]_{OB} \\ [M]_{BO} & [M]_{BB} \end{bmatrix} [T] \begin{Bmatrix} \ddot{q}_{K2} \\ \ddot{x}_B \end{Bmatrix} + [T]^T \begin{bmatrix} [K]_{OO} & [K]_{OB} \\ [K]_{BO} & [K]_{BB} \end{bmatrix} [T] \begin{Bmatrix} q_{K2} \\ x_B \end{Bmatrix} = [T]^T \{f\} \tag{226}$$

or alternately using Equation (221) and transforming the modal equilibrium Equation (171).

$$[T]_2^T \begin{bmatrix} [M]_{q11} & [M]_{q12} \\ [M]_{q21} & [M]_{q22} \end{bmatrix} [T]_2 \begin{Bmatrix} \ddot{q}_{K2} \\ \ddot{x}_B \end{Bmatrix} + [T]_2^T \begin{bmatrix} [K]_{q11} & [K]_{q12} \\ [K]_{q21} & [K]_{q22} \end{bmatrix} [T]_2 \begin{Bmatrix} q_{K2} \\ x_B \end{Bmatrix} = [T]_2^T [\Phi]_K^T \{f\} \tag{227}$$

where full generalized mass and stiffness matrices are used to include the case where the columns of the modal matrix in Equation (170) are not orthogonal. (Mass and stiffness loaded component modes are nonorthogonal with respect to the original unloaded mass and stiffness matrices, for example.)

It is to be emphasized again that the reduced modal representation given in Equations (224) through (227) is obtainable from any given free interface modal representation provided the partitioning conditions leading to Equation (222) can be met. The columns of modal matrix in Equation (219) need not be normal modes. The only necessary condition is that they be linearly independent, adequate in number, and be from a complete set, i.e., a linear combination of them should be capable of representing the deformation shapes of the component undergoing motion within the compound of the built-up system.

5.2.4 Superelement Synthesis

The superelement reduction procedures described in the preceding section yield component models with a common characteristic: the boundary degrees of freedom are explicitly retained and the internal degrees of freedom are transformed to reduced generalized coordinates. The equations of motion of a superelement component can be expressed as

$$\begin{bmatrix} [M]_{qq}^{(\alpha)} & [M]_{qB}^{(\alpha)} \\ sym. & [M]_{BB}^{(\alpha)} \end{bmatrix} \begin{Bmatrix} \ddot{q}^{(\alpha)} \\ \ddot{x}_B^{(\alpha)} \end{Bmatrix} + \begin{bmatrix} [C]_{qq}^{(\alpha)} & [C]_{qB}^{(\alpha)} \\ sym. & [C]_{BB}^{(\alpha)} \end{bmatrix} \begin{Bmatrix} \dot{q}^{(\alpha)} \\ \dot{x}_B^{(\alpha)} \end{Bmatrix} \tag{228}$$

$$+ \begin{bmatrix} [K]_{qq}^{(\alpha)} & [K]_{qB}^{(\alpha)} \\ sym. & [K]_{BB}^{(\alpha)} \end{bmatrix} \begin{Bmatrix} q^{(\alpha)} \\ x_B^{(\alpha)} \end{Bmatrix} = \begin{Bmatrix} 0 \\ f_B^{(\alpha)} \end{Bmatrix}$$

or

$$[M]^{(\alpha)} \{\ddot{p}\}^{(\alpha)} + [C]^{(\alpha)} \{\dot{p}\}^{(\alpha)} + [K]^{(\alpha)} \{p\}^{(\alpha)} = \{f\}^{(\alpha)}$$

Each component substructure of a given built-up system can be expressed in the above format. Analogous to the matrix equation of a displacement based finite element model, the generalized coordinates may be interpreted as internal DOFs. Assuming that the global structure as partitioned into N components, the assembled global matrices [M], [C], [K] relating the global displacement vector {x} and the global force vector {F} can now be synthesized by the direct stiffness approach from the component matrices of Equation (228). The direct stiffness approach postulates equal nodal displacement and nodal equilibrium of forces at the connection interfaces of adjacent components, thus

$$\{x\}_B^{(\alpha)} = \beta_B^{(\alpha)}\{x\}_B$$

$$\{f\}_B = \sum_{m}^{N} = 1\beta_B^{(\alpha)}\{f\}_B^{(\alpha)}$$

No compatibility conditions exist among the reduced generalized coordinates $\{q\}^{(\alpha)}$ and remain intact. The coupled system coordinate vector thus becomes

$$\{x\}^T = \left\{\{q\}^{(1)^T}, \{q\}^{(2)^T} \dots, \{q\}^{(N)^T}\{x\}_B^T\right\} \tag{230}$$

so that the global mass, damping, and stiffness matrices are given by

$$\begin{aligned} [M] &= \sum_{\alpha=1}^{N}[\beta]^{(\alpha)^T}[M]^{(\alpha)}[\beta]^{(\alpha)} \\ [C] &= \sum_{\alpha=1}^{N}[\beta]^{(\alpha)^T}[C]^{(\alpha)}[\beta]^{(\alpha)} \\ [K] &= \sum_{\alpha=1}^{N}[\beta]^{(\alpha)^T}[K]^{(\alpha)}[\beta]^{(\alpha)} \end{aligned} \tag{231}$$

where $[\beta]^{(\alpha)}$ is the portion of the component to global transformation matrix $[\beta]$ corresponding to the α^{th} component.

$$\begin{aligned} \{Y\} &= [\beta]\{x\} \\ [\beta]^{(\alpha)} &= \begin{bmatrix} [0] \dots & [I]^{(\alpha)} & [0] & \dots \\ [0] \dots & [0] & [0] & \dots [\beta]_B{}^{(\alpha)} \end{bmatrix} \end{aligned} \tag{232}$$

$\{Y\}$ being the vector of uncoupled superelement coordinates.

$$\{Y\}^T = \left\{\{q\}^{(1)^T}\{x\}_B{}^{(1)^T} \quad \{q\}^{(2)^T}\{x\}_B{}^{(2)^T} \quad \dots \{q\}^{(N)^T}\{x\}_B{}^{(N)^T}\right\} \tag{233}$$

and $[\beta]_B{}^{(\alpha)}$ representing the compatibility conditions for the degrees of freedom at the boundaries of the component α.

The built-up system mass, damping, and stiffness matrices are of the following form:

$$[A] = \begin{bmatrix} [a]_{qq}^{(1)} & [0] & [0] & \cdot\cdot & [a]_{qB}^{(1)} \\ [0] & [a]_{qq}^{(1)} & [0] & \cdot\cdot & [a]_{qB}^{(2)} \\ \cdot & [0] & \cdot & \cdot & \cdot \\ \cdot & \cdot & \cdot & \cdot & \cdot \\ \cdot & sym. & \cdot & [a]_{qq}^{(N)} & [a]_{qq}^{(N)} \\ \cdot & \cdot & \cdot & \cdot & [a]_{BB} \end{bmatrix} \tag{234}$$

where the coefficients $a_{ij}^{(\alpha)}$ are the mass, damping, or stiffness coefficients matrices given in Equation (228), and [A] is the corresponding global matrix. The diagonal submatrices $[a]_{qq}^{(\alpha)}$ in Equation (234) correspond to the reduced generalized coordinates of the components and are uncoupled from other components.

$$[a]_{BB} = \sum_{\alpha=1}^{N} [\beta]_B^{(\alpha)T} [a]_{BB}^{(\alpha)} [\beta]_B^{(\alpha)}$$

The submatrices are symmetric and, in general, fully populated. The system governing equations can be expressed as

$$[M]\{\ddot{x}\}+[C]\{\dot{x}\}+[K]\{x\} = \{f\} \tag{235}$$

which itself is in a superelement form since the system basis coordinate {x} contains the boundary degrees of freedom explicitly. This is particularly useful from the standpoint of coupling the system of Equation (235) to a higher level superelement.

Next, the recovery of component displacements from the system displacement vector {x} is considered. The process is essentially back substitution. The superelement displacement ($\{q\}^{(\alpha)T} \{x\}_B^{(\alpha)T}$) is recovered from the system displacement vector {x} using Equations (229) and (230). The use of superelement transformations and component transformations described in Sections 5.2.3 and 5.2.1 leads to the recovery of component displacements. The software implementation of the superelement synthesis method is described in the Appendix B.

5.3 Summary and Conclusions

This Section documents analytical investigations and software developments aimed at providing an improved procedure for component dynamic synthesis from test and/or analysis derived component dynamic models.

A set of consistent Ritz transformations was derived that lead to an exact, efficient and unified procedure for coupling component dynamic models. A broad class of test and/or analysis derived component dynamic models were considered in this work. These dynamic models are compatible with the state of the art experimental modal testing as well as analytical procedures and permit improvement of synthesis accuracy through the inclusion of flexibility, inertia and damping corrections of truncated high frequency modes in the component dynamic models. The synthesis procedure developed in this work may be considered as a generalization of the Craig-Bampton method to include free interface normal modes, residual flexibility attachment modes, loaded interface normal modes, and any general type of component modes or admissible shapes that adequately represent the dynamics of a component. Several existing methods such as MacNeal's method, and Rubin's method are shown to be the particular cases of the generalization presented in this work. As a result of this generalization, the different components of a built-up system may be characterized using any type of dynamic model which is most convenient regardless of the manner in which the other components are characterized. Furthermore the component coupling is exact and computationally efficient; no artificial coupling element or the user specification of independent coordinates is required. The developed procedure is implemented in a stand alone computer program COMSYN in Appendix C.

The component dynamics reduction method developed in this work transforms the component dynamic coordinates to the superelement coordinates containing the physical coordinates of the connection interfaces as well as any desired noninterface points. As a result of this reduction procedure the component subsystems take the form of a finite element. It is therefore possible to obtain system synthesis even with nonlinear components. The addition of the necessary data handling and solution algorithms to treat nonlinear components will greatly enhance the capabilities of COMSYN. It is recommended as a further work.

6. PRACTICAL EXAMPLES

Three examples are presented in this section to demonstrate the practical application of the theories outlined in previous chapters.

6.1 Example 1: Structural Dynamics Modification Using System Modeling Techniques

This section presents the conditions and results of the experimental testing and modeling of a H frame completed to form a practical analysis and comparison of the techniques investigated in Sections 2 and 4. Results of finite element analysis, modal modeling, component mode synthesis, and, impedance modeling using frequency response functions are summarized in Tables 2 through 6. All models are compared to experimental results as a basis to evaluate and compare the technique.

6.1.1 Development of the Experimental Modal Model

The test structure used in the modal analysis is an H frame structure (see Figure 1) constructed of two by six inch rectangular steel tubing. Bolted to each leg of the structure is a ten by eleven by one inch aluminum end plate. The combined weight of the structure with end plates is approximately 250 pounds. This structure was used in the analysis primarily because its welded steel construction closely approximates a true linear system, a basic assumption with all modeling routines. In addition , the simple geometry of the structure is easily described in the analytical model.

Preliminary analysis indicated 20 - 25 modes existing in the frequency range from 0 - 512 Hertz. Figure 2 shows a typical driving point frequency response function of the unmodified structure. Based on the modal density of the structure, resolution of 1 Hertz at this frequency range was considered sufficient to accurately identify each of the modes.

One important characteristic of this structure noted during the preliminary analysis was that the vertical and lateral modes of the structure were highly uncoupled. Because of this , three complete multi-point, burst random modal surveys were performed on the structure using dual inputs in the vertical, lateral , and skewed directions. Burst random excitation was used to minimize the leakage errors associated with the lightly damped structure.

The modal parameters from the skewed input test were extracted using the polyreference time domain algorithm [74]. Information from this skewed test generated one complete modal model since it contained both the lateral and vertical modes. The modal parameters from the lateral and vertical input test were calculated using the polyreference time domain algorithm and merged to generate a second model of the structure. This model was used primarily for reference in the analysis. Table 1 lists the frequency , damping, and modal vectors descriptions for the 19 modes of the baseline data set.

6.1.2 Rotational Degrees of Freedom

Because the aluminum end plates were known to remain rigid over the entire frequency range of interest, a rigid body program was used to generate a least squares fit of the rigid plate motion using all available measurements. In addition to generating enhanced modal vectors of the rigid bodies, the program was used to determine rotational degrees of freedom associated with each rigid body. These rotational degrees of freedom were then stored as new measurement degrees of freedom located at the center of gravity of each plate. When incorporated into the modal model, these rotational degrees of freedom improve the results of the predicted mode shapes by adding rotational constraints to the model. Ignoring these rotational degrees of freedom tends to result in high estimates of the predicted natural frequencies (especially for those modes with high rotations at the end plates) due to lack of rotational mass moment of inertia in the model. Table 2 shows the results of mass modification (the addition of 28 pound steel masses bolted to the end plates in the long ends of the H frame) using the Snyder method both with and without the rotational information included in the model.

6.1.3 Hardware Modifications

The remainder of this section presents the results of the modeling phase of these practical applications. The procedure and detail of the modifications are discussed to highlight the capabilities and limitations of each technique. The results of the various modeling programs are compared with the results of the experimental tests of the modified structure. In addition, a finite element model was constructed using SMS FESDEC finite element code. This model was tuned to match the dynamic characteristics from the baseline experimental data. Each physical modification to the structure was also performed in the analytical model and these results are included in the analysis. A percent error is calculated for each eigenvalue by dividing the difference between the experimental retest frequency and the predicted frequency by the experimental retest frequency. A more thorough comparison would include a comparison of the damping values and the computed correlation coefficients between the experimental and predicted eigenvectors.

Four modifications were implemented on the H frame to evaluate the effectiveness of the various modeling techniques. All of these modifications to the structure were made at the rigid end plates to take advantage of the calculated rotational degrees of freedom and improved modal coefficients. The experimental tests of the modified structure were multi-reference impact tests. Two triaxial accelerometers were mounted to the structure and the frequency response matrix was generated by roving the impact to generate the modified data base. The modal parameters of this modified data base were extracted using the polyreference time domain algorithm.

The first of the modifications investigated was a long thin steel rod with negligible bending stiffness connected across the two end plates on the long end of the H frame. This modification was modeled as a simple scalar stiffness, or spring element in the analytical models. Table 3 summarizes the results of the stiffness modeling results (using SDM, SYSTAN and SMURF) compared with the experimental re-test and finite element results.

The second modification investigated was the addition of 28 pound steel masses bolted to the two end plates on the long end of the H frame. These masses were modeled as lumped mass elements with the correct inertia properties about each of the three principle axis. These lumped mass elements were applied to the model at the center of the end plates to use the rotational information previously calculated for these points. Table 4 summarizes the results of the mass modification (using SDM and SYSTAN). Note that the frequency response method of general impedance modeling (SMURF) was not investigated for the mass modification, since only a single constraint equation can be modeled at one time.

The final two modifications involved elements that required a more detailed description of their properties. The first of these was a two and one half inch by one half inch beam having mass and stiffness properties in all directions connected across the long end of the H frame. The last modification involved the connection of a ten by one quarter inch steel plate across the two end plates on the long end of the H frame. Because these two modifications required matrix descriptions of their mass and stiffness properties, only the Component Mode Synthesis (SYSTAN) and finite element solutions were evaluated. The results of these modifications are summarized in Tables 5 and

6.1.4 Discussion of Modification Results

In general, the SYSTAN results compared best with the experimental test of the modified structure(s). The average error for each of the modifications were: stiffness - 2.8 %, mass - 1.1 %, beam - 3.0 %, and the plate - 3.6 %. The SMURF technique yielded excellent results for the single modification investigated. The average error was 1.7%. All of the techniques predicted the modifications within the realm of experimental accuracy. As the complexity of the modification increased the results deteriorated somewhat. This application has demonstrated that all of the methods used produce accurate results when used properly with good modal data and procedure used to obtain accurate results. More rigorous applications will determine the upper bounds of the capabilities of each of the techniques.

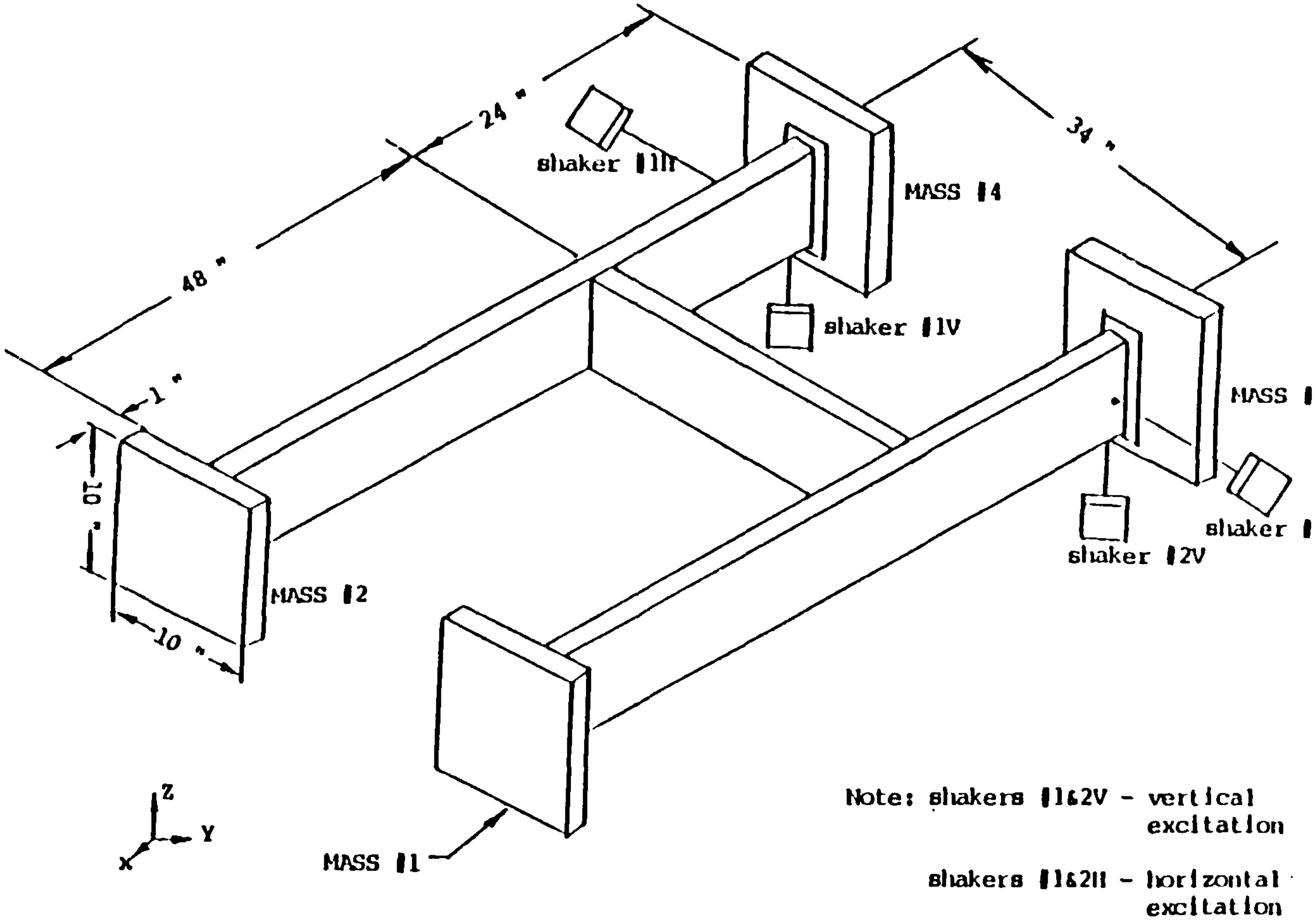

Figure 1. Sketch of the H frame

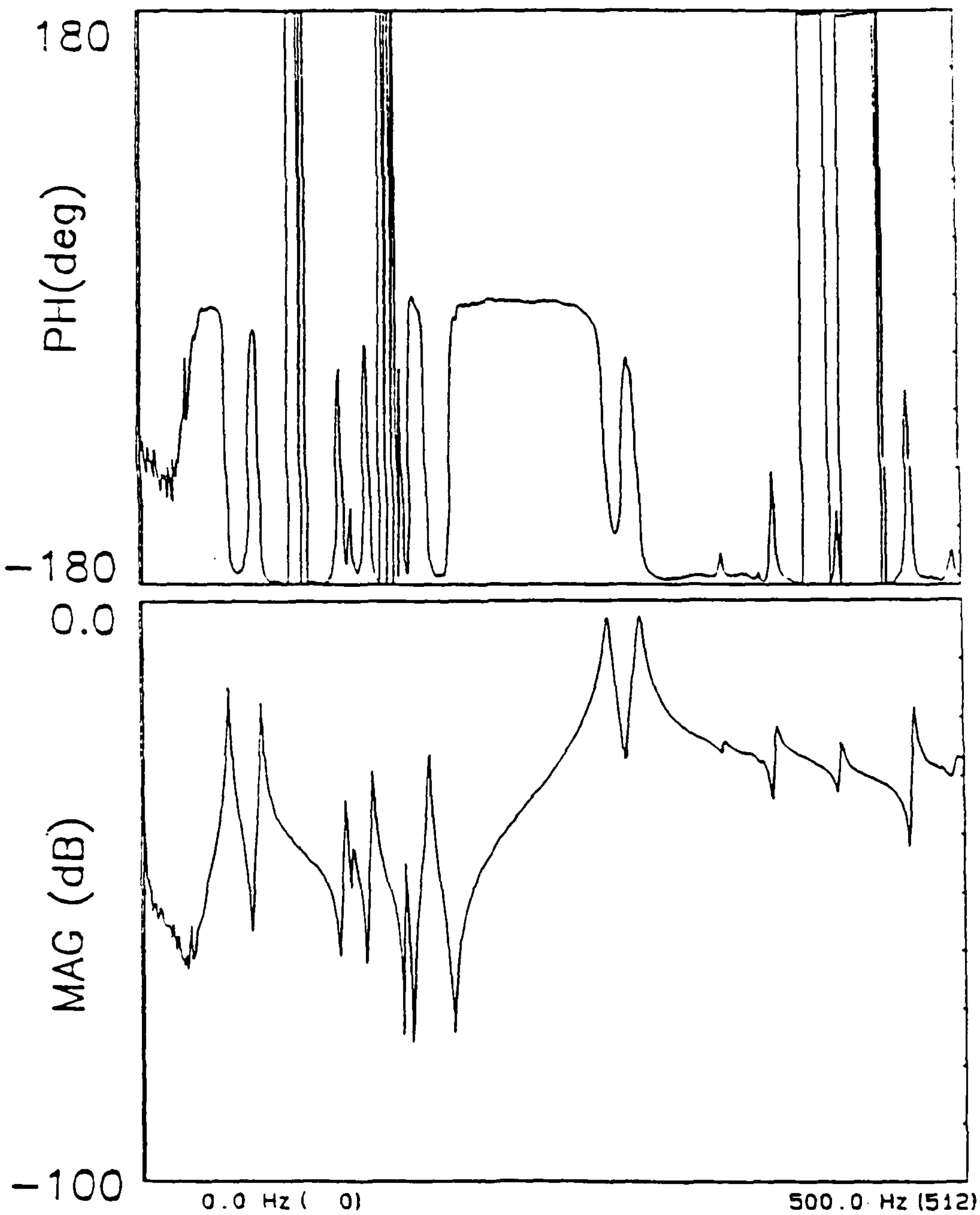

Figure 2. Typical Driving Point Frequency Response Function

TABLE 1. H frame Baseline Test Results

Mode	Frequency	Damping (%)	Description
1	14.8	0.7	1st lat. - rigid legs anti.
2	24.1	0.1	1st torsion - legs rigid
3	36.6	0.2	1st shearing
4	55.3	0.1	2nd lat. - 1st full frame anti.
5	77.4	0.1	3rd lat. - 1st full frame sym.
6	158.5	0.1	4th lat. - 2nd full frame anti.
7	162.6	0.2	1st vert. - 1st full frame sym.
8	169.5	0.2	2nd vert. - 1st full frame anti.
9	191.0	0.4	1st twist long leg - anti.
10	193.9	0.1	5th lat. - 2nd full frame sym.
11	209.1	0.4	2nd twist long legs - sym.
12	297.5	0.3	1st twist short legs - anti.
13	309.1	0.4	2nd twist short legs - anti.
14	312.6	0.1	X bar fore & aft bending
15	417.8	0.1	6th lat. - 3rd full frame sym.
16	434.1	0.1	3rd vert. -2nd full frame sym
17	438.1	0.1	7th lat. - 3rd full frame anti.
18	480.9	0.1	4th vert. - 2nd full frame anti.
19	486.1	0.1	8th lat. - 4th full frame anti.

TABLE 2. The Effects of RDOF on Modeling Results (Adding Masses)

Mode	Exp.	Snyders Method (SDM)		Description
	ω_r	ω_r w/RDOF	ω_r w/o RDOF	
1	10.50	10.85	10.87	1st lat-anti rigid
2	19.40	19.95	19.95	1st torsion
3	30.20	29.71	29.79	1st shearing
4	52.80	53.27	53.35	2nd lat-l anti
5	72.60	72.02	72.44	3rd lat-l sym
6	122.40	113.13	189.62	1 tw long-anti
7	126.80	117.77	204.81	2 tw long-sym
8	139.40	142.81	148.60	4th lat-2 anti
9	146.10	144.04	144.51	1st vertical
10	159.70	159.11	159.38	2nd torsion
11	174.20	179.14	184.28	5 lat-2 sym
12	281.80	287.22	295.80	1 tw short-anti
13	299.90	302.42	308.60	2 tw short-sym
14	370.20	387.12	307.70	6 lat-3 sym
15	382.50	397.32	413.61	7 lat-3 anti
16	395.80	400.62	411.39	3rd ver-2 sym
17	343.40	457.11	467.64	4 ver-2 anti
18	476.50	478.96	485.75	8 lat-4 anti

TABLE 3. Stiffness Modification Modeling Results (Steel Thin Rod)

Mode	Exp.	FESDEC		SDM		SYSTAN		SMURF		Description
	ω_r	ω_r	% error	ω_r	%error	ω_r	% error	ω_r	% error	
1	24.2	23.7	2.1	23.8	1.7	24.1	0.4	25.6	5.8	1st torsion
2	36.6	37.3	1.9	36.1	1.4	36.5	0.3	36.6	0.5	1st shearing
3	49.9	50.6	1.4	48.2	3.4	50.9	2.0	49.9	2.6	1 lat-1 anti
4	77.5	78.7	1.5	64.5	17.0	77.4	0.1	77.5	0.8	2 lat-1 sym
5	93.4	94.5	1.2	91.7	1.8	96.0	2.8	93.4	6.8	3 lat-2 anti
6	161.6	167.8	3.8	159.8	1.1	162.0	0.2	161.6	1.4	4 lat- 2 anti
7	164.3	169.5	3.2	162.7	0.7	164.0	0.2	164.3	0.1	1 ver-1 sym
8	168.1	176.1	4.8	171.8	2.2	169.2	0.7	186.1	0.9	2 ver-1 anti
9	191.8	198.3	3.4	193.7	1.0	194.0	1.1	191.8	1.5	5 lat-2 sym
10	211.8	216.0	2.0	201.1	6.1	209.0	1.3	211.8	0.9	1 tw l-sym
11	276.3	289.9	4.9	292.4	5.8	267.0	3.6	276.3	2.2	1 tw s-anti
12	308.9	304.4	1.2	306.1	0.6	308.0	3.2	308.0	3.2	2 tw s-sym
13	312.3	336.4	7.7	312.0	0.1	312.0	0.1	312.3	0.2	X-bar bend
14	417.7	418.1	0.1	417.1	0.1	417.0	0.2	417.7	0.2	6 lat-3 sym
15	434.0	442.6	4.9	430.9	0.7	429.0	1.2	434.0	0.0	3 ver-2 sym
16	453.1	452.9	0.4	438.0	3.3	435.0	4.0	453.0	3.5	7 lat-3 anti
17	480.1	490.5	2.2	475.2	1.0	480.0	0.0	480.1	0.0	4 ver-2 anti
18	489.6	491.9	0.5	485.8	0.8	482.0	1.6	489.6	0.0	8 lat- 4 anti

TABLE 4. Mass Modification Modeling Results (Adding Steel Plates)

Mode	Exp.	FESDEC		SDM		SYSTAN		SMURF		Description
	ω_r	ω_r	% error	ω_r	%error	ω_r	% error	ω_r	% error	
1	10.6	10.6	0.0	10.9	0.3	10.6	0.0	N/A		1 lat-anti rigid
2	19.4	19.7	1.6	19.9	2.8	19.4	0.0			1st torsion
3	30.0	31.5	4.3	29.7	1.7	29.2	3.3			1st shearing
4	52.9	53.6	1.5	53.3	0.9	53.3	0.9			2nd lat-l anti
5	72.7	74.9	3.2	72.0	0.8	71.5	1.5			3 lat-l sym
6	122.3	130.3	6.5	113.1	7.6	113.0	7.6			1 tw long-anti
7	126.8	132.1	4.2	117.8	7.1	109.6	14.0			2 tw long-sym
8	139.4	148.3	6.4	142.8	2.4	139.5	0.1			4 lat-2 anti
9	146.2	157.6	7.4	144.0	1.4	141.5	3.1			1 ver-1 sym
10	159.7	154.9	3.0	159.1	0.4	155.7	2.5			2 ver- 1 anti
11	174.2	183.2	5.2	178.1	2.8	164.3	5.7			5 lat- 2 sym
12	281.8	290.4	3.1	281.2	1.9	277.4	1.6			1 tw short-anti
13	299.7	303.6	1.2	302.4	0.8	300.5	0.2			2 tw short-sym
14	302.3	328.1	8.5	305.5	1.1	294.9	2.4			X-bar bending
15	370.1	415.3	12.0	387.7	4.6	383.8	3.7			6 lat-3 sym
16	383.5	435.5	14.0	397.3	1.2	399.2	4.5			7 lat-3 anti
17	395.8	408.7	3.3	400.6	1.2	395.2	0.2			3 ver-2 sym
18	434.4	461.5	6.2	457.1	7.5	441.6	1.7			4 ver-2 anti
19	476.4	-	-	478.9	0.5	477.3	0.2			8 lat-4 anti

TABLE 5. Beam Modification Modeling Results

Mode	Exp.	FESDEC		SDM		SYSTAN		SMURF		Description
	ω_r	ω_r	% error	ω_r	%error	ω_r	% error	ω_r	% error	
1	38.0	38.0	0.0	N/A		38.4	1.1	N/A		1st shearing
2	42.0	40.6	3.4			37.6	10.5			1st torsion
3	51.0	51.7	1.5			52.2	0.4			1st lat-short anti
4	77.0	77.7	0.9			78.1	1.4			2nd lat-1st sym
5	124.9	126.9	1.6			128.0	2.4			1st beam bending
6	154.9	160.0	4.8			155.0	0.0			2nd beam bending
7	167.9	161.9	4.5			170.0	1.7			1st ver-1st sym
8	172.9	179.1	3.5			170.0	1.7			2nd ver-1st anti
9	185.9	192.5	3.6			194.0	3.7			3rd lat-2nd sym
10	196.9	208.7	6.0			213.0	8.1			1st tw long-anti
11	286.9	291.4	1.6			287.0	0.0			1st tw short-anti
12	297.9	304.0	2.0			298.0	0.0			2nd tw short-sym
13	308.9	333.8	8.1			310.0	0.4			X-bar bending
14	366.8	373.1	1.7			381.0	3.8			3rd beam bending
15	406.8	426.6	4.0			428.0	5.2			2nd tw long-sym
16	424.8	429.4	0.6			433.0	1.4			3rd ver-2nd sym
17	426.8	459.5	2.2			459.0	2.1			4th lat-3rd sym
18	449.8	460.4	13.0			475.0	0.8			5th lat-2nd anti
19	470.8	487.8	3.6			482.0	0.8			4th ver-2nd anti
20	477.8	543.0	14.0			484.0	14.0			6th lat-3rd anti

TABLE 6. Plate Modification Modeling Results

Mode	Exp.	FESDEC		SDM		SYSTAN		SMURF		Description
	ω_r	ω_r	% error	ω_r	%error	ω_r	% error	ω_r	% error	
1	34.0	35.3	3.8	N/A		33.4	1.8	N/A		1st shearing
2	42.7	42.2	1.2			40.8	2.5			1st torsion
3	50.5	51.5	1.9			51.6	2.2			1st lat-short anti
4	62.4	66.4	6.4			54.8	18.0			1st plate bending
5	75.0	76.9	2.5			75.4	0.5			2nd lat-1st sym
6	114.9	106.2	7.5			122.0	6.1			1st plate twist
7	136.2	144.5	6.1			141.0	3.5			3rd lat-2nd anti
8	153.5	151.1	1.5			153.0	0.3			1st ver-1st sym
9	160.2	170.5	6.3			155.0	3.1			2nd plate bending
10	170.3	177.2	4.1			168.0	1.4			2nd ver-1st anti
11	193.6	202.5	4.6			186.0	3.9			4th lat 2nd-sym
12	253.7	231.8	8.6			280.0	10.0			2nd plate twist
13	275.3	289.9	5.3			273.0	0.8			1st twist-short anti
14	297.2	303.9	2.3			299.0	0.6			2nd twist-long sym
15	305.1	338.7	11.0			313.0	2.6			X-bar bending
16	319.4	329.5	3.1			311.0	2.5			3rd plate bending
17	392.2	436.6	10.0			404.0	3.1			5th lat-3rd sym
18	407.7	418.4	2.7			413.0	1.8			3rd ver-2nd sym
19	413.8	463.2	12.0			424.0	2.5			6th lat-3rd anti
20	432.7	374.4	14.0			491.0	14.0			3rd plate twist
21	446.9	321.0	30.0			405.0	9.0			Trans plate bending
22	460.3	476.3	3.5			461.0	0.2			4th ver-2nd anti
23	477.6	506.7	1.0			482.0	1.0			7th lat-4th anti

6.2 Example 2: Normalization of Complex Modes using PRA Time Domain Technique

A numerical example to determine a set of normal modes from a given set of complex modes using the time domain principal response analysis technique is demonstrated as follows:

6.2.1 Numerical Example

To demonstrate the validity of the theory outlined in Section 2.8.6, a four degree-of-freedom discrete system is used here to simulate a test structure. Mass, stiffness and damping matrices are assumed as follows:

$$[M]=\begin{bmatrix}3 & 0 & 0 & 0\\ 0 & 2 & 0 & 0\\ 0 & 0 & 1 & 0\\ 0 & 0 & 0 & 2\end{bmatrix},\quad [K]=\begin{bmatrix}200 & -60 & -80 & -40\\ -60 & 340 & -120 & -120\\ -80 & -120 & 800 & 800\\ -40 & -50 & -200 & -200\end{bmatrix},\quad [C]=\begin{bmatrix}3 & -0.9 & -0.6 & -1\\ -0.9 & 3 & -0.8 & -0.5\\ -0.6 & -0.8 & 3 & -0.6\\ -1 & -0.5 & -0.6 & 2.5\end{bmatrix}$$

Complex eigenvalues and eigenvectors are solved and listed in Tables 7 through 10. Real-normalized modes using several subsets of the identified complex modes are also presented in Tables 7 through 10.

From this example of a nonproportionally damped discrete system, it indicates that a set of real-normalized modal vectors can be obtained using the proposed method. Nevertheless, unless all modes are included in the analysis, the results are subject to modal truncation errors.

TABLE 7. First Vibration Mode

First Mode						
Complex Mode f = 1.1598 Hz ζ = 4.79 %		Normal Mode f = 1.1604 Hz				
magnitude	phase,°	analytical normal mode	include all 4 modes	include modes 1,2,3	include modes 1,2,4	include modes 1,2
100	0.	100.	100.	100.	100.	100.
37.136	3.66	37.067	37.067	37.073	37.050	37.051
18.827	3.52	18.825	18.826	18.812	18.830	18.809
8.079	7.33	8.058	8.058	8.071	8.063	8.071

TABLE 8. Second Vibration mode

Second Mode						
Complex Mode f = 2.0472 Hz ς = 6.061 %		Normal Mode f = 2.04502 Hz				
magnitude	phase,°	analytical normal mode	include all 4 modes	include modes 1,2,3	include modes 2,3,4	include modes 1,2
26.473	-173.34	-26.262	-26.263	-26.280	-26.475	-26.227
100.	0.	100.	100.	100.	100.	100.
18.047	2.06	18.047	18.047	18.057	18.066	18.075
7.807	3.88	7.794	7.794	7.801	7.831	7.818

TABLE 9. Third Vibration mode

Third Mode						
Complex Mode f = 3.8228 Hz ς = 3.134 %		Normal Mode f = 3.8237 Hz				
magnitude	phase,°	analytical normal mode	include all 4 modes	include modes 1,2,3	include modes 2,3,4	include modes 3,4
6.210	-167.34	-6.027	-6.027	-5.977	-6.228	-6.226
17.322	-174.47	-17.236	-17.236	-17.220	-17.349	-17.368
77.950	-6.86	78.318	78.318	77.980	78.344	78.381
100.	0.	100.	100.	100.	100.	100.

TABLE 10. Fourth Vibration Mode

Fourth Mode						
Complex Mode f = 4.7423 Hz ς = 5.0067 %		Normal Mode f = 4.75128 Hz				
magnitude	phase,°	analytical normal mode	include all 4 modes	include modes 1,2,4	include modes 2,3,4	include modes 3,4
2.378	-178.57	-2.413	-2.413	-2.363	-2.380	-2.367
6.882	-171.95	-6.813	-6.813	-6.768	-6.805	-6.853
100.	0.	100.	100.	100.	100.	100.
40.241	172.29	-40.552	-40.552	-40.220	-40.547	-40.564

6.3 Example 3: Superelement Dynamics Synthesis Technique

This section presents the results of a numerical study conducted in order to demonstrate the superelement dynamics synthesis procedure developed in Section 5.

Figure 3 shows a discrete spring-mass damper system and its partitioned components. The component A represents a simple model of an aircraft, while that labeled B represents a model of a store to be attached at the tip of the wing. The following types of dynamic models are employed in the study.

Component A

1. Free interface normal modes followed by a transformation to superelement coordinates.
2. Free interface normal modes plus a residual flexibility attachment mode followed by a transformation to superelement coordinates.

Component B

1. Free interface normal modes followed by superelement coordinate transformation.
2. Physical coordinate model.

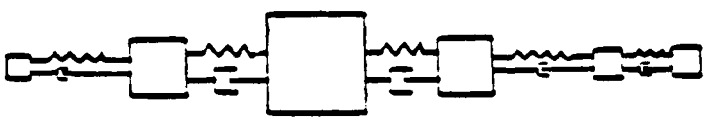

Discrete Spring-Mass Damper System.

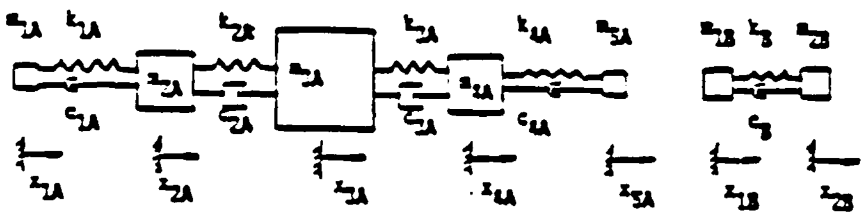

The Separated Components of the Unconstrained System.

$m_{1A} = m_{5A} = 0.1$	$m_{2A} = 36$	$m_{3A} = 100$	$m_{4A} = 40$
$k_{1A} = 60{,}000$	$k_{2A} = 120{,}000$	$k_{3A} = 100{,}000$	$k_{4A} = 50{,}000$
$m_{1B} = 0.2$	$m_{2B} = 0.4$	$k_{1B} = 2{,}000$	

Figure 3. Discrete Spring-Mass System

For comparison purposes the problem is also solved using existing MacNeal Method and Rubin Method of synthesis. The results of the synthesis are shown in Table 11. The exact results are obtained by solving the eigenproblem of the built-up system without partitioning.

TABLE 11. Direct and Synthesized System Natural Frequencies (rad/sec)

Mode No	Exact	Superelement Component Synthesis		MacNeal Method	Rubin Method
		Case I	Case II	Case II	Case II
1	0	0	0	0	0
2	52.417	52.417	52.418	52.419	52.418
3	69.348	69.348	69.829	69.886	69.829
4	72.818	72.818	291.697	504.67	291.697
5	418.029	418.03			
6	775.678	775.678			

Case I: (1 rigid body + 4 elastic modes) of Component A

Case II: (1 rigid body + 1 elastic mode + 1 residual flexibility mode) of Component of B

The superelement synthesis using complete mode sets of the components leads to exact system synthesis as expected. Superelement method using severely truncated component mode set along with residual flexibility attachment modes predicts system frequency with an accuracy better than that of the MacNeal method and equal to that of the Rubin's second order method.

It must be noted that in this study different types of component dynamics models are synthesized by virtue of the superelement formulation, and that the accuracy of system synthesis is entirely governed by the type of component dynamic models and not by the coupling procedure. No further numerical exercises are therefore undertaken to study the accuracy of synthesis with respect to component modes.

7. CONCLUSIONS

Experimental modal analysis developed in the past decade can provide a valid data base used in the application of system modeling techniques. The success of applying system modeling techniques in improving the engineering quality of the industrial products through a design cycle, is dependent on the quality of the experimental data, and the accuracy of the system modeling algorithm used to predict the altered system dynamics of a structure or combined structure(s).

Generally speaking, all system modeling techniques, which include modal or impedance modeling method, sensitivity analysis, and the component mode synthesis method, can predict satisfactory results if a complete and perfect experimental model can be obtained from testing and used as data base for system modeling predictions. In reality, there exists many uncertainties and difficulties in obtaining a complete modal or impedance model representing a physical structure. Difficulties in simulating actual boundary conditions in the testing laboratory, lack of rotational degrees of freedom measurement, incomplete modal model due to limited testing frequency range, nonlinearities existing in the structure under test, scaling errors, and mode overcomplexity, could seriously affect the quality and completeness of the experimentally-derived modal or impedance model. These deficiencies in obtaining a reliable and complete experimental model make the system modeling technique a much less powerful tool in the application of engineering design. In other words, currently, the weakness of applying system modeling techniques comes from those limitations and uncertainties to obtain a desired modal or impedance model of physical structure(s).

At the present time, many efforts have been dedicated by researchers to overcome those deficiencies in obtaining a desired experimental modal or impedance model, such as the development of rotational transducers. Further research and practices are still needed to develop a well-defined engineering procedure and criterion to make the use of the system modeling techniques a more powerful and reliable tool in engineering practices.

REFERENCES

[1] Yasuda, Chiaki, P. J. Riehle, D. L. Brown and R. J. Allemang, *An Estimation Method for Rotational Degrees of Freedom Using Mass Additive Technique,* Proceedings of the 2nd International Modal Analysis Conference, 1984

[2] Wei, M. L., R. J. Allemang and D. L. Brown, *Real-normalization of Measured Complex Modes,* Proceedings of the 5th International Modal Analysis Conference, London, 1987

[3] Kron, G., *Diakoptics* MacDonald, 1963

[4] Weissenberger, J.T., *The Effect of Local Modifications on the Eigenvalues and Eigenvectors of Linear Systems,* D.Sc. Dissertation, Washington University, 1966

[5] Simpson, A. and B. Taborrok, *On Kron's Eigenvalue Procedure and Related Methods of Frequency Analysis,* Quarterly Journal of Mechanics and Applied Mathematics, XXI, 1968,pp. 1-39.

[6] Pomazal, R. J. and V. W. Snyder, *Local Modifications of Damped Linear Systems,* AIAA Journal, IX (1971).

[7] Anonymous, *An Introduction to the Structural Dynamics Modification Systems,* Technical Information Note #1 by Structural Measurement Systems, Inc., February, 1980

[8] Hallquist, J. O. and V. W. Snyder, *Synthesis of Two Discrete Vibratory Systems Using Eigenvalue Modification,* AIAA Journal, XI (1973).

[9] Luk, Y. W. and L. D. Mitchell, *System Modeling and Modification Via Modal Analysis,* Proceedings of the 1st International Modal Analysis Conference, 1982, pp. 423-429

[10] Hallquist, J. O., *Modification and Synthesis of Large Dynamic Structural Systems,* Ph.D. Dissertation, Michigan Tech. University, 1974

[11] Avitabile, P. and J. O'Callahan, *A Structural Modification Procedure Using Complex Modes,* IMAC I, November, 1982, pp. 418-422

[12] De Landsheer, A., *Dynamic Optimization with Modal Analysis,* DYNOPS User Manual, (Spring, 1984.)

[13] O'Callahan, J.C., C. M. Chou and P. Avitabile, *Study of a Local Eigenvalue Modification Procedure Using a Generalized Beam Element,* Proceedings of the 3rd American Control Conference, June, 1984

[14] Anonymous, *Modeling Rib Stiffeners with the Structural Dynamics Modification System,* Application Note 82-1 by Structural Measurement Systems, Inc., 1982

[15] Elliott, K.B. and L. D. Mitchell, *Realistic Structural Modifications: Part I Theoretical Development,* Proceedings of the 3rd International Modal Analysis Conference, 1985, pp. 471-476

[16] O'Callahan, J. C. and C. M. Chou, *Structural Dynamics Modification Using Generalized Beam Mass and Stiffness Matrices,* Proceedings of the 3rd International Modal Analysis Conference, 1985, pp. 477-482

[17] Frazer, R. A., W. J. Duncan and A. R. Collar, *Elementary Matrices,* Cambridge University Press, 1957, p. 289

[18] Smiley, R. G. and B. A. Brinkman, *Rotational Degrees-of-Freedom in Structural Modification,* Proceedings of the 2nd International Modal Analysis Conference, 1984, pp. 937-939

[19] Lieu, I. W., *Determination of Rotational Degrees of Freedom Using Condensation/Expansion Techniques,* M.S. Thesis, Lowell, MA: University of Lowell, 1984

[20] VanHonacker, P., *The Use of Modal Parameters of Mechanical Structures in Sensitivity Analysis, System Synthesis and System Identification Methods,* Ph.D Dissertation (K.U. Leuven, 1980)

[21] O'Callahan, J. C., C. M. Chou and I. W. Lieu, *Determination of Rotational Degrees of Freedom for Moment Transfers in Structural Modifications,* Proceedings of the 3rd International Modal Analysis Conference, 1985, pp. 465-470

[22] Pomazal, R., *The Effect of Local Modification of the Eigenvalues and Eigenvectors of Damped Linear Systems,* Ph.D. Dissertation, Michigan Technological University, 1969

[23] *SDRC Modal Analysis User's Manual, Section 6.2.5*

[24] Arnold, S., *Theory of Linear Models and Multi-variate Analysis* , John Wiley, 1981

[25] Ibrahim, S. R., *Determination of Normal Modes From Measured Complex Modes,* Shock and Vibration Bulletin, Vol. 52, No. 5, 1982, pp.13-17

[26] Ibrahim,I. R., *Computation of Normal Mode from Identified Complex Modes,* AIAA Journal, Vol. 21, No. 6, 1983

[27] Zhang, Q. and G. Lallement, *New Method of Determining the Eigensolutions of the Associated Conservative Structure from the Identified Eigensolutions,* Proceedings of the 3rd International Modal Analysis Conference, 1985, pp. 322-328

[28] Natke, H. G and D. Rotert, *Determination of Normal Modes from Identified Complex Modes,* Z. Flugwiss. Weltraumforsch,g., Heft 2, 1985, pp. 82-88

[29] Allemang, R. J. and D. L. Brown, *A Correlation Coefficient for Modal Vector Analysis,* Proceedings of the 1st Modal Analysis Conference, November, 1982, pp. 110-115

[30] De Landsheer, A., *Mode Overcomplexity,* Proceedings of the Tenth International Seminar on Modal Analysis, Part IV, October, 1985

[31] Zhang, Q., G. Lallement and R. Fillod, *Modal Identification of Self-Adjoint and Non Self-Adjoint Structures by Additional Masses Techniques,* ASME Publication No. 85-DET-109, 6 pp.

[32] Deel, J. C. and W. L. Yiu, *Modal Testing Considerations for Structural Modification Applications,* Proceedings of the 3rd International Modal Analysis Conference, 1985, pp. 46-52

[33] Formenti, D. and D. Brown, *Analytical and Experimental Modal Analysis,* R.J. Allemang and R.W. Rost, eds. University of Cincinnati Modal Analysis Seminar, 1982

[34] Ramsey, K. A., *Experimental Modal Analysis, Structural Modifications and FEM Analysis on a Desktop Computer,* Sound/Vibration (February 1983,) pp. 33 - 41.

[35] Fox, R. L. and M. P. Kapoor, *Rates of Change of Eigenvalues and Eigenvectors,* AIAA Journal, VI, December, 1968 , pp. 2426-2429

[36] Garg, S., *Derivatives of Eigensolutions for a General Matrix,* AIAA Journal, XI, August, 1973, pp. 1191-1194

[37] Van Belle, H., *The Method of Construction and the Theory of Conjugated Structures,* Ph.D. Thesis, K. U. Leuven, Leuven, Belgium, 1974, pp. 142-151

[38] VanHonacker, P., *Sensitivity Analysis of Mechanical Structures, Based on Experimentally Determined Modal Parameters,* Proceedings of the 1st International Modal Analysis Conference, 1982, pp. 534-541

[39] Klosterman, A. L. and J. R. Lemon, *Building Block Approach to Structural Dynamics,* ASME Publication, VIBR-30, 1969

[40] Klosterman, A.L. *On the Experimental Determination and Use of Model Representations of Dynamic Characteristics,* Ph.D Dissertation (University of Cincinnati, 1971)

[41] Structural Dynamics Research Corporation, *SABBA V5.0 User Manual (System Analysis via the Building Block Approach),* November 1, 1984

[42] Crowley, J. R., A. L. Klosterman, G. T. Rocklin and H. Vold, *Direct Structural Modification Using Frequency Response Functions,* Proceedings of the 2nd International Modal Analysis Conference, 1984, pp. 58-65

[43] Klosterman, A. L. and W. A. McClelland, *Combining Experimental and Analytical Techniques for Dynamic System Analysis,* Tokyo Seminar on Finite Element Analysis, November, 1973

[44] Wang, B.P., G. Clark and F. H. Chu, *Structural Dynamic Modification Using Modal Analysis Data,* Procedures of the 3rd International Modal Analysis Conference, February, 1985, pp. 42-45

[45] Przemieniecki, J. S., *Matrix Structural Analysis of Substructures,* AIAA J., Vol. I, No. 1, 1963, pp. 138-147

[46] Guyan, R. J., *Reduction of Stiffness and Mass Matrices,* AIAA J., Vol. 3, No. 2, February, 1965, p. 380

[47] Hurty, W., *Vibrations of Structural Systems by Component Mode Synthesis,* Journal of the Engineering Mechanics Division, August, 1960, pp. 51-69

[48] Hurty, W., *Dynamic Analysis of Structural Systems Using Component Modes,* AIAA Journal, 3(4) (1965), pp. 678-685

[49] Craig, R. and M. Bampton, *Coupling of Structures for Dynamic Analysis,* AIAA Journal, July 1968, pp. 1313 - 1319.

[50] Bamford, R. M., *A Modal Combination Program for Dynamic Analysis of Structures,* Technical Memorandum 33-290, Jet Propulsion Laboratory, July 1967

[51] Goldman, R. L., *Vibration Analysis by Dynamic Partitioning,* AIAA Journal, Vol. 7, No. 6, 1969, pp. 1152-1154

[52] Hou, S., *Review of Modal Synthesis Techniques and a New Approach,* Shock and Vibration Bulletin, US Naval Research Laboratory, Proc. 40(4) (1969), pp. 25-39.

[53] Gladwell, G. M. L., *Branch Mode Analysis of Vibrating Systems,* Journal of Sound and Vibration, Vol. 1, 1964, pp. 41-59.

[54] Bajan, R. L., C. C. Feng and I. J. Jaszlics, *Vibration Analysis of Complex Structural System by Modal Substitution,* Shock and Vibration Bulletin, Vol. 39, No. 3, 1969, pp. 99-106

[55] Benfield, W. A. and R. F. Hruda, *Vibrational Analysis of Structures by Component Mode Substitution,* AIAA Journal, Vol. 9, No. 7, 1971, pp. 1255-1261

[56] MacNeal, R. H., *A Hybrid Method of Component Mode Synthesis,* Computers and Structures, Vol. 1, 1971, pp. 581-601

[57] Rubin, S., *Improved Component Mode Representation for Structural Dynamic Analysis,* AIAA Journal, Vol. 13, 1975, pp. 995-1006

[58] Klosterman, A.L. *A Combined Experimental and Analytical Procedure for Improving Automotive System Dynamics,* SAE Paper No.720093, January, 1972, pp. 343-353.

[59] Hintz, R. M., *Analytical Methods in Component Modal Synthesis,* AIAA Journal, Vol. 13, No. 8, 1975, pp. 1007-1016

[60] Baker, M., *Component Mode Synthesis Methods for Test-Based, Rigidly Connected, Flexible Components,* AIAA Journal, Paper 84-0943, 1984, pp. 153-163

[61] Hale, A. L. and L. Meirovitch, *A General Substructure Synthesis Method for Dynamic Simulation of Complex Structures,* Journal of Sound and Vibration, Vol. 69, No. 2, 1980, pp. 309-326

[62] *SYSTAN Users Manual,* General Electric CAE International, Inc., Milford, OH

[63] Herting, D. N. and M. J. Morgan, *A General Purpose Multi-Stage Component Modal Synthesis Method,* AIAA/ASME/AHCE/AHS 20th Structural Dynamics and Materials Conference, (St. Louis, MO: 1979)

[64] Hasselman, T. K. and A. Kaplan, *Dynamic Analysis of Large Systems by Complex Mode Synthesis,* Journal of Dynamical Systems, Measurement and Control (Sept. 1974), pp. 327-333.

[65] Kana, D. D. and J. F. Unruh, *Substructure Energy Methods for Prediction of Space Shuttle Modal Damping,* Journal of Spacecraft, Vol. 12 (1975), pp. 294-301

[66] Soni, M. L., *Prediction of Damping for Flexible Spacecraft Appendages,* Proceedings of the 2nd International Modal Analysis Conference, 1984

[67] Soni, M. L., M. Kluesener and M. L. Drake, *Damping Synthesis and Damped Design for Flexible Spacecraft Structures,* Computers and Structures, Vol. 20, No. 1, 1985, pp. 53-574

[68] Jezuquel, L., *A Method of Damping Synthesis from Substructure Tests,* Journal of Mechanical Design Trans. ASME, Vol. 102, April 1980, pp. 286-294

[69] *Combined Experimental/Analytical Modeling of Dynamic Structural Systems,* Papers presented at ASCE/ASME Mechanics Conference, Albuquerque, NM, June 24-26, 1985, ASME publication AMD VOL. 67, edited by D. R. Martinez and A. K. Miller.

[70] Walton, W. C. Jr. and E. C. Steeves, *A New Matrix Theorem and Its Application for Establishing Independent Coordinates for Complex Dynamic Systems with Constraints,* NASA TR R-326, 1969.

[71] Craig, R. Jr., *Structural Dynamics: An Introduction to Computer Methods,* John Wiley & Sons, 1981

[72] Lamontia, M. A., *On the Determination of Residual Flexibilities, Inertia Restraints, and Rigid Body Modes,* Proceedings of International Modal Analysis Conference, pp. 153-159

[73] Kramer, D. C. and M. Baker, *A Comparison for the Craig-Bampton and Residual Flexibility Methods for Component Substructure Representation,* AIAA Paper 85-0817

[74] O'Callahan, J. C. and C. M. Chou, *Study of a Structural Modification Procedure with Three Dimensional Beam Elements Using a Local Eigenvalue Modification Procedure,* Proceedings of the 2nd International Modal Analysis Conference, pp. 945-952

BIBLIOGRAPHY

[1] Richardson, M. H., *Measurement and Analysis of the Dynamics of Mechanical Structures,* Hewlett-Packard, 1976

[2] Sulisz, D., *Component Test Design Using Structural Dynamic Criteria,* Undergraduate Thesis, General Motors Institute, December 1983

[3] Sulisz, D.W., et al., *Final Report - System Dynamics Analysis III,* University of Cincinnati, September 1985

[4] *An Introduction to the Structural Dynamics Modification System,* Structural Measurement Systems (SMS), 3350 Scott Blvd., Bldg. 28, Santa Clara, CA 95051, November 1979, pp. 56

[5] Adelman, H. M. and R. T. Haftka, *Sensitivity Analysis of Discrete Structural Systems,* AIAA Journal, 24, 5, May 1986, pp. 823-832

[6] Akaike, H., *A New Look at the Statistical Model Identification,* IEEE Transactions on Automatic Control, AC-19, 6, December 1974, pp.716-723

[7] Allemang, R. J. and D. L. Brown, *A Correlation Coefficient for Modal Vector Analysis,* Proceedings of the 1st Modal Analysis Conference, November 1982, pp. 110-115

[8] Anonymous, *An Introduction to the Structural Dynamics Modification Systems,* Technical Information Note #1 by Structural Measurement Systems, Inc., February 1980

[9] Anonymous, *Modeling Rib Stiffeners with the Structural Dynamics Modification System,* Application Note 82-1 by Structural Measurement Systems, Inc., 1982

[10] Arnold, S., *Theory of Linear Models and Multi-variate Analysis,* John Wiley, 1981

[11] Avitabile, P. and J. O'Callahan, *A Structural Modification Procedure Using Complex Modes,* IMAC I, November 1982, pp. 418-422

[12] Bajan, R. L., C. C. Feng and I. J. Jaszlics, *Vibration Analysis of Complex Structural System by Modal Substitution,* Shock and Vibration Bulletin, Vol. 39, No. 3, 1969, pp. 99-106

[13] Baker, M., *Component Mode Synthesis Methods for Test-Based, Rigidly Connected, Flexible Components,* AIAA Journal, Paper 84-0943, 1984, pp. 153-163

[14] Bamford, R. M., *A Modal Combination Program for Dynamic Analysis of Structures,* Technical Memorandum 33-290, Jet Propulsion Laboratory, July 1967

[15] Benfield, W. A. and R. F. Hruda, *Vibrational Analysis of Structures by Component Mode Substitution,* AIAA Journal, Vol. 9, No. 7, 1971, pp. 1255-1261

[16] Bennetts, R. D., *Impedance Concepts in Interconnection Theory,* SDRC

[17] Berman, A., *A Generalized Coupling Technique for the Dynamic Analysis of Structural Systems,* American Institute of Aeronautics and Astronautrics, Paper No. 79-0735, 1979, pp. 76-85

[18] Berman, A., *Mass Matrix Correction Using an Incomplete Set of Measured Modes,* AIAA Journal, 17, 10, October 1979, pp. 1147-1148

[19] Brandon, J., *Reply by Auther to A. H. Flax (to comment of "Derivation & Significance of Second-Order Modal Design Sensitivities"),* AFAA Journal, 23, 3, March 1985, p. 479

[20] Brandon, J. A., *Derivation and Significance of Second-Order Modal Design Sensitivites,* AIAA Journal, 22, 5, May 1984, pp. 723-724

[21] Brauch, M. and Y. B. Itzhack, *Optimal Weighted Orthogonality of Measured Modes,* AIAA Journal, Vol. 16, No. 4, 1978

[22] Brown, D. L. and W. G. Halvorsen, *Impulse Technique for Structural Frequency Response Testing*, Sound and Vibration, November 1977, pp. 8-21

[23] Chang, C., *A General Method for Substructure Coupling in Dynamic Analysis*, Ph.D. Dissertation, University of Texas, 1977

[24] Chen, J. C. and J. A. Garba, *Matrix Perturbation for Analytical Model Improvement*, AIAA Journal, Paper No. 79-0831, pp. 428-436

[25] Chen, S. and J. Fuh, *Application of the Generalized Inverse in Structural System Identification*, AIAA Journal, 22, 12, December 1984, pp. 1827-1828

[26] Chou, Y. F. and J. S. Chen, *Structural Dynamics Modification Via Sensitivity Analysis*, Proceedings of the 3rd International Modal Analysis Conference, 1985, pp. 483-489

[27] Chou, C.M., *Structural Dynamics Modification of 3D Beam Elements Using a Local Eigenvalue Modification Procedure*, Ph.D. Dissertation , University of Lowell, 1984

[28] *Combined Experimental/Analytical Modeling of Dynamic Structural Systems*, Papers presented at ASCE/ASME Mechanics Conference, Albuquerque, NM, June 24-26, 1985, ASME publication AMD VOL. 67, edited by D. R. Martinez and A. K. Miller.

[29] Craig, R. and C. J. Chang, *A Review of Substructure Coupling Methods of Dynamic Analysis*, Advances in Engineering Science II, NASA-CP-2001, November 1976, pp. 393-408

[30] Craig, R. Jr., *Structural Dynamics: An Introduction to Computer Methods*, John Wiley & Sons, 1981

[31] Craig, R. and M. Bampton, *Coupling of Structures for Dynamic Analysis*, AIAA Journal, July 1968, pp. 1313- 1319.

[32] Crowley, J., D. L. Brown and G. T. Rocklin, *Uses of Rigid Body Calculations in Test*, Proceedings of the 4th International Modal Analysis Conference, February 1986

[33] Crowley, J. R., A. L. Klosterman, G. T. Rocklin and H. Vold, *Direct Structural Modification Using Frequency Response Functions*, Proceedings of the 2nd International Modal Analysis Conference, 1984, pp. 58-65

[34] Crowley, J. R., G. T. Rocklin, S. M. Crowley and T. E. Gorman, *A Comparison of SMURF and Modal Modeling*, Proceedings of the 3rd International Modal Analysis Conference, 1985

[35] Crowley, S. M., M. Javidinejad and D. L. Brown, *An Investigation of Structural Modification Using an H-Frame Structure*, Proceedings of the 4th International Modal Analysis Conference, 1986, pp. 1268-1278

[36] De Landsheer, A., *Dynamic Optimization with Modal Analysis*, DYNOPS User Manual, Spring, 1984.

[37] De Landsheer, A., *Mode Overcomplexity*, Proceedings of the Tenth International Seminar on Modal Analysis, Part IV, October 1985

[38] Deblauwe, F. and R. J. Allemang, *A Possible Origin of Complex Modal Vectors*, Proceedings of the Eleventh International Seminar on Modal Analysis, Leuven, Belgium, 1986

[39] Deel, J. C. and W. L. Yiu, *Modal Testing Considerations for Structural Modification Applications*, Proceedings of the 3rd International Modal Analysis Conference, 1985, pp. 46-52

[40] Elliott, K.B. and L. D. Mitchell, *Realistic Structural Modifications: Part I Theoretical Development*, Proceedings of the 3rd International Modal Analysis Conference, 1985, pp. 471-476

[41] Flax, A. H., *Comment on "Derivation and Significance of Second-Order Modal Design Sensitivities,"* AIAA Journal, 23, 3, March 1985

[42] Formenti, D. and D. L. Brown, *Analytical and Experimental Modal Analysis,* R.J. Allemang and R.W. Rost, eds. University of Cincinnati Modal Analysis Seminar, 1982

[43] Formenti, D. and S. Welaratna, *Structural Dynamics Modification - An Extension to Modal Analysis,* SAE Technical Paper Series No. 811043, Aerospace Congress and Exposition, Anaheim, California, Oct. 5-8, 1981, pp. 619-642

[44] Fox, R. L. and M. P. Kapoor, *Rates of Change of Eigenvalues and Eigenvectors,* AIAA Journal, VI, December 1968, pp. 2426-2429

[45] Frazer, R. A., W. J. Duncan and A. R. Collar, *Elementary Matrices,* Cambridge University Press, 1957, p. 289

[46] Fuh, J. and S. Chen, *Constraints of the Structural Modal Synthesis,* AIAA Journal, 24, 6, June 1986, pp. 1045-1047

[47] Garbow, B. S., J. M. Boyle, J. J. Dongarra and C. B. Moler, *Matrix Eigensystem Routines - EISPACK Guide Extension,* Lecture Notes in Computer Science V.51, Springer-Verlag, New York, 1977.

[48] Garg, S., *Derivatives of Eigensolutions for a General Matrix,* AIAA Journal, XI, August 1973, pp. 1191-1194

[49] Gaylord, M. E., *Smoothed Frequency Responses for Matrix-Characterized Vibrating Structures,* Journal of Sound and Vibration, 93, 2, March 1984, pp. 249-271

[50] Gladwell, G. M. L., *Branch Mode Analysis of Vibrating Systems,* Journal of Sound and Vibration, Vol. 1, 1964, pp. 41-59.

[51] Goldman, R. L., *Vibration Analysis by Dynamic Partitioning,* AIAA Journal, Vol. 7, No. 6, 1969, pp. 1152-1154

[52] Guyan, R. J., *Reduction of Stiffness and Mass Matrices,* AIAA J., Vol. 3, No. 2, February 1965, p. 380

[53] Haftka, R. T., Z. N. Martinovic and W. L. Hallaver Jr., *Enhanced Vibration Controllability by Minor Structural Modifications,* AIAA Journal, 23, 8, August 1985, pp. 1260-1266

[54] Hale, A. L., *Substructure Synthesis and its Iterative Improvement for Large Nonconservative Vibratory Systems,* AIAA Journal, 22, 2, February 1984, pp. 265-272

[55] Hale, A. L. and L. Meirovitch, *A General Substructure Synthesis Method for Dynamic Simulation of Complex Structures,* Journal of Sound and Vibration, Vol. 69, No. 2, 1980, pp. 309-326

[56] Hallquist, J. O., *Modification and Synthesis of Large Dynamic Structural Systems,* Ph.D. Dissertation, Michigan Tech. University, 1974

[57] Hallquist, J. O. and V. W. Snyder, *Synthesis of Two Discrete Vibratory Systems Using Eigenvalue Modification,* AIAA Journal, XI (1973).

[58] Hasselman, T. K. and A. Kaplan, *Dynamic Analysis of Large Systems by Complex Mode Synthesis,* Journal of Dynamical Systems, Measurement and Control (Sept. 1974), pp. 327-333.

[59] Haug, E. J. and K. K. Choi, *Structural Design Sensitivity Analysis with Generalized Global Stiffness Mass Matrices,* AIAA Journal, 22, 9, September 1984, pp. 1299-1303

[60] Herbert, M. R. and D. W. Kientzy, *Applications of Structural Dynamics Modification,* SAE Technical Paper, Series No. 801125, October 1980, pp. 607-615

[61] Herting, D. N. and M. J. Morgan, *A General Purpose Multi-Stage Component Modal Synthesis Method,* AIAA/ASME/AHCE/AHS 20th Structural Dynamics and Materials Conference, (St. Louis, MO: 1979)

[62] Heylen, I. W., *Model Optimization with Measured Modal Data by Mass and Stiffness Changes,* Proceedings of the 4th International Modal Analysis Conference, Los Angeles, CA., 1986, pp. 94-100

[63] Hintz, R. M., *Analytical Methods in Component Modal Synthesis,* AIAA Journal, Vol. 13, No. 8, 1975, pp. 1007-1016

[64] Hou, S., *Review of Modal Synthesis Techniques and a New Approach,* Shock and Vibration Bulletin, US Naval Research Laboratory, Proc. 40(4) (1969), pp. 25-39.

[65] Hughes, P. E., *Modal Identities for Elastic Bodies, with Application to Vehicle Dynamics and Control,* The Journal of Applied Mechanics, Paper No. 79-WA/APM-34

[66] Hurty, W., *Dynamic Analysis of Structural Systems Using Component Modes,* AIAA Journal, 3(4) (1965), pp. 678-685

[67] Hurty, W., *Vibrations of Structural Systems by Component Mode Synthesis,* Journal of the Engineering Mechanics Division, August 1960, pp. 51-69

[68] Huston, R. L. and C. E. Passerello, *Finite Element Methods: An Introduction,* New York: Marcel Dekker, Inc., 1984

[69] Ibrahim, S. R., *Determination of Normal Modes From Measured Complex Modes,* Shock and Vibration Bulletin, Vol. 52, No. 5, 1982, pp.13-17

[70] Ibrahim, S. R., *Dynamic Modeling of Structures from Measured Complex Modes,* AIAA Journal, Vol. 21, No. 6, 1982.

[71] Ibrahim,I. R., *Computation of Normal Mode from Identified Complex Modes,* AIAA Journal, Vol. 21, No. 6, 1983

[72] Javidinejad, M., S. Crowley and D. L. Brown, *An Investigation of Structural Modification Using an H- Frame Structure,* Proceedings of the 4th International Modal Analysis Conference, February 1986

[73] Jezuquel, L., *A Method of Damping Synthesis from Substructure Tests,* Journal of Mechanical Design Trans. ASME, Vol. 102, April 1980, pp. 286-294

[74] Jones, R., *Structural Modification Using Modal and Frequency Domain Techniques,* 10th International Conference at Leuven

[75] Kana, D. D. and J. F. Unruh, *Substructure Energy Methods for Prediction of Space Shuttle Modal Damping,* Journal of Spacecraft, Vol. 12 (1975), pp. 294-301

[76] Kanievsky A.M., *Experimental Error Estimation of Rotational DOF Calculated From Measured Rigid Body Motion*

[77] Kanievsky, A.M., M.Sc., *Structure Modification-Sensitivity Study*

[78] Klahs, J., M. Goldstein, R. Madabusi and R. Russel, *Assembling Large Scale System Models from Test and Analysis Using Interactive Computing,* Proceedings of the 1st International Modal Analysis Conference, November 1982, pp. 46-52

[79] Klosterman, A. L. and J. R. Lemon, *Building Block Approach to Structural Dynamics,* ASME Publication, VIBR-30, 1969

[80] Klosterman, A. L., *A Combined Experimental and Analytical Procedure for Improving Automotive System Dynamics,* SAE Paper No.720093, January 1972, pp. 343-353.

[81] Klosterman, A. L. and W. A. McClelland, *Combining Experimental and Analytical Techniques for Dynamic System Analysis,* Tokyo Seminar on Finite Element Analysis, November 1973

[82] Kramer, D. C. and M. Baker, *A Comparison for the Craig-Bampton and Residual Flexibility Methods for Component Substructure Representation,* AIAA Paper 85-0817

[83] Kron, G., *Diakoptics* MacDonald, 1963

[84] Lamontia, M. A., *On the Determination of Residual Flexibilities, Inertia Restraints, and Rigid Body Modes,* Proceedings of International Modal Analysis Conference, pp. 153-159

[85] Lieu, I. W., *Determination of Rotational Degrees of Freedom Using Condensation/Expansion Techniques,* M.S. Thesis, Lowell, MA: University of Lowell, 1984

[86] Luk, Y. W. and L. D. Mitchell, *System Modeling and Modification Via Modal Analysis,* Proceedings of the 1st International Modal Analysis Conference, 1982, pp. 423-429

[87] MacNeal, R. H., *A Hybrid Method of Component Mode Synthesis,* Computers and Structures, Vol. 1, 1971, pp. 581-601

[88] Martinez, D. R., A. K. Miller and T. G. Carne, *Combined Experimental/Analytical Modeling Using Component Mode Synthesis,* Proceedings of 25th AIAA Structures, Dynamics & Materials Conference, May 1984, Paper 84-0941

[89] Massoud, M., *Impedance Methods for Machine Analysis: Modal Parameters Extraction Techniques,* The Shock and Vibration Digest, May 1984, pp. 5-14

[90] Meirovitch, L., *Analytical Methods in Vibrations,* New York: The MacMillan Company, 1967, pp. 388-434

[91] Nagamatsu A., and M. Ookuma, *Analysis of Forced Vibration with Reduced Impedance Method (Part I. Introduction of Analytical Procedure,* Bulletin of the JSME, 24, 189, March 1981, pp. 578-584

[92] Nagamatsu, A. and Y. Kagohashi, *Analysis of Forced Vibration by Reduced Impedance Method (Part 2 - Introduction of New Curve Fitting Technique),* Bulletin of the JSME, 25, 199, January 1982, pp. 76-80

[93] Natke, H. G and D. Rotert, *Determination of Normal Modes from Identified Complex Modes,* Z. Flugwiss. Weltraumforsch,g., Heft 2, 1985, pp. 82-88

[94] O'Callahan, J.C., C. M. Chou and P. Avitabile, *Study of a Local Eigenvalue Modification Procedure Using a Generalized Beam Element,* Proceedings of the 3rd American Control Conference, June 1984

[95] O'Callahan, J. C. and C. M. Chou, *Structural Dynamics Modification Using Generalized Beam Mass and Stiffness Matrices,* Proceedings of the 3rd International Modal Analysis Conference, 1985, pp. 477-482

[96] O'Callahan, J. C., C. M. Chou and I. W. Lieu, *Determination of Rotational Degrees of Freedom for Moment Transfers in Structural Modifications,* Proceedings of the 3rd International Modal Analysis Conference, 1985, pp. 465-470

[97] O'Callahan, J. C. and P. Avitabile, *A Structural Modification Procedure Using Complex Modes,* Proceedings of the 1st International Modal Analysis Conference, 1983, pp. 418-422

[98] Olson, N., *Excitation Functions for Structural Frequency Response Measurement,* Proceedings of the 2nd International Modal Analysis Conference, Orlando, Fl., 1984, pp. 894-902

[99] Pal, T.G. and R. A. Schmidtberg, *Combining Analytical and Experimental Modal Analysis for Effective Structural Dynamic Modeling,* Proceedings of the Third International Modal Analysis Conference, 1985, pp. 265-271

[100] Pomazal, R., *The Effect of Local Modification of the Eigenvalues and Eigenvectors of Damped Linear Systems,* Ph.D. Dissertation, Michigan Technological University, 1969

[101] Pomazal, R. J. and V. W. Snyder, *Local Modifications of Damped Linear Systems,* AIAA Journal, IX (1971).

[102] Przemieniecki, J. S., *Matrix Structural Analysis of Substructures,* AIAA J., Vol. I, No. 1, 1963, pp. 138-147

[103] Rades, M., *System Identification Using Real-Frequency-Dependent Modal Characteristics,* The Shock and Vibration Digest, 18, 8, August 1986, pp. 3-10

[104] Reiss, R., *Design Derivatives of Eignenvalues and Eigenfunctions for Self-Adjoint Distributed Parameter Systems,* AIAA Journal, 24, 7, July 1987, pp. 1169-1172

[105] Rubin, S., *Improved Component Mode Representation for Structural Dynamic Analysis,* AIAA Journal, Vol. 13, 1975, pp. 995-1006

[106] *SDRC Modal Analysis User Manual,* Section 6.2.5, Version 9.0

[107] *SYSTAN Users Manual,* General Electric CAE International, Inc., Milford, OH

[108] Simpson, A. and B. Taborrok, *On Kron's Eigenvalue Procedure and Related Methods of Frequency Analysis,* Quarterly Journal of Mechanics and Applied Mathematics, XXI, 1968, pp. 1-39.

[109] Smiley, R. G. and B. A. Brinkman, *Rotational Degrees-of-Freedom in Structural Modification,* Proceedings of the 2nd International Modal Analysis Conference, 1984, pp. 937-939

[110] Snyder, V. W., *Modal Synthesis Using Eigenvalue Modification,* Proceedings of the Third International Modal Analysis Conference, February 1985, pp.1134-1137

[111] Soni, M. L., *Prediction of Damping for Flexible Spacecraft Appendages,* Proceedings of the 2nd International Modal Analysis Conference, 1984

[112] Soni, M. L., M. Kluesener and M. L. Drake, *Damping Synthesis and Damped Design for Flexible Spacecraft Structures,* Computers and Structures, Vol. 20, No. 1, 1985, pp. 53-574

[113] Starkey, J. M. and J. E. Bernard, *A Constraint Function Technique for Improved Structural Dynamics,* Journal of Vibration, Acoustics, Stress & Reliability in Design, 108, January 1986, pp. 101-106

[114] Structural Dynamics Research Corporation, *SABBA V5.0 User Manual* (*System Analysis via the Building Block Approach*), November 1, 1984

[115] Taber, R. C., H. Vold, G. T. Rocklin and D. L. Brown, *Exponential Window for Burst Random Excitation,* Proceedings of the 3rd International Modal Analysis Conference, January 1985

[116] Van Belle, H., *The Method of Construction and the Theory of Conjugated Structures,* Ph.D. Thesis, K. U. Leuven, Leuven, Belgium, 1974, pp. 142-151

[117] VanHonacker, P., *Sensitivity Analysis of Mechanical Structures, Based on Experimentally Determined Modal Parameters,* Proceedings of the 1st International Modal Analysis Conference, 1982, pp. 534-541

[118] Vold, H., J. Kundrat, G.T. Rocklin and R. Russel, *A Multi-Input Modal Estimation Algorithm for Mini-Computers,* SAE Paper No.820194, February 1982

[119] Walton, W. C. Jr. and E. C. Steeves, *A New Matrix Theorem and Its Application for Establishing Independent Coordinates for Complex Dynamic Systems with Constraints,* NASA TR R-326, 1969.

[120] Wang, B. P. and W. D. Pilkey, *Eigenvalue Reanalysis of Locally Modified Structures Using a Generalized Rayleigh's Method,* AIAA Journal, 24, 6, June 1986, pp. 983-990

[121] Wang, B.P., G. Clark and F.H. Chu, *Structural Dynamic Modification Using Modal Analysis Data,* Procedures of the 3rd International Modal Analysis Conference, February 1985, pp. 42-45

[122] Wei, M. L., R. J. Allemang and D. L. Brown, *Real-normalization of Measured Complex Modes,* Proceedings of the 5th International Modal Analysis Conference, London, 1987

[123] Wei, M. L., R. J. Allemang and D. L. Brown, *Structural Dynamic Modifications Using Mass Additive Technique,* Proceedings of the 4th International Modal Analysis Conference, L.A., Ca., 1986, pp. 691-699

[124] Weissenberger, J.T., *The Effect of Local Modifications on the Eigenvalues and Eigenvectors of Linear Systems,* D.Sc. Dissertation, Washington University, 1966

[125] Weissenberger, J.T., *Effect of Local Modifications on the Vibration Characteristics of Linear Systems,* Journal of Applied Mechanics, XXXV, June 1968

[126] Wittmeyer, V. H., *Eine,, Orthogonalitats methode "Zur Ermitthing der dynamischen Kennwerteeines elastischen Korpers...,"* Ingenieur-Archiv, 42, 1973, pp. 104-115

[127] Yasuda Chiaki, P. J. Riehle, D. L. Brown and R. J. Allemang, *An Estimation Method for Rotational Degrees of Freedom Using Mass Additive Technique,* Proceedings of the 2nd International Modal Analysis Conference, 1984

[128] Zhang, Q. and G. Lallement, *New Method of Determining the Eigensolutions of the Associated Conservative Structure from the Identified Eigensolutions,* Proceedings of the 3rd International Modal Analysis Conference, 1985, pp. 322-328

[129] Zhang, Q., G. Lallement and R. Fillod, *Modal Identification of Self-Adjoint and Non Self-Adjoint Structures by Additional Masses Techniques,* ASME Publication No. 85-DET-109, 6 pp.

[130] Zimmerman, R. and D. L. Hunt, *Multiple-Input Excitation Using Burst Random for Modal Testing,* Sound and Vibration XIX, pp. 12-21.

NOMENCLATURE

Matrix Notation

$\{..\}$	braces enclose column vector expressions
$\{..\}^T$	row vector expressions
$[..]$	brackets enclose matrix expressions
$[..]^H$	complex conjugate transpose, or Hermitian transpose, of a matrix
$[..]^T$	
$[..]^{-1}$	inverse of a matrix
$[..]^+$	generalized inverse (pseudoinverse)
$[..]_{q \times p}$	size of a matrix: q rows, p columns
$\lceil .. \rfloor$	diagonal matrix

Operator Notation

A^*	complex conjugate
F	Fourier transform
F^{-1}	inverse Fourier transform
H	Hilbert transform
H^{-1}	inverse Hilbert transform
ln	natural logrithm
L	Laplace transform
L^{-1}	inverse Laplace transform
$\mathrm{Re} + j\mathrm{Im}$	complex number: real part "Re", imaginary part "Im"
$\dot{x}$	first derivative with respect to time of dependent variable x
$\ddot{x}$	second derivative with respect to time of dependent variable x
$\overline{y}$	mean value of y
$\hat{y}$	estimated value of y
$\sum_{i=1}^{n} A_i B_i$	summation of $A_i B_i$ from i = 1 to n
$\frac{\partial}{\partial t}$	partial derivative with respect to independent variable "t"
det[..]	determinant of a matrix
$\lVert .. \rVert_2$	Euclidian norm

Roman Alphabet

A_{pqr}	residue for response location p, reference location q, of mode r
C	damping
COH	ordinary coherence function[†]
COH_{ik}	ordinary coherence function between any signal i and any signal k[†]
COH^n	conditioned partial coherence[†]
e	base e (2.71828...)
F	input force
F_q	spectrum of q^{th} reference[†]
GFF	auto power spectrum of reference[†]
GFF_{qq}	auto power spectrum of reference q[†]
GFF_{ik}	cross power spectrum of reference i and reference k[†]

$[GFFX]$	reference power spectrum matrix augmented with the response/reference cross power spectrum vector for use in Gauss elimination
GXF	cross power spectrum of response/reference†
GXX	auto power spectrum of response†
GXX_{pp}	auto power spectrum of response p†
$h(t)$	impulse response function†
$h_{pq}(t)$	impulse response function for response location p, reference location q †
$H(s)$	transfer function†
$H(\omega)$	frequency response function, when no ambiguity exist, H is used instead of $H(\omega)^{\dagger}$
$H_{pq}(\omega)$	frequency response function for response location p, reference location q, when no ambiguity exist, H_{pq} is used instead of $H_{pq}(\omega)^{\dagger}$
$H_1(\omega)$	frequency response function estimate with noise assumed on the response, when no ambiguity exist, H_1 is used instead of $H_1(\omega)^{\dagger}$
$H_2(\omega)$	frequency response function estimate with noise assumed on the reference, when no ambiguity exist, H_2 is used instead of $H_2(\omega)^{\dagger}$
$H_S(\omega)$	scaled frequency response function estimate, when no ambiguity exist, H_S is used instead of $H_S(\omega)^{\dagger}$
$H_v(\omega)$	frequency response function estimate with noise assumed on both reference and response, when no ambiguity exist, H_v is used instead of $H_v(\omega)^{\dagger}$
$[I]$	identity matrix
j	$\sqrt{-1}$
K	stiffness
L	modal participation factor
M	mass
M_r	modal mass for mode r
$MCOH$	multiple coherence function†
N	number of modes
N_i	number of references (inputs)
N_o	number of responses (outputs)
$_p$	output, or response point (subscript)
$_q$	input, or reference point (subscript)
$_r$	mode number (subscript)
R_I	residual inertia
R_F	residual flexibility
s	Laplace domain variable
t	independent variable of time (sec)
t_k	discrete value of time (sec) $t_k = k\,\Delta t$
T	sample period
x	displacement in physical coordinates
X	response
X_p	spectrum of p^{th} response†
z	Z domain variable

Greek Alphabet

$\delta(t)$	Dirac impulse function
Δf	discrete interval of frequency (Hertz or cycles/sec)
Δt	discrete interval of sample time (sec)
ϵ	small number
η	noise on the output
λ_r	r^{th} complex eigenvalue, or system pole

	$\lambda_r = \sigma_r + j\omega_r$
$\lceil \Lambda \rfloor$	diagonal matrix of poles in Laplace domain
ν	noise on the input
ω	variable of frequency (rad/sec)
ω_r	imaginary part of the system pole, or damped natural frequency, for mode r (rad/sec)
	$\omega_r = \Omega_r \sqrt{1 - \varsigma_r^2}$
Ω_r	undamped natural frequency (rad/sec)
	$\Omega_r = \sqrt{\sigma_r^2 + \omega_r^2}$
ϕ_{pr}	scaled p^{th} response of normal modal vector for mode r
$\{\phi\}_r$	scaled normal modal vector for mode r
$[\Phi]$	scaled normal modal vector matrix
$\{\psi\}$	scaled eigenvector
ψ_{pr}	scaled p^{th} response of a complex modal vector for mode r
$\{\psi\}_r$	scaled complex modal vector for mode r
$[\Psi]$	scaled complex modal vector matrix
σ	variable of damping (rad/sec)
σ_r	real part of the system pole, or damping factor, for mode r
ς	damping ratio
ς_r	damping ratio for mode r
†	vector implied by definition of function

APPENDIX A: TEST DERIVED COMPONENT DYNAMICS MODELS

The appendix served as a supplement to the theory developed in Section 5, describes the construction of the fixed interface modal model and the residual flexibility modal model from experimental test data. Also given is the derivation of free interface modal model using measured loaded interface normal modes.

A.1 Fixed Interface Modal Model

Consider the component Equation 195. The component is tested with $\{X\}_B = 0$ and the constraint modal matrix $[\Phi]$ results for which:

$$[\Phi]^T [K]_{OO} [\Phi] = \lceil K_{q\rfloor} \qquad \text{(A-1)}$$
$$[\Phi]^T [M]_{OO} [\Phi] = \lceil M_{q\rfloor}$$

Multiplying by $[\Phi]^T$ in the upper partition of Equation 195 and substituting the transformation $\{X\} = [\Phi]\{q\}$ results in

$$\begin{bmatrix} \left[\lceil K_{q\rfloor} - \lambda^2 \lceil M_{q\rfloor}\right] & \left[[\Phi]^T [K]_{OB}\right] \\ \left[[K]_{OB}^T [\Phi]\right] & [K]_{BB} \end{bmatrix} \begin{Bmatrix} q \\ x_B \end{Bmatrix} = \begin{Bmatrix} 0 \\ f_B \end{Bmatrix} \qquad \text{(A-2)}$$

The modal matrix $[\Phi]$, modal mass $\lceil M_{q\rfloor}$, and modal stiffness $\lceil K_{q\rfloor}$ are readily available from constraint modal test, but the stiffness $[K]_{BB}$ and $[K]_{OB}$ must be derived from additional static testing. From Equation (A-2) for $\{x\}_B = \{0\}$

$$[K]_{OB}^T [\Phi]\{q\} = \{f\}_B \qquad \text{(A-3)}$$

The matrix on the left hand side of Equation (A-3) is made up of reaction forces for each mode. This expression is expanded out into:

$$[K]_{OB}^T [\Phi]\{q\} = \left\{\{R\}_1, \{R\}_2, \ldots, \{R\}_{n_m}\right\} = [R] \qquad \text{(A-4)}$$

The matrix [R] is the modal reaction force matrix and is measured directly by placing a force transducer at the connect DOF during the modal test.

The other unknown $[K]_{BB}$ is found by substituting the modal reaction force matrix [R] and rearranging Equation (A-2) into:

$$\begin{bmatrix} \lceil K_{q\rfloor}^{-1} & \left[-\lceil K_{q\rfloor}^{-1} [R]^T\right] \\ \left[[R] \lceil K_{q\rfloor}^{-1}\right] & \left[[K]_{BB} - [R] \lceil K_{q\rfloor} [R]^T\right] \end{bmatrix} \begin{Bmatrix} \lambda^2 \lceil M_{q\rfloor} \\ x_B \end{Bmatrix} = \begin{Bmatrix} q \\ f_B \end{Bmatrix} \qquad \text{(A-5)}$$

the term $\lambda^2 \lceil M_{q\rfloor}$ represents the forces on the unconstrained DOFs of the component. For static case $\lambda=0$ and the static stiffness of the boundary DOF is obtained from the lower partition of Equation

(A-5) as

$$[K]'_{BB} = [K]_{BB} - [R]\,[K_q]^{-1}\,[R]^T \tag{A-6}$$

If the component restraints are statically non-redundant, that is, just sufficient to prevent rigid body motion, then there is no stiffness among the boundary DOF and $[K]_{BB}' = 0$.

$$[K]_{BB} = [R]\,[K_q]^{-1}\,[R]^T \tag{A-7}$$

the boundary stiffness can be obtained from the modal stiffness and modal reaction forces alone.

For redundantly restrained components, $[K]_{BB}'$ is not zero and therefore some additional static test or analysis is required. Consider the partitions of $\{x\}_B$ nonredundant subset $\{x\}_C$ and remainder $\{x\}_f$.

$$\{x\}_B = \begin{Bmatrix} x_f \\ x_C \end{Bmatrix}$$

With the coordinates $\{x\}_C$ restrained, the static deflection due to some applied force $\{f\}_f$ of the remainder $\{x\}_f$ coordinates can be expressed as the sum of the rigid body motion and elastic deformation of the component:

$$\{x\}_f = [G]\{f\}_f + [T]\{x\}_C \tag{A-8}$$

where [G] is the static flexibility and [T] is the rigid body transformation. Also from static equilibrium, the forces applied at $\{x\}_f$ must be balanced by forces at $\{x\}_C$; therefore

$$-[T]^T\{f\}_f = \{f\}_C \tag{A-9}$$

Rearranging Equations (A-8) and (A-9) results in the following equations

$$\begin{bmatrix} [G]^{-1} & \left[-[G]^{-1}[T]\right] \\ \left[-[T]^T[G]^{-1}\right] & \left[-[T]^T[G]^{-1}[T]\right] \end{bmatrix} \begin{Bmatrix} x_f \\ x_C \end{Bmatrix} = \begin{Bmatrix} f_f \\ f_C \end{Bmatrix} \tag{A-10}$$

The square matrix in Equation (A-10) is the required $[K]_{BB}'$ which completes the definition of the constrained interface modal model.

Therefore, to construct the constrained interface modal model following information must be obtained from tests: $\lceil M_{q\rfloor}$ $\lceil K_{q\rfloor}$, $[\Phi]$, $[R]$, $[G]^{-1,}$ and $[T]$. The first four are obtained from modal testing. The matrix $[G]^{-1}$ must be measured from static tests using a nonredundant subset of $\{x\}_B$ constrained. The rigid body transformation matrix [T] can be obtained from geometry alone.

A.2 Residual Flexibility Modal Model

The dynamic flexibility G_{pq} is the response at coordinate q due to excitation at coordinate p. It can be expressed in terms of the modal stiffness k_r , mass m_r , and mode shape vector $\{\phi\}_r$ by the following summation over the number of modes:

$$G_{pq} = \sum_{r=1}^{m_K} \frac{\phi_{rp}\,\phi_{rq}}{k_r - \lambda^2 m_r} + \sum_{r=m_K+1}^{\infty} \frac{\phi_{rp}\,\phi_{rq}}{k_r - \lambda^2 m_r} \tag{A-11}$$

where the subscript r denotes the r^{th} mode and m_K denotes the number of retained modes. The second term on the right hand side in the above equation is called the residual flexibility G_{Rpq} due to modes deleted in a simulation. If the magnitude of the forcing frequency ω, is within the range of lower frequencies of the component containing the number of modes retained for synthesis, $\omega << \omega_r$; $r > n_k + 1$, a first order approximation to the flexibility of omitted modes is obtained as

$$G_{Rpq} = \sum_{n=m_k+1}^{\infty} \frac{\phi_{rp}\,\phi_{rq}}{\omega_n^2}$$

Experimentally the term G_{Rpq} can be obtained by exciting the component at DOF q, measuring the response at DOF p, and subtracting the first sum in Equation (A-11), which can be evaluated after the modal analysis has determined the properties of the first m_k modes.

The residual mass term $[H]_{BB}$ in Equation 192 must however be obtained from the knowledge of the residual flexibility and the component mass matrix as no method has yet been demonstrated for its determination from direct measurements. Note that the computation of the residual mass requires the full mass matrix of the component in physical coordinates and also the full $n \times n_B$ partition $[G]_B$ of the residual flexibility matrix. This includes residuals for both boundary $[G]_{BB}$ and other $[G]_{OB}$ DOFs.

A.3 Inertia-Loaded Interface Modal Model

Let the experimentally measured modal parameters of the loaded interface component be stiffness k_r, mass m_r, modes $[\Phi]$, frequency ω_r, and $[\Delta M]$ be the matrix of added mass. The procedure to analytically unload the component and obtain the resulting modal parameters is as follows.

Consider the equations of motion of loaded component in modal coordinates

$$\lceil m_{\rfloor} \{\ddot{q}\} + \lceil k_{\rfloor} \{q\} = \{Q\} \tag{A-12}$$

where $\{q\}$ is the generalized coordinate such that

$$\{x\} = [\Phi]\{q\} \tag{A-13}$$

{x} being the physical displacement vector of the component. The equation of motion of the added mass can be written as

$$[\Delta M]\{\ddot{x}\}_a = \{f\}_a \tag{A-14}$$

where $\{x\}_a$ is a subset of the component boundary DOF $\{x\}_B$ where extra masses are attached during test, and $\{F\}_a$ is the force on the added mass from the component at the attachment points. Analytical unloading of the component is accomplished by combining the dynamical equation of the loaded component and the negative of Equation (A-14). Thus,

$$\begin{bmatrix} -[\Delta M] & [0] \\ [0] & \lceil m_\eta \rfloor \end{bmatrix} \begin{Bmatrix} \ddot{x}_a \\ \ddot{q} \end{Bmatrix} + \begin{bmatrix} [0] & [0] \\ [0] & \lceil k_\eta \rfloor \end{bmatrix} \begin{Bmatrix} x_a \\ q \end{Bmatrix} = \begin{Bmatrix} -f_a \\ Q \end{Bmatrix} \tag{A-15}$$

Displacement compatibility at the attachment interface requires

$$\{x\}_a = [\Phi]|_A \{q\} \tag{A-16}$$

where $[\Phi]|_A$ is the partition of $[\Phi]$ corresponding to the attachment degrees of freedom. Thus,

$$\begin{Bmatrix} x_a \\ q \end{Bmatrix} = \begin{bmatrix} [\Phi]|_A \\ [I] \end{bmatrix} \{q\} \tag{A-17}$$

The use of Equation (A-17) in Equation (A-15) leads to the equation of motion of unloaded component as

$$\left[\lceil m_\eta \rfloor - \lambda^2 [\Phi]^T_A [\Delta M] [\Phi]|_A\right]\{\ddot{q}\} + \lceil k_\eta \rfloor \{q\} = \left[-[\Phi]^T_C \{F\}_a + \{Q\}\right] = 0$$

Solve the above eigenvalue problem

$$\left[\lceil k_\eta \rfloor - \lambda_r^2 \left(\lceil m_\eta \rfloor - [\Phi]^T_A [\Delta M] [\Phi]_a\right)\right]\{\psi\}_r = \{0\}$$

where λ_r and $\{\hat{\psi}\}_r$ are respectively the eigenvalue and mode shapes of the unloaded component. The modal properties of the unloaded component are then

$[\hat{\Psi}]^T \lceil k_\eta \rfloor [\hat{\Psi}]$ = Generalized stiffness

$[\hat{\Psi}]^T \left[\lceil m_\eta \rfloor - [\Phi]^T_A [\Delta M] [\Phi]_a\right] [\hat{\Psi}]$ = Generalized mass and since

$$\{q\} = [\hat{\Psi}]\{\eta\}$$

where $\{\eta\}$ is the modal participation factor with respect to $[\hat{\Psi}]$.

and

$$\{x\} = [\Phi]\{q\}$$

the mode shapes of the unloaded component are given as the product

$$[\Phi][\hat{\Psi}]$$

Thus in effect, the kinetic energy of the added mass has been subtracted from the mass loaded component modal data. If the added mass possesses flexibility as well, then the unloaded generalized stiffness is given as

$$[\Psi]^T \left[\lceil k_{\eta \rfloor} - [\Phi] \,|\, _a^T [\Delta M] [\Phi]_a \right] [\Psi]$$

where $[\Delta K]$ is the stiffness of added mass systems referred to attachment DOFs.

APPENDIX B: SOFTWARE DEVELOPMENT

The primary computer software developed in the component dynamic synthesis (Section 5) task of this contract is a computer program COMSYN for the synthesis and analysis of dynamics of built-up systems from component subsystem test or analysis data. The objective of this appendix is to describe the design, operation, and usage of the computer program. The mathematical formulation on which COMSYN is based is contained in Section 5.2 of this report. The overall organization of the program is discussed, together with procedures for operation and selected programming information required to operate and modify the program. A description of the organization of the program is first given, followed by details concerning the usage of the program. Input instructions, sample data and procedure to execute the program is given in Appendices C and D respectively.

All COMSYN coding is done in ANSI-77 FORTRAN, and the present version is configured to run on VAX/VMS machines. The program interfaces to component analysis and/or modal testing software through data files described in Appendix C.

B.1 Program Organization

A block diagram of the COMSYN system is shown in Figure B-1. The program operation is divided into three phases; component dynamics data processing; superelement reduction; and system synthesis solution and back substitution.

In the component data processing phase, the following operations are performed: component and system sizing parameters, topology, and other control information is read from user input files; and component coordinate rotations and modal truncations are performed and the processed data is written to sequential access internal files.

In the reduction phase, the component dynamics models are transformed to superelement coordinates and the reduced dynamic matrices are written to internal files for assembly.

In the synthesis phase, the following operations are performed: assembly of superelement matrices; system eigensolution and modal transformations; and back substitution to recover component displacements, stored energy, etc.

The flow of information between various modules is through unformatted low speed sequential system files indicated in Figure B-1.

COMSYN Call Tree:

The hierarchy of COMSYN subroutines is given in the following tree. Here the order in which the subroutines are called is given by the row number. The level at which the subroutines are called is given by the column number. All utility subroutines are grouped under the fourth level.

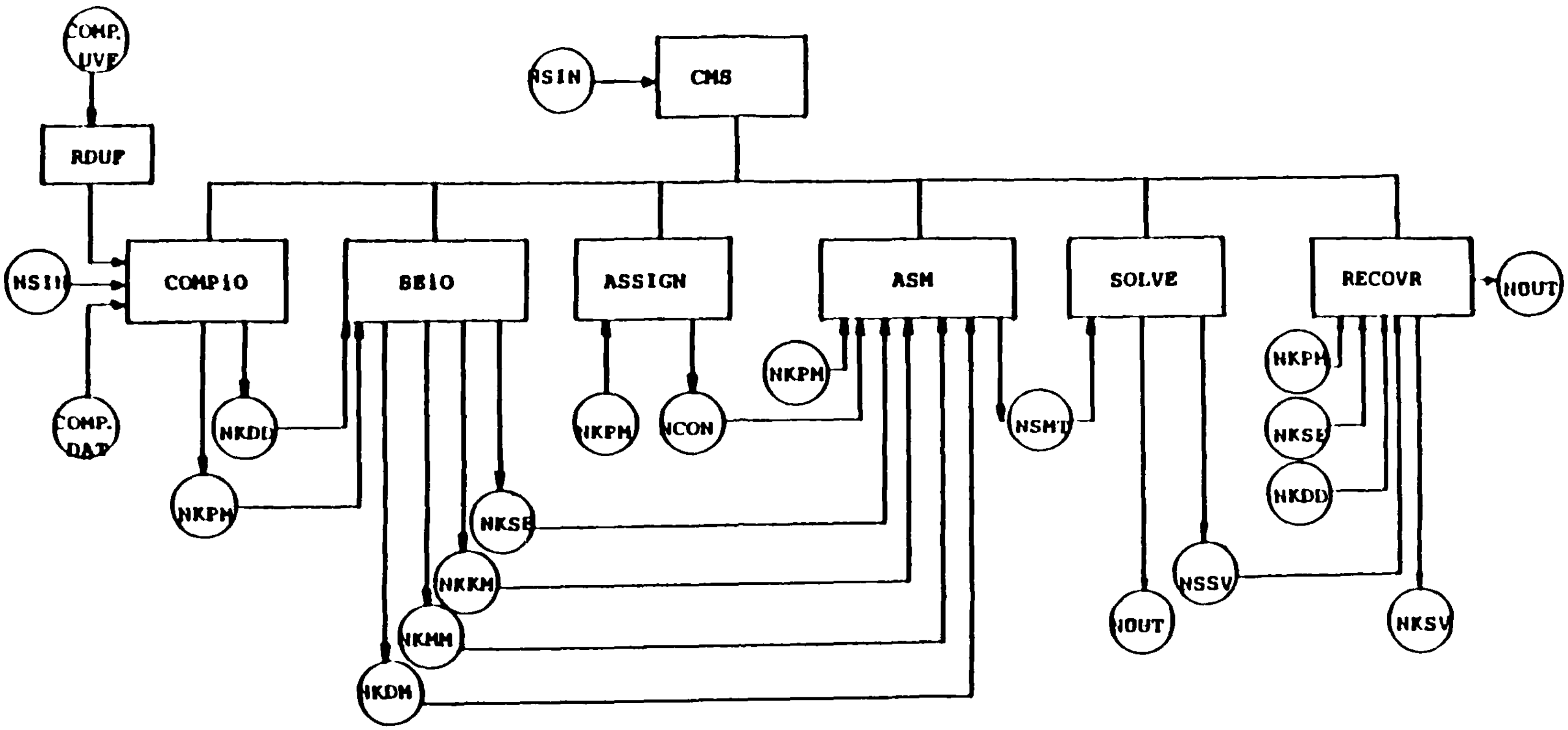

PROGRAM MODULE

NXXX Logical Unit

NSIN	System Input File	NCON	Component-System Correspondence Table
NFIL	Component Dynamics Data File	NSMT	Synthesized System Dynamic Matrices
NKPM	Component Sizing, Topology, and Connectivity Data	NSSV	System Solution Vector
NKDD	Component Dynamics Matrices	NKSV	Component Solution Vector
NKSE	Superelement Transformation	NOUT	Output Print File
NKKM	Superelement Mass	COMP.UVF	Universal File Input
NKDM	Superelement Damping	COMP.DAT	Neutral File Input

Figure B-1. COMSYS Program Organization and Internal File Utilization

	1	2	3	4
1	CMS			
2		COMPiO	RDPRM	
			GETFL	RDUVF
			RDiO	RDMAT
				WRMAT
				ROTMAT
				SINTLZM
				SCALEM
				RMVSR
				RMVSM
				COLX
				ROWX
3		SEiO	RDPRM	TRIPLE
				MTRAN
				MULT
				ADDSM
				TRANS
				MULT
				COPY
				SELECT
				ZNEW
				INVERT
				ERRMSG
				PRINTP
				PRINTSM
				INVERT
				SYMINV
				INITCM
				PRIMAT
4		ASM	ASMBL	PRIVEC
				SKM
5		SOLVE	EIGEN	REDUC
				TQL2
				TRED2
				REBAK
				ENRG
6		RECOVR	DISPiO	

The overall logical flow of the program and the function of the major program segments is given below. Third and fourth level subroutines perform rudimentary operations such as read, write, matrix manipulations, etc. and are documented in the program listings. The program uses VAX INCLUDE utility to maintain consistency between labeled common blocks used to pass data between different modules of the program.

CMS

CMS is the main driver program. It reads problem definition and system parameters and directs calls to component processing, superelement reduction, synthesis, and backsubstitution segments of the program.

COMPiO

Processes component dynamics matrices of component type i (i=1: finite element component; i=2: free interface modal component with residual flexibility attachment modes; i=3: free interface component with/without interface loading; i=4: constrained interface component). The subroutine RDPRM reads component sizing and topological information from the system input file. Subroutine GETFL assigns logical units from which component dynamic data is read. Subroutine RDiO performs the component dynamic data manipulations such as modal truncation, coordinates rotation, matrix partitioning etc.

SEiO

Reduces component type i dynamic matrices to superelement coordinate. The reduction procedures use the fourth level subroutines.

ASSIGN

Assigns system equation numbers to superelement degrees of freedom for assembly.

ASM

Forms system dynamic matrices from superelement matrices.

SOLVE

Solves system eigenproblem. Subroutine EIGEN calls the EISPAC routines REDUC, TRED2, TQL2, and REBAK for eigencalculation. Subroutine MTRAN computes system generalized mass, stiffness, and damping matrices.

RECOVR

Back transforms superelement partition of system displacement vector to component generalized as well as physical coordinates. The component stored energy is computed in subroutine ENRG.

The subroutine RDUVF provides an interface of the COMSYN with the SDRC modal software generated component universal data file. Component dynamic data generated by any other means such as NASTRAN or ANSYS may be supplied in the Universal File format. The program also accepts the component dynamic data in an alternate simpler format called Neutral file format described in Appendix C.2.

Solution Method:

COMSYN uses the similarity transformation based QL method of eigensolution. The system mass and stiffness matrices are symmetric and fully populated with possibly singular stiffness matrix and a positive definite mass matrix. The eigenproblem is solved as follows. Consider the system equations

$$[K]\{\psi\} = \lambda[M]\{\psi\} \tag{B-1}$$

Since M is symmetric and positive definite, its Choleski factorization

$$[M] = [L][L]^T$$

exits enabling the Equation (B-1) to be transformed to an equivalent standard symmetric eigenproblem

$$[\hat{K}]\{Y\} = \lambda \{Y\} \qquad \text{(B-1)}$$

with

$$[\hat{K}] = [L]^{-1}[K][L]^{-T} \quad \text{and} \quad \{Y\} = [L]^{T}\{\psi\}$$

The eigenvalues of the Equation (B-2) are obtained by first reducing the symmetric matrix $[\hat{K}]$ into a tridiadonal form using the orthogonal similarity transformation. Starting with j=N the elements in the j^{th} row to the left of the diagonal are first scaled. The sum of squares of these scaled elements is next formed. Then a vector {U} and a scalar H, where

$$H = \{U\}^{T}\{U\}/2,$$

define an operator,

$$[P] = [I] - \{U\}\{U\}^{T}/H,$$

which is orthogonal and symmetric and for which the similarity transformation $[P]^{T}[K][P]$ eliminates the elements in the j^{th} row of [K] to the left of the subdiagonal and the symmetric elements in the j^{th} column. The eigenvalues and eigenvectors of the symmetric tridiagonal matrix $[\hat{K}]^{*}$ are found using QL transformation, where [Q] is an orthogonal matrix and [L] is a lower triangular matrix such that

$$[\hat{K}]^{*} = [Q][L]$$

A sequence of symmetric tridiagonal matrices is formed which converges to a diagonal matrix. The rate of convergence of the sequence is improved by shifting the origin at each iteration. The similarity transformations are the orthogonal eigenvectors of the matrix [K]. Backward substitution in

$$[L]^{T}\{Z\} = \{Y\}$$

then leads to the eigenvalues of the matrix system of Equation (B-1). The subroutines required for the above operations are extracted from EISPACK [75].

Program Compatibility:

COMSYN is written for use with the VAX standard operating system to run on the Wright-Patterson Air Force Base VAX-11/780. All programming is done using VAX FORTRAN 77, machine language is not used. All I/O is accomplished with VAX FORTRAN 77 statements and does not use as an integral part of the operation program any on-line card reader, card punch, or printer. The standard system logical unit 5 (SYS$INPUT) for card reading and unit 6 (SYS$OUTPUT) for printing is used to facilitate compatibility with other computers. Fortran logical unit 5 is equated to system input file NSIN and Fortran logical unit 6 is equated to output file NOUT. The disk file organization type is sequential access available with VAX Record Manager. The program uses standard VAX issued basic function routines such as SQRT, SINE, etc.

Tape Capability

The program accepts unlabeled or ANSI standard labels in ASCII format recorded at either 800, 1600, or 6250 bpi density. However, it is recommended that the tapes be 9 track (1600 characters per inch), unlabelled, with block size less than or equal to 5720 characters.

Dynamic Storage Allocation

Due to the wide potential range of component and resulting system sizes and the desirability of maximizing efficient usage of the central memory by minimizing page faults, dynamic storage allocation is important to the practical utility of COMSYN. Implementation of dynamic storage allocation is accomplished by using the main program segment to set up pointers to the start of every dynamic array. The basic advantage of the scheme is that except for this program segment which establishes pointer set, the array dimensions are dummy argument as opposed to fixed. The means for accomplishing the dynamic dimensioning is by passing the pointer set as dummy arguments from the main program segment to lower subroutines. These lower level subroutines then refer to each pointer by the actual array name which that pointer references. The complete process involves the following steps: read in data describing problem size; use this data to establish pointers to all dynamic arrays, compute total size of dynamic memory; increment pointer set to point to locations within new memory block; pass pointer set to lower level subroutines. Sufficiently large memory block must be included in the blank common to accommodate the total dynamic memory required. Oversizing this dynamic block does not adversely impact the VMS system in any way, since pages which are never accessed do not impact the program in any way.

B.2 Data Input Instructions

The following describes the preparation of input for the COMSYN program. The program requires two sets of data:

Set 1: Sizing and Topological Data
Set 2: Component Dynamics Data

The first set of input contains the definition of the problem, sizing, and other control information for the system as well as the components and component connectivity definition. The second set of input data contains the component dynamics data as obtained in independent component tests and/or analyses. Because each component may be analyzed and/or tested independent of other components, a separate data file for each component is required. The specification formats for these data sets are described in Appendix C. Specific order is required to data input.

B.3 Program Usage

The usage of the program involves preparation of the program input data and execution of the program. Component dynamics data in most cases is obtained from separate test and/or analysis software. The program accepts this data in the industry standard universal file format and also in the neutral file format as described in Appendix C. The program is executed by entering @CMS P1 P2 P3 which accesses the executable binary and all the needed component data files; the parameters P1,P2 and P3 are respectively the name of the executable binary, system input and system output files. Appendix D describes the procedure to use the program through an example problem.

APPENDIX C: COMSYN INPUT INSTRUCTIONS

COMSYN data consists of two parts : (a) sizing and topological data, and (b) component dynamics data. Contents of the two data types are described below.

C.1 SIZING AND TOPOLOGICAL DATA

Record	Column	Format	Data Item	Description	Notes
1-3	1-80	20A4	TITLE1	System Header Data	
4	1-5	I5	NG	No. of System Nodes	(1)
	6-10	I5	NDFN	No. of Degrees of Freedom at each Node	(2)
5	1-5	I5	NC	No. of Components in the System	
6	1-5	I5	IRES	Solution Type Flag	(3)
7	1-5	I5	METHOD	Method of Eigensolution	(4)
	6-10	I5	NVEC	No. of System Modes to output	
8	1-10	A10	KEYWORD	*"COMPONENT "*	(5)
	11-15	I5	KID	Component Identification Number	
9	1-5	A5	TYPE	"TYPE "	
	1-5	I5	KTYPE	Component Dynamics Data Type	(6)
10	1-5	I5	KN	No. of Component Grid Points	(7)
11	1-5	I5	KB	No. of Component Boundary Nodes	(8)
12	1-80	16I5	KBLI5T(I), I=1,KB	List of Boundary Nodes	(9)
13	1-80	16I5	KSLIST(I), I=1,KB	Component to System Correspondence Table	(10)

Record	Column	Format	Data Item	Description	Notes
14	1-5	I5	KM	No. of Modes Supplied in input data	(11)
15	1-5	I5	KK	No. of Modes to be Used in Synthesis (KK.LE.KM)	
16	1-80	16I5	KKLIST(I), I=1,KK	List of Modes to be Used	(12)
17	1-60	I3	KFLAG(I), I=1,20	Flags for Specifying Type and Data Storage Mode	(13)
	61-70	E10.3	EPS	Residual Mass Parameter if KFLAG(8)=0	
18	1-30	3F10.0	ANGL(I), I=1,3	Three Sequential Angles (Roll, Pitch, Yaw) Defining Orientation of of Component Axes with Respect to System Axes (see Figure 5)	
19	1-13	A13	KEYWORD	"DYNAMICS DATA"	
	14-15	I2	IOPT	Dynamic Data File Option	(14)
	16-25	A10	FNAME	File Name for Dynamic Data File	(15)
	26-30	I5	IDEN	Tape Density	(16)
	31-35	I5	IRDWR	Read/Write Flag	(16)
	3-45	A10	MGTPFN	Magnetic Tape File Name	(16)
	46-50	I5	IBLF	Blocking Factor	

Record numbers 12, 13, and 16 may run into several cards each.

Repeat record numbers 8 through 19 for each component.

Data for each component must be in sequence; that is, component i must precede component i+1 and for each component the data must be ordered as per instructions above.

NOTES:

1. Number of system nodes includes all the connection nodes plus the number of nodes which are to be restrained in system analysis.
2. Valid input for the number of degrees of freedom is one of:
   1 : One translational degree of freedom per node
   2 : Two translational degrees of freedom per node
   3 : Three translational degrees of freedom per node
   6 : Three translational and three rotational degrees of freedom per node, referred to three mutually orthogonal axes

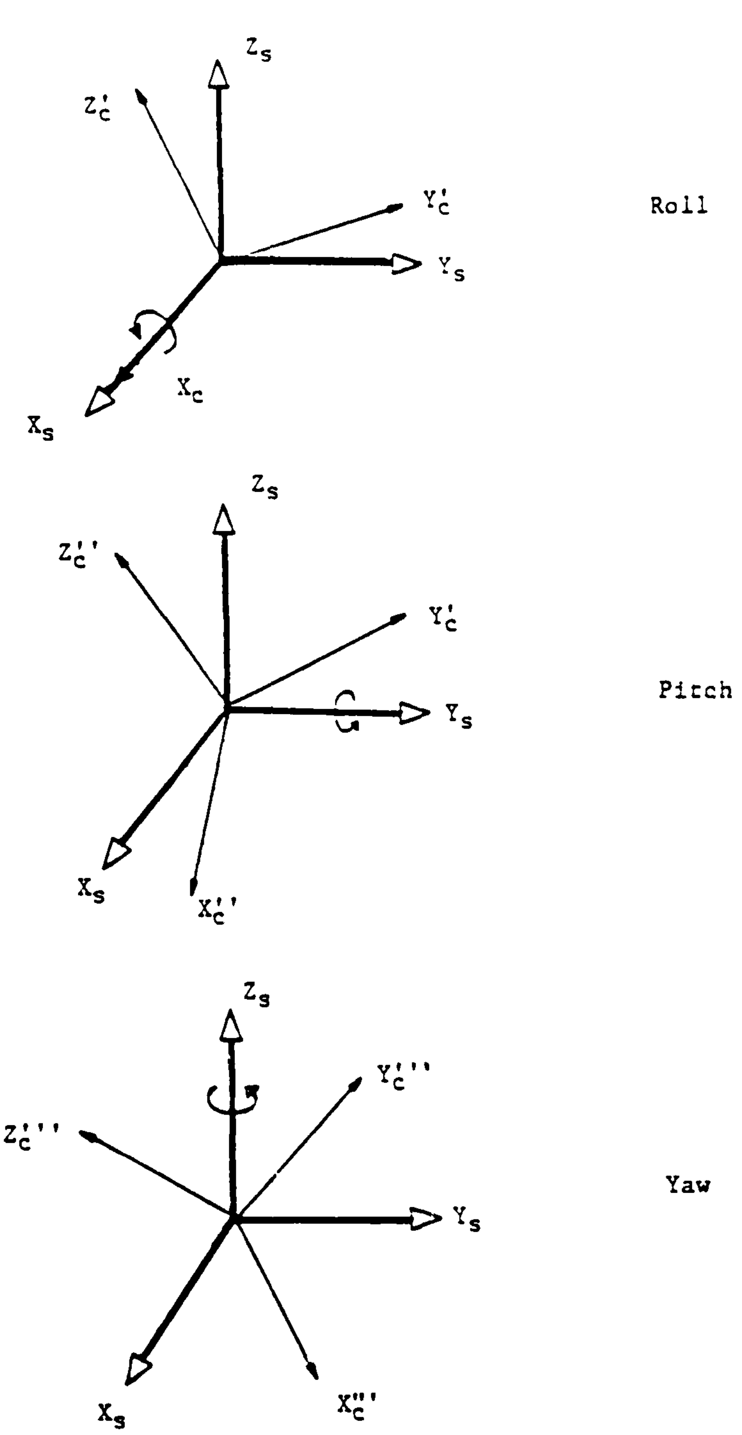

Figure C-1. Roll, Pitch and Yaw Orientation of Component Axes (X_c, Y_c, Z_c) with respect to System Axes (X_s, Y_s, Z_s)

3. IRES=1 for eigensolution.

4. Method of eigensolution used is QL method.

5. Repeat record numbers 8 through 19 for each component. Data for each component must be in sequence; that is, component i must precede component i+1 and for each component the data must be ordered as per instructions above.

6. Component data types allowed are:

   10 : Finite element stiffness mass and/or damping data
   20 : Free interface normal modes plus residual flexibility data
   30 : Free interface normal mode data
   40 : Constrained interface normal mode data

7. Component grid points must include the component partition of system nodes; that is, all of its connection points and any other node which is to be carried into system synthesis. Each node has NDFN degrees of freedom (see Note 2).

8. Boundary nodes include nodes connected to adjacent components plus nodes that will be restrained in system analysis. The node labels are those used in component grid point numbering.

9. Record type 12 is to be repeated in-place as necessary, if the number of component boundary nodes (KB) is greater than 16.

10. Connectivity of the component is specified by the component to system correspondence table that lists the system node number for each of the nodes specified in KBLIST.
    Record type 13 is to be repeated in-place as necessary, if the number of component boundary nodes (KB) is greater than 16.

11. Number of nodes supplied on the component data file. For type 10, component KM=0. For Type 20 and Type 30, the number of nodes include rigid body nodes (if any) plus elastic normal nodes.

12. Record 16 is to be repeated in-place as necessary, if the number of modes to be used (KK) is greater than 16.

13. Flags refer to the type and storage mode for component dynamic data, in the following manner:

ENTITY	KFLAG	VALUE	MEANING
Stiffness Matrix K_x	1	0	Absent
		1	Vector of diagonals
		2	Full matrix, row-wise
		3	Full matrix, symmetric upper triangular (row)
		4	Full matrix, symmetric lower triangular (row)
Mass Matrix M_x	2	0	
		1	
		2	(same as for KFLAG(1))
		3	
		4	
Damping Matrix C_x	3	0	
		1	

		2 3 4	(same as for KFLAG(1))
Modal Stiffness K_q	4	0 1 2 3 4	(same as for KFLAG(1))
Modal Mass M_q	5	0 1 2 3 4	(same as for KFLAG(1))
Modal Damping C_q	6	0 1 2 3 4	(same as for KFLAG(1))
Residual Flexibility ,G_B	7	0	Absent
		1	G_{BB} partition only. Size KBFxKBF, listed row-wise.
		2	G_B: KNFxKBF size listed row-wise.
Residual Mass H_B	8	0	Absent
		1	H_{BB} partition only KBFxKBF size, listed row-wise.
		2	H_B partition KNFxKBF size, listed row-wise
		3	Compute $G_B.M_x.G_B$ (full mass matrix in physical coordinates must be supplied as per KFLAG(2))
Residual Damping C_B	9	0	Absent
		1	C_{BB} partition only. Listed row-wise
		2	Full C_B partition. Listed row-wise.
		3	Compute $G_B.C_X.G_B$ (Full damping must be supplied as per KFLAG(3))
Constraint Mode Stiffness K_{CC}	10	0	Absent
		1	Full matrix, row-wise
		2	Full matrix, symmetric, upper triangular (row)
		3	Full matrix, symmetric,

			lower triangular (row)
Constraint Mode Mass M_{CC}	11	0	Absent
		1	Full matrix, row-wise
		2	Full matrix, symmetric, upper triangular (row)
		3	Full matrix, symmetric, lower triangular (row)
Normal Mode-Constraint Mode Coupling Mass M_{nc}	12	0	Absent
		1	Full matrix row-wise
Hysteretic Damping H_x	13	0	
		1	
		2	(same as for KFLAG(1))
		3	
Modal Inverse Method	14	0	Generalized inverse using Gaussian elimination
		1	Generalized inverse using singular value decomposition

KFLAG(15) through KFLAG(20) are used for controlling level of printed output in various modules. Thus a unit value of the respective flag outputs data in subroutines COMPi0, SEi0, ASSIGN, ASMBL, SOLVE and RECOVR.

14. Dynamic data may be read in two ways: IOPT=1 Read dynamic data from user supplied file in Neutral file format defined in Appendix C.2. IOPT=2 Read dynamic data from universal file format defined in Appendix C.3.
15. On VAX the program automatically accesses the file named FNAME.DAT.
16. The tape density, read/write flags, magnetic tape file name, and the blocking factor refer to the SDRC software created universal file.

C.2 COMPONENT DYNAMICS DATA: NEUTRAL FILE FORMAT

The specification format for component dynamic data differs with the type of component dynamic model as described below.

Finite Element Component: Type 10

Record	Column	Format	Data Item	Description	Notes
1	1-80	A80	TITLE2	Component Header Data	
2	1-80	8E10.3	K_X	Stiffness Matrix in Physical Coordinates	(1)
3	1-80	8E10.3	M_X	Mass Matrix in Physical Coordinates	(1)
4	1-80	8E10.3	C_X	Viscous Damping Matrix in Physical Coordinates	(1)

Free Interface Modal Component with Residual Flexibility: Type 20

Record	Column	Format	Data Item	Description	Notes
1	1-80	20A4	TITLE2	Component Header Data	
2	1-5	I5	MOD	Mode Number	(15)
3	1-10 11-20 21-30	E10.3 E10.3 E10.3	G_K G_M G_C	Modal Stiffness Modal Mass Modal Damping	(2,15)
4	1-4 6-65	I4 6E10.3	NUM U(I), I=1,6	Node Number Node Point Modal Coefficients	(3) (14,15)
5	1-80	8E10.3	G_B or G_{BB}	Residual Flexibility	(4)
6	1-80	8E10.3	H_B or H_{BB}	Residual Inertia	(5)
7	1-80	8E10.3	M_X	Mass Matrix	(6)
8	1-80	8E10.3	C_B or C_{BB}	Residual Damping	(7)
9	1-80	8E10.3	C_X	Damping Matrix	(8)

Free Interface Modal Component With or Without Interface Loading:

Type 30

Record	Column	Format	Data Item	Description	Notes
1	1-80	20A4	TITLE2	Component Header Data	
2	1-5	I5	MOD	Mode Number	(15)
3	1-10	E10.3	G_K	Modal Stiffness	(9)
	11-20	E10.3	G_M	Modal Mass	(15)
	21-30	E10.3	G_C	Modal Damping	
4	1-4	I4	NUM	Mode Number	(10)
	6-65	6E10.3	U(I), I=1,6	Node point Modal coefficients	(14) (15)
5	1-80	8E10.3	K_Q	Generalized Stiffness Matrix (KM*KM size)	(9)
6	1-80	8E10.3	M_Q	Generalized Mass Matrix (KM * KM size)	(9)
7	1-80	8E10.3	C_Q	Generalized Damping Matrix (KM * KM size)	(9)

Constrained Interface Modal Component: Type 40

Record	Column	Format	Data Item	Description	Notes
1	1-80	20A4	TITEL2	Component Header Data	
2	1-5	I5	MOD	Constrained Normal Mode Number	(11) (15)
3	1-10	E10.3	G_K	Constrained Normal Mode Stiffness	(2) (15)
4	11-20	E10.3	G_M	Constrained Normal Mode Mass	(2) (14,15)
5	21-30	E10.3	G_C	Constrained Normal Mode Damping	(2) (16)
6	1-4 6-65	I4 6E10.3	NUM U(I), I=1,6	Node Number Node Point Moda Coefficients	(10) (16)
7	1-5	I5	MOD	Constraint Mode Number	(12)
8	1-4 6-65	I4 6E10.3	NUM U(I), I=1,6	Node Number Node point Modal Coefficient	(10)
9	1-80	6E10.3	K_{CC}	Constraint Mode Stiffness Matrix (KBF * KBF size)	(13)
10	1-80	6E10.3	M_{CC}	Constraint Mode Mass Matrix (KBF * KBF size)	(13)
11	1-80	8E10.3	M_{NC}	Normal Mode-Constraint Mode Inertia Coupling Matrix (KM * KBF size)	(13)

NOTES:

1. The specification of the matrix coefficients A(I,J) should be consistent with the corresponding flags specified in record 17 of sizing data described in Appendix C.1. Each record may run into several data cards. The matrices should conform with the free interface boundary conditions of the component.
2. Physical units of the generalized mass, damping, and stiffness are at the user's discretion; any consistent units may be selected.
3. The node point modal coefficients should be ordered as u,v,w,rx,ry,rz, where u, v, w, and rx, ry, rz are respectively the three translational displacements and three rotations with respect to Cartesian axes x, y, z.
4. Residual flexibility matrix coefficients are input row-wise as ((GBB(I,J),J=1,KBF),I=1,KBF) if KFLAG(7)=1 and as ((GB(I,J),J-1,KBF),I=1,KNF) if KFLAG(7)=2. KBF and KNF are respectively the number of boundary DOFs and total nodal DOFs of the component.

5. Residual inertia matrix coefficients are input row-wise as (HBB(I,J),J=1,KBF),I=1,KBF) if KFLAG(8)=1 or ((HB(I,J),J=1,KBF),I=1,KNF) if KFLAG(8)=2. Omit this record set if KFLAG(8)=0 or 3.

6. If KFLAG(8)=3, physical mass matrix and the full G partition of the residual flexibility matrix is required ((KFLAG(7) must be 2) to compute residual mass matrix. Input mass matrix as per KFLAG(2). Omit this record if KFLAG(8).NE.3.

7. Residual damping matrix coefficients are input row-wise as ((CBB(I,J),J=1,KBF),I=1,KBF) if KFLAG(9)=1 or ((CBB(I,J),J=1,KBF),I=1,KNF) if KFLAG(9)=2. Omit this record set if KFLAG(9)=0 or 3.

8. If KFLAG(9)=3, physical damping matrix and the full G partition of the residual flexibility matrix is required ((KFLAG(7) must be 2) to compute residual damping matrix. Input damping matrix as per KFLAG(3). Omit this record if KFLAG(9).NE.3.

9. Physical units of the generalized mass, damping, and stiffness are at the user's discretion; any consistent units may be selected.

   When nonorthogonal modes are used one or more of the generalized matrices may be fully populated. Full matrices are specified in records 4 through 6 as per KFLAG(4), KFLAG(5), and KFLAG(6).

10. The node point modal coefficients should be ordered as u, v, w, rx, ry, rz, where u, v, w, and rx, ry, rz are respectively the three translational displacements and three rotations with respect to cartesian axes x, y, z.

    Record type 4 must be repeated as many times as there are nodes in the component; that is, KN times, where variable KN has been set in record type 10 in the Sizing and Topological Input Data File.

11. Constrained normal modes are normal modes of the component obtained with connection interface degrees held fixed. The input formats for the constrained normal mode data is similar to that of the normal mode data.

12. The constraint modes are static deflection shapes as defined in Equations 183 through 186. The component and nodal degrees of freedom arrangement and the mode shape data input is same as that of the normal mode shape data. Record types 5 through 6 must be repeated for each constraint mode. The number of constraint modes equals the number of boundary degrees of freedom, NBDG. This can be calculated by multiplying the number of boundary nodes, KB, times the number of degrees of freedom per node NDFN. That is, NBDG = (KB*NDFN), where KB and NDFN are the values specified in the Sizing and Topological Data Input File on records 11 and 4, respectively.

13. Stiffness, mass and damping matrices associated with the constraint modes are defined in Equation 200. Note the matrix partitions required.

14. Record Number 4 should be repeated as many times as there are number of nodes in the component.

15. Record 2 through 4 should be repeated for each mode.

16. Records 5 and 6 should be repeated for each constraint mode.

C.3 COMPONENT DYNAMICS DATA: UNIVERSAL FILE FORMAT

The universal file format is a widely accepted form for interfacing data between different software. Details of the universal file are given in Reference 76. Subroutine RDUVF translates the universal file contents and creates a neutral file for the component. The data requirement for a certain type of component is the same as those defined in Appendix C.2; only the specification format differs. The following describes the universal file formats for all the dynamic data types needed by COMSYN.

The general characteristics of a universal file data set are as follows:

- The first record of the data contains "-1" right justified in columns 1 through 6. Columns 7 through 80 of this physical record is blank.

- The second record of the data set contains the data TYPE number, numeric range 1 through 32767, right justified in columns 1 through 6. The remaining columns, 7 through 80, are blank.

- The last record of the data set contains "-1" right justified in columns 1 through 6. Columns 7 through 80 of this record are blanks.

The following lists the universal data sets for the four component types and the specifics of each data set.

Universal Data Set for Physical Coordinate Component (TYPE 10)

Dataset Type	Description
241	Component Header Data
250	Stiffness Matrix (IMAT=9)
250	Mass Matrix (IMAT=6)
250	Viscous Damping Matrix (IMAT=7)

Universal Dataset for Residual Flexibility Component (TYPE 20)

Dataset Type	Description
241	Component Header Data
55	Eigenvector and Modal Parameters
250	Residual Flexibility Matrix
250	Residual Mass Matrix (if KFLAG(8)=1 or 2)
250	Total Mass Matrix (if KFLAG(8)=3)
250	Residual Damping Matrix (if KFLAG(9)=1 or 2)
250	Total Damping Matrix (if KFLAG(9)=3)

Universal Dataset for General Coordinate Component (TYPE 30)

Dataset Type	Description
241	Component Header Data
55	Mode Shape Vector and Modal Parameters
250	Generalized Stiffness Matrix (if KFLAG(4)>0)
250	Generalized Mass Matrix (if KFLAG(5)>0)
250	Generalized Damping Matrix (if KFLAG(6)>0)

Universal Dataset for Constrained Interface Component (TYPE 40)

Dataset Type	Description
241	Component Header Data
55	Eigenvector and Modal Parameters
55	Constraint Mode Vector
250	Constraint Mode Stiffener Matrix (K partition)
250	Constraint Mode Mass Matrix (M partition)
250	Normal Mode-Constraint Mode Mass Coupling (M partition)

Dataset Type 55

Record	Column	Format	Data Item	Description
1-5	1-80	80A1	TITLE	Identifying Title (5 lines)
6	1-10	I10	1	Structural Model Flag
	11-20	I10	1	Constraint Mode
			2	Normal Mode Shape
	21-30	I10	3	3 DOF (Translation) per Node
			6	6 DOF (Translations + Rotations) per node
	31-40	I10	8	Flag for Displacement Vector
	41-50	I10	2	Real Coefficients
	51-60	I10	NDV	No. of Data Values per Node (=data in field 2 above)
7	1-10	I10	1	No. of integer data values for constant mode
			2	No. of integer data values for normal mode
	11-20	I10	1	No. of real data values for constant mode
			4	No. of real data values for normal mode
	21-30	I10	MOD	Constraint Mode Number
	31-40	I10	MOD	Normal Mode Number
8	1-13	E13.5	ω	Normal Mode Frequency in Hz (blank for constraint mode)
	14-26	E13.5	G_M	Modal Mass (normal mode) (blank for constraint mode)
	27-39	E13.5	G_C	Modal Viscous Damping (blank for constraint mode)
9	1-10	I10	NOD	Node Number
10	1-78	6E13.5	U(I), I=1,NDV	Node Point Modal Coefficient

NOTES:

1. Records 9 and 10 are repeated for each node.
2. Title lines may not be blank. If no information is required the word "NONE" must appear in columns 1-4.
3. The order of data values U(I),I=1,NDV is

   3 DOF Vector X,Y,Z
   6 DOF Vector X,Y,Z,$\theta X, \theta Y, \theta Z$

4. Modal stiffness is obtained computed in the program as $G_K = 4.0 \pi^2 \omega^2 G_m$, where ω is natural frequency in Hertz.

Dataset Type 250

Record	Column	Format	Data Item	Description
1	1-10	I10	IMAT	Matrix Identification
2	1-10	I10	MDTYPE	Matrix Data Type (=2 for real)
	11-20	I10	MFORM	Matrix Form (=3 General Rectangular
	21-30	I10	NROWS	Number of Rows
	31-40	I10	NCOLS	Number of Columns
	41-50	I10	MKEY	Storage Key (=1 Row, =2 Column)
3	1-10	I10	ISR	Starting Row for Submatrix
	11-20	I10	ISC	Starting Column for Submatrix
	21-30	I10	NR	No. of Rows in Submatrix
	31-40	I10	NC	No. of Columns in Submatrix
	41-50	I10	MFORMS	Submatrix Form (=3 General Rectangular, =5 Diagonal)
	51-60	I10	MKEYS	Submatrix Storage Key (=1 Row, =2 Column)
4	1-80	4E10.12	A(I,J)	Real Matrix Data

- Repeat record 4 as necessary to fulfill requirements of record 3.
- Records 3 and 4, as a group, are repeated as necessary to define all non-zero submatrices.

APPENDIX D: EXAMPLE JCL AND INPUT DATA

The following describes a sample VAX/VMS command procedure to execute program COMSYN. The example shown in Figure D-1 uses input data files which are all resident on disk as permanent files. The example problem uses one system input file and four component dynamic data files. These are declared as LV.DAT, COMP1.DAT, COMP2.DAT, COMP3.DAT and COMP4.DAT, respectively. The procedure file and the input data file are listed in Figures D-2 through D-7.

The system considered is that of the longitudinal motion of a launch vehicle-like structure. It is partitioned into four components as shown in Figure D-1. In order to cover the full modeling capabilities of the synthesis program, a different type of dynamic model is used to represent the component dynamics. Thus the four components are modeled respectively as free interface normal modes plus residual flexibility; free interface modes alone; finite element matrices in physical coordinates; and constrained interface modes. The system input and component data file are as follows. The component dynamic data files are input to the program in universal file format. In generating the component data, the connection interfaces are left unrestrained. Only those component nodes are restrained in component model generation which correspond to the restrained system nodes. Thus the node 1 of the component 1 is restrained because the built-up system is also restrained at the same location. In the following the background information needed to create the data is also given for the sake of completeness.

Component 1 Residual Flexibility Component

The normal modal and static residual flexibility properties of the component are derived from the following stiffness and mass matrices. Node 2 is the boundary node and is kept unrestrained.

Stiffness Matrix: $[K]_o = \begin{bmatrix} 1 & -1 & 0 & 0 \\ -1 & 2 & -1 & 0 \\ 0 & -1 & 2 & -1 \\ 0 & 0 & -1 & 1 \end{bmatrix}, \quad [M]_o = \begin{bmatrix} 1 & 0 & 0 & 0 \\ 0 & 2 & 0 & 0 \\ 0 & 0 & 2 & 0 \\ 0 & 0 & 0 & 1 \end{bmatrix}$

Normal modes and modal properties are:

$$[\Phi]_N = \begin{bmatrix} 0 & 0 & 0 \\ -.288675 & .57735 & .288675 \\ -.5 & 0 & -.5 \\ -.57735 & -.57735 & .57735 \end{bmatrix}$$

$$[K]_q = \begin{bmatrix} .13397 & 0 & 0 \\ 0 & 1.0 & 0 \\ 0 & 0 & 1.86603 \end{bmatrix}$$

$$[M]_q = \begin{bmatrix} 1.0 & 0 & 0 \\ 0 & 1.0 & 0 \\ 0 & 0 & 1.0 \end{bmatrix}$$

Residual Flexibility Properties:

Modes to be kept

$$[\Phi]_K = \begin{bmatrix} 0 & 0 \\ -.28865 & .57735 \\ -.5 & 0 \\ -.57735 & -.57735 \end{bmatrix}, \quad [K]_q = \begin{bmatrix} .13397 & 0 \\ 0 & 1.0 \end{bmatrix}, \quad [M]_q = \begin{bmatrix} 1.0 & 0 \\ 0 & 1.0 \end{bmatrix}$$

Total Static Flexibility

$$[G] = [K]_o^{-1} = \begin{bmatrix} 0 & 0 & 0 & 0 \\ 0 & 1 & 1 & 1 \\ 0 & 1 & 2 & 2 \\ 0 & 1 & 2 & 3 \end{bmatrix}$$

Static Flexibility of Truncated Mode (Residual Flexibility)

$$[G]_R = [K]_o^{-1} - [\Phi]_K [K]_q^{-1} [\Phi]_K^T$$

$$= \begin{bmatrix} 0 & 0 & 0 \\ .044658 & -.07735 & -.089316 \\ -.07735 & .133975 & -.154701 \\ .089316 & -.154701 & .178633 \end{bmatrix}$$

Residual Flexibility Attachment Mode:

$$[G]_B = \begin{bmatrix} 0 \\ .089316 \\ -.154701 \\ .178633 \end{bmatrix}$$

The universal data set for the above component COMP1.DAT is listed in Figure D-3.

Component 2: Free Interface Normal Mode Component

The modal properties are derived from the stiffness and mass matrices in physical coordinates given for the Component 1. the mode shapes, modal stiffness, and modal mass are given as

$$[\Phi]_N = \begin{bmatrix} .408 & .577 & .577 & -.408 \\ .408 & -.2887 & -.2887 & .408 \\ .408 & -.2887 & -.2887 & -.408 \\ .408 & .577 & .577 & .408 \end{bmatrix}$$

$$[K]_q = \begin{bmatrix} 0 & 0 & 0 \\ 0 & 0.5 & 0 \\ 0 & 0 & 1.5 \end{bmatrix}, \quad [M]_q = \begin{bmatrix} 1. & 0 & 0 \\ 0 & 1. & 0 \\ 0 & 0 & 1. \end{bmatrix}$$

The universal data set for the above component COMP2.DAT is listed in Figure D-4.

Component 3: Finite Element Component

The stiffness and mass matrices for this component are as shown above for the Component 1. The universal data set for this component is listed in Figure D-5.

Component 4: Constrained Interface Modal Component

The component is constrained at the nodes 1 and 4. The Node 4 is treated as a boundary node since it is to be represented in the system equation in physical coordinates. The normal mode properties are obtained from the solution of the following eigenproblem.

$$\left[\begin{bmatrix} 2 & -1 \\ -1 & 2 \end{bmatrix} - \omega^2 \begin{bmatrix} 2 & 0 \\ 0 & 2 \end{bmatrix} \right] \begin{Bmatrix} x_2 \\ x_3 \end{Bmatrix} = \{0\}$$

leading to

$$[\Phi]_N = \begin{bmatrix} 0 & 0 \\ .5 & .5 \\ .5 & -.5 \\ 0 & 0 \end{bmatrix}, \quad [K]_q = \begin{bmatrix} .5 & 0 \\ 0 & 1.5 \end{bmatrix}, \quad [M]_q = \begin{bmatrix} 1. & 0 \\ 0 & 1. \end{bmatrix}$$

The constraint modes are derived by solving the two statics problems obtained by (a) constraining node 1 and imposing a unit displacement to node 2, and (b) constraining node 2 and imposing a unit displacement to node 1. The two constraint nodes are

$$[\Phi]_C = \begin{bmatrix} 1. & 0 \\ .667 & .333 \\ .333 & .667 \\ 0 & 1. \end{bmatrix}$$

and the corresponding stiffness and mass properties are

$$[K]_{CC} = \begin{bmatrix} .333 & -.333 \\ -.333 & .333 \end{bmatrix}, \quad [M]_{CC} = \begin{bmatrix} 2.1111 & .8889 \\ .8889 & 2.1111 \end{bmatrix}, \text{ and } [M]_{NC} = \begin{bmatrix} 1. & 1. \\ .333 & -.333 \end{bmatrix}$$

In the above normal and constraint mode, matrices are obtained by first arranging the displacement transformation as

$$\{X\} = \begin{Bmatrix} \{q\} \\ \{X\}_B \end{Bmatrix} = [\Phi]_N\{q\} + [\Phi]_C\{X\}_B, \text{ where } \{q\} = \begin{Bmatrix} q_1 \\ q_2 \end{Bmatrix}, \quad \{X\}_B = \begin{Bmatrix} X_1 \\ X_4 \end{Bmatrix}$$

and also rearranging the physical stiffness and mass matrices accordingly as

$$[\hat{K}]_x = \begin{bmatrix} 2 & -1 & -1 & 0 \\ -1 & 2 & 0 & -1 \\ -1 & 0 & 1 & 0 \\ 0 & -1 & 0 & 1 \end{bmatrix}$$

$$[\hat{M}]_x = \begin{bmatrix} 2 & 0 & 0 & 0 \\ 0 & 2 & 0 & 0 \\ 0 & 0 & 1 & 0 \\ 0 & 0 & 0 & 1 \end{bmatrix}$$

Transformation of the above matrices to the $\{q\}$ and $\{X\}_B$ coordinates leads to

$$[\Phi]^T[\hat{K}]_x[\Phi] = \begin{bmatrix} .5 & 0 & 0 & 0 \\ 0 & 1.5 & 0 & 0 \\ 0 & 0 & .33 & -.33 \\ 0 & 0 & -.33 & .33 \end{bmatrix}$$

$$[\Phi]^T[\hat{M}]_x[\Phi] = \begin{bmatrix} 1. & 0 & 1. & 1. \\ 0 & 1. & .33 & -.33 \\ 1. & .33 & 2.111 & .889 \\ 1. & -.33 & -.33 & 2.111 \end{bmatrix}$$

The universal data set for this component is listed in Figure D-6.

Built-Up System:

The input data for the built-up system is listed in Figure D-7. It consists of 4 component and 4 system nodes (three connection nodes plus a non-interface node to be carried into system synthesis) with one DOF at each node. The dynamics data type, sizing, connectivity, and other control information for each component is also shown in Figure D-7.

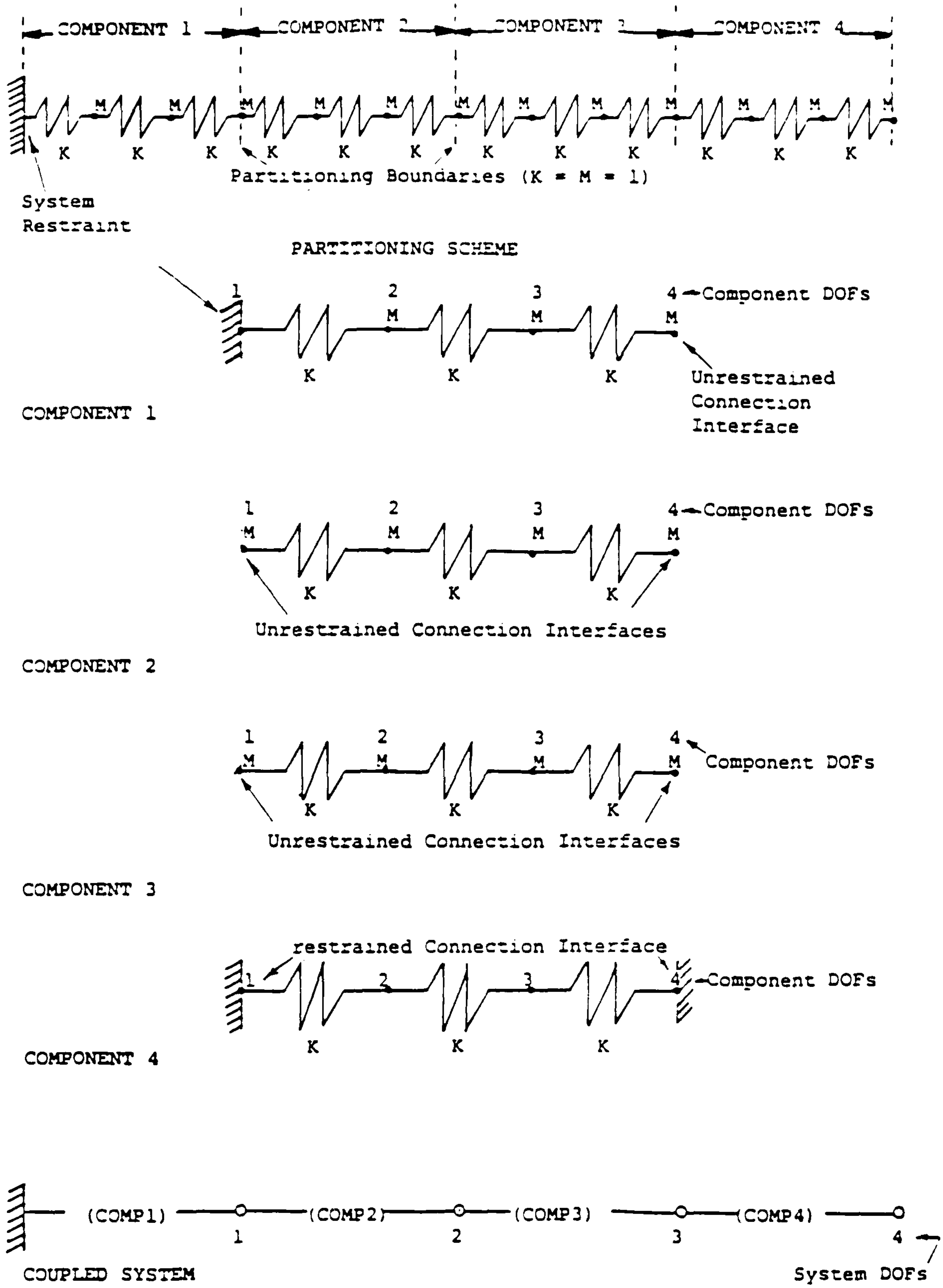

Figure D-1. Example Problem

```
$!Command Procedure File CMS.COM :
$!
$! PROCEDURE TO RUN COMSYS INTERACTIVELY
$!
$!----SYSTEM INPUT FILE
$!
$ ASSIGN/USER_MODE 'P2' FOR005
$!
$!----OUTPUT PRINT FILE
$!
$ ASSIGN USER_MODE 'P3' FOR006
$!
$!----EXECUTION STEP
$!
$ RUN 'P1'
$ EXIT

TO Start Execution Enter:

@CMS.COM  P1  P2  P3

Where:
      P1 = File Name Containing COMSYN Executable Binary
      P2 = File Name Containing System Input Data
      P3 = File Name for Output File
```

Figure D-2. Procedure File for COMSYS Execution

```
    -1
   241 (Component Header Data)
     6
KM01
DYNAMIC DATA FOR COMPONENT 1 - UNIVERSAL FILE INPUT
15-OCT-86
     1     6
    -1
    -1
    55 (Mode Shape Data at Nodes: Mode 1)
COMPONENT 1:  RESIDUAL FLEXIBILITY COMPONENT
NORMAL MODE 1
NONE
NONE
NONE
         1         2         1         8         2         1
         2         4         1         1
 .0582538          1.0          0.            0.
         1
 .0                0.           0.            0.
         2
 -.288675          0.           0.            0.
         3
 -.5               0.           0.            0.
         4
 -.577350          0.           0.            0.
    -1
    -1
    55 (Mode Shape Data at Nodes : Mode 2)
COMPONENT 1: RESIDUAL FLEXIBILITY COMPONENT
NORMAL MODE 2
NONE
NONE
NONE
         1         2         1         8         2         1
         2         4         1         2
 .15915            1.0          0.            0.
         1
 .0                0.           0.            0.
         2
 .57735            0.           0.            0.
         3
 .0                0.           0.            0.
         4
 -.577350          0.           0.            0.
    -1
```

Figure D-3. Universal File for Component 1

```
    -1
    55 (Mode Shape Data at Nodes : Mode 3)
COMPONENT 1: RESIDUAL FLEXIBILITY COMPONENT
NORMAL MODE 3
NONE
NONE
NONE
         1          2          1          8          2          1
         2          4          1          3
 .21745            1.0          0.             0.
         1
 .0                0.           0.             0.
         2
 .288675           0.           0.             0.
         3
 -.5               0.           0.             0.
         4
 -.57735           0.           0.             0.
    -1
    -1
   251 (Residual Flexibility DOF Data)
         1
         1          1
    -1
    -1
   250 (Residual Flexibility Matrix Data)
   149
         2          3          4          1          1
         1          1          4          1          3          1
       0.                  .089316            -.154701
 .178633
    -1
```

Figure D-3 (continued)

```
    -1
   241 (Component Header Data)
     6
KM02
DYNAMIC DATA FOR COMPONENT 2 - UNIVERSAL FILE INPUT
15-OCT-86
     1     6
    -1
    -1
    55 (Mode Shape Data)
COMPONENT 2:  FREE INTERFACE MODAL COMPONENT
NORMAL MODE 1
NONE
NONE
NONE
         1         2         1         8         2         1
         2         4         1         1
         0.        1.0         0.            0.
         1
 .408248            0.          0.           0.
         2
 .408248            0.          0.           0.
         3
 .408248            0.          0.           0.
         4
 .408248            0.          0.           0.
    -1
    -1
    55 (Mode Shape Data)
COMPONENT 2: FREE INTERFACE COMPONENT
NORMAL MODE 2
NONE
NONE
NONE
         1         2         1         8         2         1
         2         4         1         2
 .5                1.0         0.            0.
         1
 .57735            0.          0.            0.
         2
-.288675           0.          0.            0.
         3
-.288675           0.          0.            0.
         4
 .57735            0.          0.            0.
    -1
```

Figure D-4. Universal File for Component 2

```
    -1
    55 (Mode Shape Data)
COMPONENT 2 FREE INTERFACE MODAL DATA (TYPE 30)
NORMAL MODE 3
NONE
NONE
NONE
         1         2         1         8         2         1
         2         4         1         3
  1.5              1.0         0.            0.
         1
  .57735           0.          0.            0.
         2
 -.288675          0.          0.            0.
         3
 -.288675          0.          0.            0.
         4
  .57735           0.          0.            0.
    -1
    -1
    55 (Mode Shape Data)
COMPONENT 2 FREE INTERFACE MODAL DATA (TYPE 30)
NORMAL MODE 4
NONE
NONE
NONE
         1         2         1         8         2         1
         2         4         1         4
  2.0              1.0         0.            0.
         1
 -.408248          0.          0.            0.
         2
  .408248          0.          0.            0.
         3
 -.408248          0.          0.            0.
         4
  .408248          0.          0.            0.
    -1
```

Figure D-4 (continued)

```
    -1
   241
     6
KM03
DYNAMIC DATA FOR COMPONENT 3 - UNIVERSAL FILE INPUT
15-OCT-86
     1     6
    -1
    -1
   250   (Mass Matrix)
          6
          2      3      4      4      1
          1      1      4      4      5      1
          1.0           2.0           2.0           1.0
    -1
    -1
   250   (Stiffness Matrix)
          9
          2      3      4      4      1
          1      1      4      4      3      1
          1.0          -1.0           0.0           0.0
         -1.0           2.0          -1.0           0.0
          0.0          -1.0           2.0          -1.0
          0.0           0.0          -1.0           1.0
    -1
    -1
   250   (Viscous Damping Matrix)
          7
          2      3      4      4      1
          1      1      4      4      5      1
          0.05         -0.05          0.0           0.0
         -0.05          0.1          -0.05          0.0
          0.0          -0.05          0.1          -0.05
          0.0           0.0          -0.05          0.05
    -1
```

Figure D-5. Universal File for Component 3

```
    -1
   241
     6
KM04
DYNAMIC DATA FOR COMPONENT 4 - UNIVERSAL FILE INPUT
15-OCT-86
     1     6
    -1
    -1
    55
COMPONENT 4  CONSTRAINED INTERFACE MODAL COMPONENT
NORMAL MODE 1
NONE
NONE
NONE
         1        2        1        8        2        1
         2        4        1        1
        .5       1.0         0.          0.
         1
      .0         0.          0.          0.
         2
      .5         0.          0.          0.
         3
      .5         0.          0.          0.
         4
      .0         0.          0.          0.
    -1
    -1
    55
COMPONENT 4  CONSTRAINED INTERFACE MODAL MODEL
NORMAL MODE 2
NONE
NONE
NONE
         1        2        1        8        2        1
         2        4        1        2
       1.5       1.0         0.          0.
         1
        .0       0.          0.          0.
         2
        .5       0.          0.          0.
         3
       -.5       0.          0.          0.
         4
        .0       0.          0.          0.
    -1
```

Figure D-6. Universal File for Component 4

```
     -1
     55
COMPONENT 4  CONSTRAINED INTERFACE MODAL MODEL
CONSTRAINT MODE 1
NONE
NONE
NONE
             1        1        1        8        2        1
             1        1        1
            0.
             1
            1.          0.          0.          0.
             2
        .666666         0.          0.          0.
             3
        .333333         0.          0.          0.
             4
            0.          0.          0.          0.
     -1
     -1
     55
COMPONENT 4  CONSTRAINED INTERFACE MODAL MODEL
CONSTRAINT MODE 2
NONE
NONE
NONE
             1        1        1        8        2        1
             1        1        2
            0.
             1
            0.          0.          0.          0.
             2
        .333333         0.          0.          0.
             3
        .666666         0.          0.          0.
             4
            1.          0.          0.          0.
     -1
     -1
    250
    142  (Kcc partition of constraint mode stiffness matrix)
             2        3         2       2       1
             1        3         2       2       3       1
        .333333      -.333333      -.333333      .333333
     -1
```

Figure D-6 (continued)

```
 -1
250
134  (Mcc partition of constraint mode mass matrix)
       2        3         2       2        1
       1        3         2       2        3        1
  2.11111         .888889          .888889        2.11111
 -1
 -1
250
132  (Knc partition of constraint mode mass matrix)
       2        3         2       2        1
       1        3         2       2        3        1
     1.0         1.0               .33333         -.33333
 -1
```

Figure D-6 (continued)

```
LAUNCH VEHICLE SYSTEM DYNAMICS SYNTHESIS USING COMPONENT MODELS
COMP. 1: RESIDUAL FLEXIBILITY COMP. 2:FREE INTERFACE NORMAL MODES
COMP. 3: CONSTRAINED INTERFACE MODES COMP. 4 DISCRETE SPRING-MASS
    4
    1    4
COMPONENT       1
TYPE    20
    4
    1
    4
    1
    3
    1    2
 0 0 0 1 1 0 2 0 0 0 0 0 0 0 0 0 0 0 0    .001
     0.          0.         0.
     0.
DYNAMICS DATA 2 COMP1.DAT
COMPONENT     2
TYPE    30
    4
    2
    1    4
    1    2
    4
    4
    1    2    3    4
 0   0   0  1  1  0  0  0  0  0  0  0
     0.          0.         0.
     0.
DYNAMIC DATA 2 COMP2.DAT
COMPONENT    3
TYPE    10
    4
    2
    1    4
    2    3
    0
    0
    0
 2   1  0  0  0  0  0  0  0  0  0
     0.          0.         0.
     0.
DYNAMICS DATA 2 COMP3.DAT
COMPONENT     4
TYPE    40
    4
    2
```

Figure D-7. System Input File

```
     1    4
     1    4
     3    4
     2
     2
     1    2
  0  0  0  1  1  0  0  0  0  2  2  0
     0.          0.          0.
     0.
DYNAMIC DATA 2 COMP.DAT
```

Figure D-7 (continued)